JIMMA UNIVERSITY

JIMMA INSTITUTE OF TECHNOLOGY

SCHOOL OF CHEMICAL ENGINEERING

PRODUCTION AND CHARACTERIZATION OF BIOPLASTIC FROM WHEAT BRAN STARCH REINFORCED WITH WHEAT STRAW FIBER

By

Asfaw Adeko

A Thesis Submitted to Jimma University, Jimma Institute of Technology, School of Chemical Engineering in Partial Fulfillment of the Requirement for the Degree of Masters of Science in Chemical Engineering (Process Engineering stream)

December 2021

Jimma, Ethiopia

JIMMA UNIVERSITY

JIMMA INSTITUTE OF TECHNOLOGY

SCHOOL OF CHEMICAL ENGINEERING

This is to certify that the thesis prepared by Asfaw Adeko, entitled: "**Production and Characterization of Bioplastic from wheat bran Starch reinforced with wheat straw Fiber"** is submitted in partial fulfillment of the requirement for the degree of Master of Science in Chemical (Process Engineering) complies with the regulations of the university and meets the accepted standards concerning originality and quality.

Approved by the Examining Committee:

Approved by the Examining Committee:

Girma Gonfa (PhD)	_Signature_	30/12/2021
External Examiner	Signature	Date
Desalegn Abdissa (MSc)	_____	_____
Internal Examiner	Signature	Date
Ermias Girma (Ass. Prof.)	_____	_____
Advisor	Signature	Date
Yasin Ahmed (MSc)	_____	_____
Chair Person	Signature	Date
Ermias Girma (Ass. Prof.)	_____	_____
School dean	Signature	Date

Declaration

I hereby declare that thesis entitled "**Production and Characterization of Bioplastic from wheat bran Starch reinforced with wheat straw Fiber**" is my original work and has not been presented for any other degree award in any other university. Where material has been used from other sources it has been properly acknowledged.

Submitted by:

Asfaw Adeko   _____   _____

 Approved by: Signature   Date

Ermias Girma (Ass. Prof.)   _____   _____

Advisor   Signature   Date

Alfiya Demoze (MSc)   _____   _____

Co-advisor   Signature   Date

Ketema Beyecha (MSc)   _____   _____

Program coordinator   Signature   Date

Acknowledgments

ABSTRACT

Nowadays, environmental pollution due to plastic waste taking too long to decay has become a serious problem in the world. Existence without plastics looks like to be difficult because of their important role in society and their applications in virtually all the ranges of daily life. However, there are still a number of drawbacks to plastic, one of which is that it is not easily biodegradable. Therefore, environmentally friendly materials to substitute non-biodegradable materials, such as bioplastics, are urgently needed. Bioplastics made entirely on starch have high water sensitivity, lower mechanical and thermal stability, which can be enhanced by adding cellulosic fillers. In this work, wheat bran starch incorporated with wheat straw cellulosic fiber was used to make bioplastic film. An investigation of proximate analysis of wheat bran and wheat straw was undertaken. The physicochemical characteristics of the prepared starch and fiber samples were examined using analytical techniques. The effect of oven drying temperature (35 - 55 ℃), the concentration of glycerol (30 - 40 %) w/v, and concentration of fiber (5 - 15 %) w/w of starch basis was investigated on the tensile strength (TS), elongation at break (EA), and water absorption (WA) of bioplastic film by using Response Surface Methodology (RSM) and physicochemical characteristics of bioplastic film at the optimum point was determined. The obtained results at the optimal point were 20.528 Mpa TS, 8.1 % EA, and 19.44 % WA at a combination of 55 ℃ oven drying temperature, 31.97 % concentration of glycerol, and 14.40 % concentration of fiber with a high value of (97.1 %) desirability. A statistical model was validated and found to have an insignificant difference between experimental and predicted results. At the optimum point, the value of density (1.54 g/ml), moisture content (16.66 %), water solubility (35 %), transparency (5.6 %) and thickness (0.47 mm) of bioplastic film was determined, and also, the result was analyzed by TGA, XRD, and FTIR. The duration of bioplastic degradation (86.7 %) was produced from the optimum value within 16 days.

Keywords: *Bioplastic, Starch, cellulose, temperature, glycerol, characterization*

Table of Contents

List of Tables

List of Figures

List of Abbreviations

ANOVA	Analysis of Variance
ASTM	American Society for Testing and Materials
ASTU	Adama Science and Technology University
CCD	Central Composite Design
CSA	Central Statistics Agency
D.B	Dry basis
EA	Elongation at break
ECAE	Ethiopia conformity assessment enterprise
EGTE	Ethiopia Grain Trade Enterprise
FTIR	Fourier-transformed infrared ray spectroscopy
GHG	Greenhouse gases
JIT	Jimma Institute of Technology
LCA	Life Cycle Assessment
MCC	Microcrystalline cellulose
PE	Polyethylene
PP	Polypropylene
PVA	Polyvinyl alcohol
RSM	Response Surface Methodology
SNNP	Southern nation, nationalities, and peoples
TGA	Thermogravimetric analysis
TS	Tensile strength
UK	United Kingdom
UV	Ultra Violet
WA	Water absorption
WPI	Wheat processing industry
WS	Wheat straw
XRD	X-ray diffraction

1 INTRODUCTION

1.1 Background of the study

The word "plastic" comes from the Greek word "plastikos," which means "able to be formed or molded." Plastic can be molded and cast into several different shapes (Hammer *et al*.,2012). The capacity of a material to be cast, compressed, or extruded into several forms during manufactures, such as films, fibers, plates, tubes, bottles, and boxes, is referred to as plastic. Plastic is a broad term that encompasses a wide range of synthetic and semi-synthetic materials used in a variety of applications. Plastics may be found almost everywhere on earth's surface. Plastic items help to make lives cleaner, simpler, safer, and more enjoyable (Zhou, 2016). Plastics are now commonly used in packaging, catering goods, consumer electronics, automotive, agriculture or horticulture, and toys from textiles, among other markets. Packaging is the most efficient use of plastics, accounting for roughly 65 percent of the overall plastic demand (Chozhavendhan *et al*., 2020)

Plastic production requires natural materials such as cellulose, starch, protein fiber (silk, wool), paper, wood, coal, natural gas, salt, and crude oil (Orezzoli *et al*., 2018). Polymers, additives, and other components make up plastics. Polymerization and polycondensation are the two most important processes in the production of plastics. Both of them require specific catalysts. Polymers are long molecular chains formed by joining together short repeating subunits or monomers in a chemical process known as polymerization (Kershaw, 2016). Additives are compounds that are used to preserve materials, such as lubricants, pigments, and various fillers. While these additions account for a small percentage of all materials used in plastics, they are critical for biodegradable plastics to be biodegradable (Aviles Trujillo, 2017). There are several diverse categories of plastics and classified on the two key polymer families: thermoplastics and thermosets (Zhou, 2016).

Almost all current plastics are petroleum-based; manufactured via chemical extraction and synthesis giving rise to materials that are low cost, easily manufactured, versatile, impervious to water, and some possess the added capability of being resistant to corrosive chemicals. Plastic is wonderful because of its durability and is too alarming because of supposed durability. Almost every piece of man-made synthetic plastic ever produced is largely non-biodegradable and tend to remain in the natural environment in one form or the other (Gertz, 2016).

Bioplastics are also known as biodegradable plastics because they are made from biomass. Biodegradable plastics are substances that can be broken down by microorganisms in the

atmosphere over some time. Specific environmental conditions, such as temperature and aeration, are needed for effective biodegradation, enabling microorganisms to turn natural materials into other natural substances such as compost, water, and carbon dioxide (Halley, 2016). Bioplastics are created by turning sugar found in plants into plastic. The majority of the starch manufactured worldwide is resulting from corn. In addition to cassava, wheat, rice, pea, tapioca, potato are other main sources of starch. High manufacturing costs are a known drawback that has hampered the growth of bioplastics. Bioplastic production from a low-cost and sustainable raw material source is a promising techniques for addressing environmental problems caused by plastic waste (Jain *et al*., 2015). As a result, bioplastics made from starches are more sustainable and environmental friendly than traditional plastics (Washam, 2010). Starch from agricultural waste is a solution for an alternative that comes from a variety of plentiful and easily accessible sources.

Starch, on the other hand, has its own set of drawbacks. As compared to most current plastics, which are mainly water-soluble and have low mechanical properties, so this makes it difficult. The use of natural fibers as a reinforcement (filler) for starch is one of the best alternatives since it not only improves starch's water sensitivity but also increases its power. This property has now been attributed to the chemical similarity of polysaccharides and plant fibers, resulting in good compatibility (Nattakan *et al*., 2012). Cellulose has been secured to be the most promising material for reinforcing fillers because of their environmental friendly. Straw is a by-product of agriculture that is typically made up of cellulose. Converting low-cost agricultural, commercial, and kitchen waste into usable products is critical not only for waste reduction but also for farmers' income. Agriculture is the cornerstone of Ethiopia's economy, with the agricultural sector accounting for more than 85 % of the country's national growth domestic product. Many African countries produce wheat for both domestic consumption and export. Ethiopia is one of the world's largest wheat producers, both in terms of total wheat area cultivated and total output (Anteneh & Asrat, 2020).

Nowadays, there are around 300 flour mills in Ethiopia. The by-product of large and modern flour factories converts 1 kg of wheat into 0.21 kg of wheat bran, whereas the small-medium flour factory converts 1 kg wheat into 0.26 kg wheat bran. From the total wheat bran, 90 % is sold as animal feeds at a very low price. A miller often disposes of wheat bran since the cost of transportation is more than its worth, and such waste also causes potential environmental distresses. Furthermore, wheat bran has many high-value components, for instance, phenolic

compounds, starches, soluble and insoluble dietary fiber (CSA, 2017). And also, wheat straw is one of the most preferable biomass in Ethiopia because of its availability. Therefore, just a small quantity of wheat straw is used for animal feed, while the rest is burned, causing environmental problems. Furthermore, by taking into account all of these factors, wheat straw can be considered as a biomaterial for a variety of residential and industrial purposes (Nigussie *et al*., 2015). The solution casting method is the most widely used technique for the production of bioplastic at the laboratory scale. Bioplastics have comparable or better characteristics than commercial plastics due to their simple process and biodegradability, with the added benefit of reducing the negative impact of waste disposal (Naseri *et al*., 2019).

This study was done on the production and characterization of bioplastic from wheat bran starch via wheat straw fiber by using glycerol as a plasticizer.

1.2 Statement of the problem

Nowadays, the world has tackled side effects from fossil fuel dependence such as greenhouse gas (GHG) emissions, environmental pollution, and ocean acidification during its biodegradability. The exponential growth of the human population has led to the gathering of large quantities of non-degradable waste materials on earth (Zhou, 2016). Currently, life without plastics looks like to be impossible because of their significant role in society and their applications in almost all the areas of daily life. The majority of these plastics that are used nowadays are based on very unmaintainable fossil resources such as natural gas, oil, or coal, producing toxic waste that distresses the entire environment (Geyer *et al*., 2017).

In the follow-up of objectives of sustainable development and the minimization of environmental impacts, biodegradable plastics from renewable resources appropriately represent the best possibility. In this regard, the development of environmentally friendly materials to replace non-biodegradable materials is necessary. Starch is the most promising alternative material for the replacement of petroleum-based polymers, and it offers a very attractive base for new biodegradable polymers due to its environmentally beneficial, available, recyclable, and low cost and its ability to be processed with conventional plastics processing equipment (Nattakan *et al*., 2012). But it has its number of drawbacks, including high water sensitivity (hydrophilic character), poor mechanical efficiency, and gas permeability when compared to conventional industrial polymers (Balaji, A. N., & Nagarajan, K. J, 2017). To overcome the above-mentioned problems

starch is reinforced with cellulosic fiber to advance the mechanical strength, thermal stability of the film. The raw material used was wheat by-products that do not contradict any food security and advantages to minimize waste disposal. Wheat bran for instance, frequently discarded as waste has around 25-39 % starch content (Apprich *et al*., 2014). High percentage of starch contents are found abundantly in wheat bran and cellulose are found in wheat straw.

Many studies have been conducted on the starch as the raw material to produce bioplastics, however, using starch from wheat bran and the effects of process parameters (oven drying temperature, the concentration of glycerol, and concentration of fiber) on the consistency and flexibility of the bioplastic have been rarely investigated.

Therefore, the current study was try to address the effect of those process parameters and optimized them in a way that enables the production of good quality bioplastic.

1.3 Objectives of the research

1.3.1 General objective

The general objective of this study is to produce and characterize bioplastic from wheat bran starch reinforced with wheat straw fiber.

1.3.2 Specific objectives

- To determine the proximate analysis of wheat bran and wheat straw.
- To extract and characterize starch from wheat bran and cellulose from wheat straw.
- To investigate the effect of process variables (oven drying temperature, concentration of glycerol, and concentration of fiber) on the production of bioplastic film and to optimize the process parameters.
- To characterize physicochemical properties of synthesized bioplastic film at the optimum point.

1.4 Significance of the study

The successful accomplishment of this research will be able to play a great role by providing a remedy for the bottlenecked problems of environmental pollution due to the discharge of waste plastics. Besides that, it also reduces packaging problems with prolonged shelf life owi-ng to reinforcement with cellulosic fiber. Through this research, conventional petroleum-based plastics

were replaced by this wheat straw fiber incorporated wheat bran starch-based biodegradable films. This research will be significant to the whole scientific community; subsequently, it would offer added information about how to make a good, environmentally friendly, inexpensive, and toxic-free bioplastic from wheat byproducts. The additional advantage of this research is to be responsible for a way of converting agricultural wastes into treasured products, which in turn, increases income for farmers, creates a job for generations, and enhances industrial contacts.

1.5 Scope and Limitations of the Study

This research generally covers lab-scale production and characterization of bioplastic from wheat bran starch via wheat straw fiber. The materials used in this study were locally available. It includes the collection of wheat bran from wheat flour factor in Jimma city and wheat straw from Dawro zone Zaba Gazo woreda Gazo koysha kebele and proximate analysis, as well as pretreatment of raw materials, was made. In this study, the extraction of starch from wheat bran, cellulose from wheat straw, and their characterization were performed. The production of the bioplastic from the wheat bran starch via wheat straw cellulose and glycerol as a plasticizer. Then, the optimization of processes parameters (TS, EA, and WA) of bioplastic film was performed by using process variables (oven drying temperature, concentration of glycerol, and concentration of fiber). The effect of those process parameters was studied and optimized through a central composite design (CCD). The investigation of the optimum value of bioplastic film using XRD, FTIR, and TGA tests was performed. The challenges that occurred during the experimental work were the unavailability of testing materials; for example, scanning electron microscope.

2 LITERATURE REVIEW

2.1 Definition and production of plastic

"A plastic is a synthetic or man-made material that, in some ways, looks like natural resins found in trees and other plants." Polymerization produces a variety of complex organic compounds that can be molded, extruded, cast into various shapes and films, or pulled into filaments and utilized as textile fibers," according to Webster's Dictionary (Al-Enizi *et al*., 2018). Plastics are considered a special subset of polymers. Therefore, understand polymers before understanding plastics. Polymers (Greek: poly-many, meros-particle). Plastic is material that have lightweight, inexpensive, and durable, which can be shaped readily into a variety of products should be used in a wide range of applications (Brazel, C. S., & Rosen, S. L. 2012).

Plastics are mainly used for the production of a wide range of packaging materials due to their all-around functionalities. Bakelite (polyoxybenzylmethylenglycolanhydride) was the first synthetic plastic, appearing in the Second World War in the form of pilot's goggles, field telephones, patriotic jewelry, and other products. Plastic's growth is extremely intelligent, even surpassing that of most artificial materials. According to researchers from the University of California and the University of Georgia, the production of plastic material has reached 8300 million metric tons (Mt) to date. According to reports from 2015, almost 6300 Mt of plastic garbage was collected, of which 9 % was recycled, 12 % was burnt, and the rest (79 %) was stored in landfills or the natural environment (Rajam & Parthasarathi, 2020).

Thermoplastics and thermoset plastics are the two major categories of plastic families. Commodity, engineering, and specialty plastics are the three types of plastics. Commodity plastics are inexpensive, simple to make, and relatively strong. Engineering plastics are two to three times more expensive than commodity plastics, but they have better heat resistance and strength. Specialty plastics are very expensive, but they have unique properties that make them desirable, such as being able to withstand high temperatures. A resin is an unprocessed form of plastic (Reddy *et al*., 2013). To recapitulate, plastics are differentiated from other polymers by a combination of their organic composition and their capacity to be molded or cast into a variety of shapes.

2.2 Development of bioplastic

Biodegradable plastics began being arousing interest amid the oil crisis in the 1970s. As oil prices climbed, so did the planning and development of biodegradable materials. Biodegradable films,

sheets, and mold forming materials were introduced in the 1980s. Green materials are becoming increasingly popular. This is because they are a renewable resource that is far more cost-effective than it was previously (Mashek *et al*., 2016). The research and development of new materials are ongoing. To create a suitable biodegradable material, researchers must balance several variables. Wheat, potatoes, rice, and corn are the most common sources of starch-based plastics. Corn is the most widely used and the least expensive of these four starch sources. The United States, which generates about \$1.8 million in annual starch sales, accounts for the majority of starch sales. Because starch is such a flexible substance, around 20 % of it is used for non-food things. Many non-food goods, such as paper, cardboard, textile sizing, and adhesives, are made with starch. Eating utensils, plates, cups, and other things have already been made using starch-based polymers (Glenn *et al*., 2014).

The creation of biodegradable plastics has numerous advantages. It has been proven that starch-based plastics are more environmentally friendly. Biodegradable plastics based on starch have been shown to degrade 10 to 20 times faster than conventional plastics. When typical plastics are burned, harmful gases are released, potentially harming people's health and the environment. There are few if any, hazardous compounds or gases discharged into the air when biodegradable films are burned. It has been proven that biodegradable plastics increase soil quality. This process occurs when microbes and bacteria in the soil digest the debris, resulting in a more fertile ground (Jouhara et al., 2017).

2.3 Global overview of bioplastics

A bioplastic is a part of plastic that is manufactured partly or wholly from polymers derived from biological sources like sugar cane, potato starch, avocado seed, or the cellulose from trees, straw, stalk, cotton, and the like. Bioplastics are not considered a single substance because they comprise a whole family of materials with different properties and applications. As stated by Europeans's a plastic material is said to be a bioplastic if it is either bio-based, biodegradable, or features both properties (Shamsuddin *et al*., 2017). The general misunderstanding exists between "bio-based" and "biodegradable" polymers because all biodegradable bioplastic may not be bio-based [e.g. polybutylene adipate-co-terephthalate and polycaprolactone] and a bioplastic that is all bio-based may not essentially be biodegradable (e.g. polyethylene-terephthalate and bio polyethylene) (Abioye *et al.*,2018).

Because of its advantages such as high availability, low cost, renewability, and the ability to degrade without leaving harmful residues, starch is intended to be one of the most commonly used biopolymers as a replacement for traditional plastics. However, its main drawback is low water resistance and mechanical strength. Reinforcements, either microparticle or nanoparticle, have been incorporated into starch to address these inherent problems. Mainly the properties of starch and cellulose fiber blends are primarily determined by the compatibility between their components by using the solution casting method (Jianlei *et al*., 2019). Nowadays in general, the bioplastic family can be categorized into three main classes according to their properties: Both bio-based and biodegradable bioplastic, bio-based or partly bio-based non-biodegradable bioplastics, and fossil fuel-based and biodegradable bioplastic.

i) Both bio-based and biodegradable bioplastic

Bioplastics contain products of both bio-based and biodegradable. They can be synthesis from; several different natural sources such as plants, cellulose, protein, chitin (prawn shells), and bacteria. These materials are comfortable for disposable items due to their biodegradability, such as packaging, drink bottles, single-use food containers, and cutlery. They are more sustainable and renewable because they save fossil fuel resources and if disposed of appropriately, support further plant growth. Examples: polylactic acid (PLA) and polyhydroxyalkanoate (PHA) (Babu *et al*., 2013).

ii) Bio-based or partially bio-based non-biodegradable plastics

Drop-ins are bio-based or partially bio-based bioplastics that are not biodegradable. Simply, drop-in solutions are plastics that are a hybrid of classic plastics. Drop-ins bioplastic differs from conventional counterparts only in terms of their partially renewable raw material foundation, while remaining functionally equivalent (Halley, 2016). Examples: bio-polyethylene (PE), bio-polypropylene (PP) and bio-polyethylene terephthalate (PET), and polyvinyl chloride (PVC) can be synthesis from renewable resources, like bioethanol.

iii) Fossil fuel-based and biodegradable bioplastic

New polymers based on fossil fuels that are nonetheless biodegradable make up the final classes of bioplastics. Microorganisms in their natural environment (e.g., in soil, surface waters, or compost) should be able to mineralize biodegradable polymers, which produce energy, biomass,

water, and carbon dioxide or methane, depending on the presence or lack of oxygen (Geueke, 2014). Polybutyrate adipate terephthalate (PBAT) and polycaprolactone (PCL) are two examples of polybutyrate adipate terephthalate.

2.4 Bioplastic market in the world

The world bioplastics market is thought to prefer about 20%~25 % per year. Estimated 10~15 % bioplastics of the total plastics market will raise its market share to 25~30 % by 2020. The bioplastic market come to 1 billion US$ in 2007 and it will be over 10 billion by 2020. Rising numbers of companies are entering and investing in this market, as new applications and innovations in the automotive and electronics industries are creating a market boom (Arikan *et al*., 2015). Bioplastics have a prompt growing market share; enlarge at a rate of more than 8-10 % per year. Over 500 BPs processing companies are already available; more than 5,000 are expected by 2020. In the world, less than 3 % of all waste plastic gets recycled, compared with recycling rates of 30 % for paper, 35 % for metals, and 18 % for glass (Mostafa *et al*., 2015).

Nowadays availability of bioplastic covers approximately 10-15 % of the plastics market and is expected to grow between 8-10 % per year. Due to the shortage of crude oil reserves, Europe is intended as one of the most important markets. Currently, bioplastics have been used in the food and packaging industry, medical, toys, and textile industries. Demand for bioplastics is expanding nowadays. Advances in technology will improve product quality and versatility by lowering production costs. This, in conjunction with increasing fossil-fuel costs, has resulted in more companies entering the bioplastic market, promoting further research and competition. The renewability and availability of raw materials, the various disposal choices for bioplastics, coupled with increasing consumer demand for environmentally responsible products has directed some to claim the industry has collided with its tipping point (Halley, 2016).

2.5 Biodegradation of bioplastics

Biodegradation of plastic is a process that occurs at a boundary of solid/liquid whereby the enzymes in the liquid phase depolymerize the solid phase. Both bioplastics and conventional plastics comprising additives are capable to biodegrade. Bioplastics are capable to biodegrade in diverse environments because they are more suitable than conventional plastics. Biodegradability of bioplastics arises under several environmental situations including soil, aquatic environments, and compost. Both the structure and composition of biopolymer or bio-composite influence the

process, hence varying the composition and structure might rise biodegradability (Gómez *et al*, 2013).

Soil and compost through environmental situations are more effective in biodegradation owing to their great microbial range. Composting not only biodegrades bioplastics competently but also considerably diminishes the emission of greenhouse gases. The biodegradability of bioplastics in compost environments can be advanced by rising temperatures. Soil environments on the other hand have a great variety of microorganisms creating it easier for biodegradation of bioplastics to happen. However, bioplastics in soil environments want greater temperatures and a longer time to biodegrade. Some bioplastics biodegrade more competently in water bodies and marine systems; nevertheless, this causes danger to marine ecosystems and freshwater. Therefore, it is truthful to conclude that biodegradation of bioplastics in water bodies leads to the death of aquatic organisms, and unhealthy water can be famous as one of the harmful environmental influences of bioplastics (Emadian *et al*, 2017).

Most, but not all, bioplastics can be broken down in the environment by micro-organisms (as part of the 'carbon cycle'- see below) in a process called 'biodegradation'. This process produces carbon dioxide (CO_2) and water (H_2O) under aerobic conditions or methane (CH_4) under anaerobic conditions (in the absence of air) such as in a landfill.

The biodegradation of polymers contains three significant stages:

1) Biodeterioration: this is a type of environmental degradation that affects polymer mechanical, physical, and chemical structures due to the development of microorganisms within or surface of the polymer environment.

2) Biofragmentation: This is conversion of polymers into oligomers and monomers by the acquisition of microorganisms.

3) Assimilation: when microorganisms are supplied with essential carbon, energy, and nutrient sources from the breakdown of polymers and converts plastic into CO_2, water, and biomass.

During bio-deterioration, changes in surface features and mass loss occur simultaneously, whereas, during bio-fragmentation and microbial assimilation, changes in surface features and bulk loss occur simultaneously (Lucas *et al*., 2008).

The significant issues that disturb the plastic's biodegradation in the environment are the chemical structure, the polymer chain, crystallinity, and the complexity of the polymer formula. The

particular functional groups are carefully chosen by enzymes and can be processed. In general, polymers with a shorter chain, more amorphous part, and less complex formula are more susceptible to biodegradation by microorganisms. Furthermore, the environment, in which the polymers are located or disposed of, plays a key factor in their biodegradation. The pH, temperature, moisture, and oxygen content are among the top important environmental issues that must be measured in the biodegradation of polymers. Finally, biodegradable material thickness (the thicker the substance, the longer it takes to degrade) (Gómez *et al*, 2013).
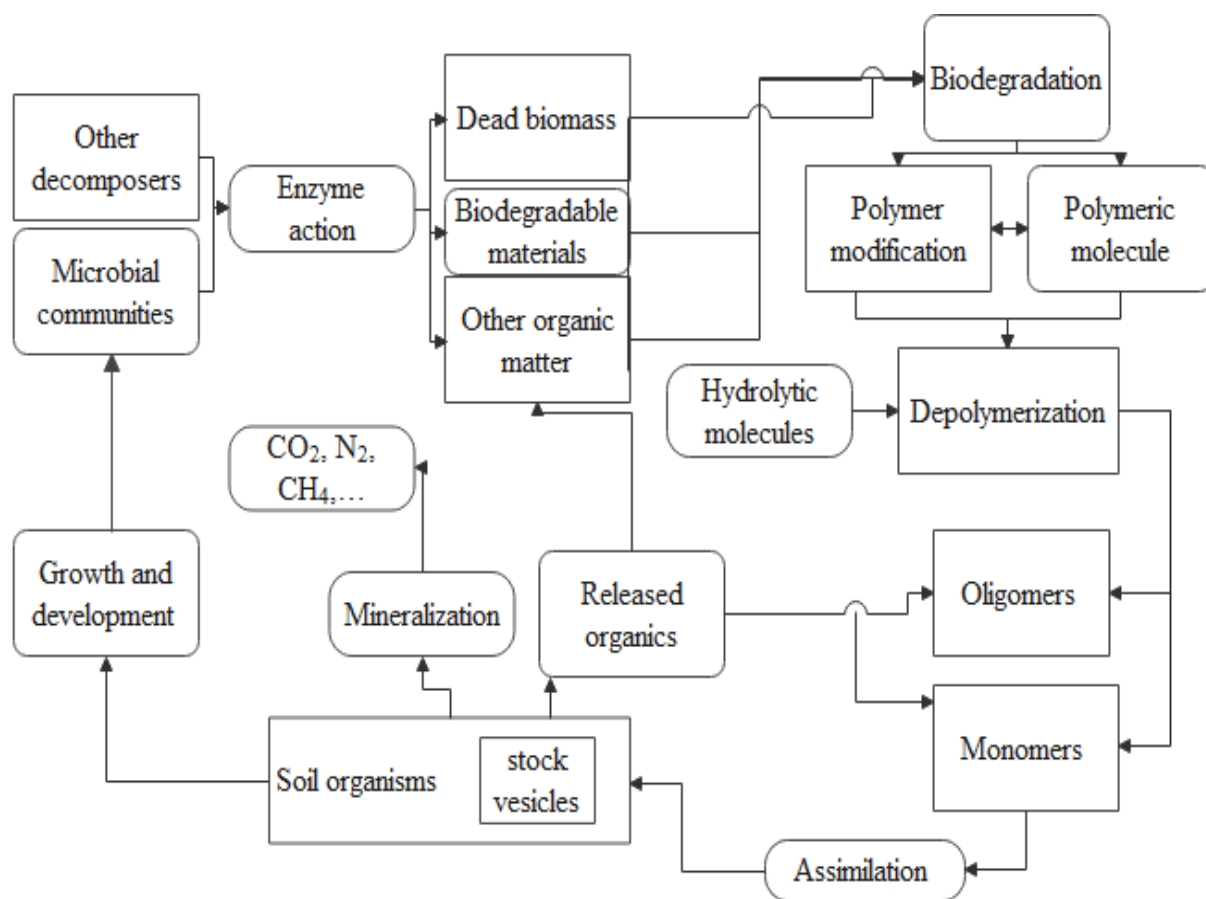
Figure 2.1: Polymer biodegradation scheme.

2.6 Advantages of bio-plastics

i. Lower CO$_2$ emissions: A metric ton of bio-plastics emits between 0.8 and 3.2 metric tons less CO$_2$ than a metric ton of petroleum-based plastics.

ii. A less expensive option: As oil costs fluctuate, bio-plastics are becoming more viable. On the other hand plastics are made from ~4% of the oil that the world uses every year. With oil shortage the production of plastics becomes increasingly exposed to fluctuating prices.

iii. Do not use scarce crude oil: In contrast each kilogram of plastic typically requires 20 kilowatt hours of energy to production, more than the amount needed to make the same weight of steel. Almost all this originates from fossil sources.

iv. The economic benefit to rural areas: Crop prices, such as maize, have risen substantially in response to worldwide interest in the manufacture of biofuels and bioplastics, as governments around the world seek alternatives to oil to protect the environment and achieve energy security.

v. Lower carbon footprint: Oil-based polymers rely on fossil fuel as a primary source of energy. Furthermore, when compared to bio-polymers, oil-based plastics such as PP and PS demand more energy throughout the development process. A typical PP or PS plastic has a carbon footprint of about 2.0 kg CO_2 equivalents per kg of plastic, according to a Life Cycle Analysis (from cradle to factory gate). These CO_2 emissions are four times higher than those from PLA (Poly Lactic Acid) resin.

vi. Multiple end-of-life options: Valuable raw materials can be reclaimed and recycled into new goods, lowering the demand for new virgin material and reducing, if not eliminating, the negative environmental impact of 'used' plastic products. Bio-plastics may be recycled into bio-diesel in the future (Reddy *et al*., 2013).

2.7 Challenges of bioplastics in industry

The development, extensive acceptance and production of bioplastics have to face numerous challenges. The greatest challenging point for bioplastic production is to disturb the potential food sources that it needs high production cost. This requirement can be overcome by employing non-food resources for the purpose. These are known as second-generation bioplastics. On the other hand, these must be processable via common processing routes like extrusion, compression, and injection molding. Several amounts of bioplastics (e.g. derived from bacterial polymer polylactic acid) are only biodegradable in controlled environments of temperature and moisture. This limitation must be overcome and bioplastics must be capable of degrading in landfills. Additionally, bioplastics made from starch have poor mechanical properties and are quite brittle, highly viscous, and hydrophilic. As a result, they must be reinforced with a fiber to improve mechanical properties. Bioplastics, when endangered to biodegradation under anaerobic conditions, release methane in landfills (Imre *et al*., 2013). To compete with the problem and to create appreciated biodegradability as well as to enhance mechanical, water absorption and thermal

stability, current study was done on the production of bioplastic from wheat bran starch reinforced with wheat straw fiber.

2.8 Sustainability of bio-based bioplastics

As stated in the initial section, there are sustainability concerns of petro-based plastics that have been vividly shown. Plastics made from fossil fuels are largely unsustainable because of their negative social, environmental, and health consequences (Markus et *al*., 2014). As a result, significant efforts are being made to develop sustainable bioplastics production from wheat bran starch reinforced with wheat straw fiber. Therefore the bioplastics made from those renewable materials must have the following properties to be considered a truly sustainable resource.

- ❖ Limited resource utilization (energy, cost, biomaterial)
- ❖ The material used should be renewable.
- ❖ The material should be compostable or biodegradable.
- ❖ The material must be able to be produced locally to prevent the environmental and economic impact of transportation.
- ❖ The material must be sustainable throughout its lifecycle, including biomass resource development, polymer manufacture, conversion to a biodegradable plastic product, and end-user consumption (Sustainable bioplastic guidelines, 2007).

As described in the (Figure 2.1), bioplastics' long-term viability must be demonstrated on all three levels: such as social, economic, and environmental levels. As a result, wheat bran and wheat straw as a resource material, as well as the biodegradable films and bioplastics developed from them, could be sustainable because they have no long-term environmental impact and are interesting on social and economic levels.
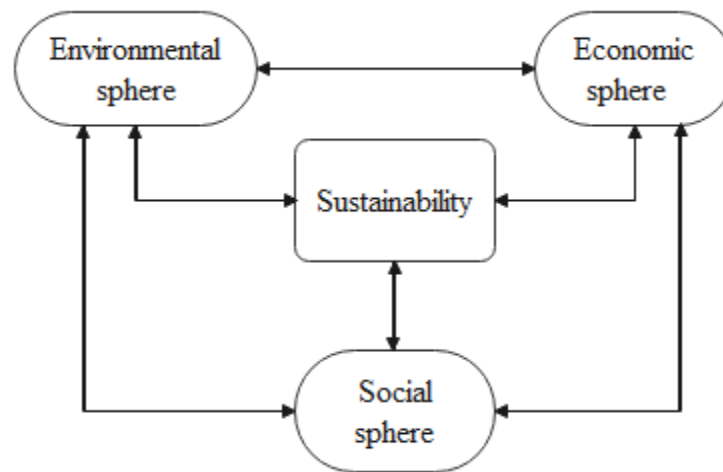
Figure 2.2: The concept of sustainability at the economic, social, and environmental levels from the production of sustainability.

- **Environmental sphere**

Biodegradability, decreased GHG emission, and water management

- **Economic sphere**

Cost-effectiveness, job potential, and beneficial for the rural economy

- **Social sphere**

Public acceptance, industry development, and manpower.

2.9 Measuring the environmental impact of bioplastics

A Life Cycle Assessment (LCA) is a collection of techniques for accumulating and assessing the inputs and outputs of materials and energy, as well as the accompanying environmental impacts, which are directly traceable to the operation of a product or service system during its life cycle. An approach known as life cycle analysis (LCA) can be used to estimate the net environmental impact of bioplastics. LCA quantifies the overall environmental impact of a product by combining input and output data from each phase of the manufacturing process (also known as 'cradle-to-grave'). There is currently no single LCA standard, making it difficult to compare identical products created from various polymers. A publically available specification (PAS) 2050 was recently created to establish a standard LCA methodology for UK products and services (Van der Harst *et al*., 2014). In this study, LCA would look at things like GHG emissions from starch and cellulose extraction, its characterization, bioplastic production, and characterization.

2.10 Wheat production in Ethiopia

Agriculture is the backbone of the Ethiopian economy from earlier to now, and more than 85 % of the national growth domestic product of the country originates from the agricultural sector. Its economy registered a 7.7 % growth in 2017/2018 that was slower than the 10.9 % expansion recorded in 2015/2016. This growth was characterized by a 12.2 % increase in industrial output, an 8.8 % expansion in the service sector, and a 3.5 % growth in agriculture (Shiferaw *et al*., 2019). In Ethiopia wheat is grown in most highlands of the northern, central, and south-eastern parts. This means that wheat can be grown in almost all regions of the country, including pastoral and agro-pastoral areas such as Afar, Gambela, and Somali regions (Leta, S., & Mesele, 2014). There are 4.7 million wheat-growing farmers in our country. Among them, more than three-quarters (78 %) live in Oromia and Amhara regions. Southern Nations, Nationalities, and Peoples' of Ethiopia (SNNP) estimates for 13 % and the Tigray region accounts for only 8 %. In our country, less than 1 % of the wheat farmers live in other regions (Anteneh & Asrat, 2020).

Wheat is one of the important essential food crops in Ethiopia, mainly in urban areas. It is an essential food in the diets of several Ethiopians, providing about 15 percent of the caloric intake in the world, making wheat the second most important food after maize (19 %) and ahead of teff (10 %), sorghum (11 %), and enset (12 %) (Wakeyo, M., & Lanos, 2019). Ethiopia is the second-largest wheat producer in sub-Saharan Africa next to South Africa. Wheat production has significantly increased over the past two decades following several government programs and initiatives implemented to flavor agricultural development and food security in the country. Wheat production in our country increased from around 1.1 million tons in 1995/96 to 3.9 million tons in 2013/14, which is an average annual growth of 7.5 percent. In our country agriculture is dominated by smallholders. In Ethiopia, the year of 2014 close to 5 million wheat farmers engage in wheat production (Gebreselassie *et al*., 2017).

Table 2.1: Trends of wheat in area coverage, production, and yield by different regions of the country between 2016/2017 and 2017/2018

Region	2016/2017 production season			2017/2018 production season		
	Area (000 ha)	Production (000 qt)	Yield (qt/ha)	Area (000 ha)	Production (000 qt)	Yield (qt/ha)
Oromia	898.46	26,640.24	29.65	898.68	26,699.18	29.71
Amhara	554.28	13,190.62	23.80	554.66	14,047.07	25.33
SNNPR	127.21	3,287.59	25.84	127.25	3,391.96	26.66
Tigray	107.72	2,128.67	19.76	107.93	2,140.03	19.83
Benishangulgumz	2.08	-		2.46	59.08	24.06

Source: (Anteneh & Asrat, 2020).

2.11 The flour milling industry in Ethiopia

There are around 300 flour mills in Ethiopia now, with a joint milling capacity of 3.7 million tons per year. The Ethiopia Grain Trade Enterprise (EGTE), which supervises all commercial wheat imports and makes wheat available to flour mills at a government-subsidized rate, can give the flour mills the requisite wheat (CSA, 2017).

Wheat is processed through various sectors and activities in the wheat processing industries (WPI) before reaching final consumers. Wheat processing industries turn wheat into flour and bran, and flour into biscuits, pasta, macaroni, and bread, all of which add value to the product and meet market demand. Wheat processing industries buy domestically or nationally produced wheat at market price from traders and farmers, and imported wheat from the government at a subsidized price. They sell the first one at market price to wholesalers and retailers, and the second one at a discounted fixed price to bakeries. WPI buys about 80 % of raw materials from wholesalers, 10 % from government quota wheat, and 10 % directly from farmers. The result shows that the capacity use of wheat processing industries rises from 41 to 72 % for flour, 42 to 80 % for macaroni and biscuits, and 5 to 19 in numbers because of industrial policy, but till now they have worked below capacity due to inadequate supply of raw material which leads to low supply of wheat products. Exactly, the total capacity was 156 tons per day before the 2010 year. There are only 10 wheat processing industries in Adama town which used about 65 % of their full capacity, Addis Ababa town and around Addis Ababa, Jimma, town, etc. (Habte *et al.*, 2016).

About 50-60 % is wheat bran (furushca) and about 30 % is wheat shorts/middlings (furiskello), and the rest goes as fine flour-like material (fino) and aspiration dust out of the total by-products produced from wheat. Nowadays, the total amount of wheat bran produced in our country is 1,872,368 tonnes (CSA, 2017).

2.12 Classification of bioplastic

The following diagram tries to classify bioplastic productions from different raw materials.

- First agricultural polymers mixed with biodegradable synthetic polymers or used in it are alone.

- Second microbial polymers, made by the fermentation of agricultural products which performances as the substrate. Within this class occurs polyhydroxyalkanoates (PHA) it's most important derivative being polyhydroxybutyrate covalerate (PHBV).

- Third oligomers or monomers that got from the fermentation of agricultural raw materials (substrate) and polymerized via commonly recognized chemical processes. Polylactic acid (PLA) is the greatest recognized material within this class.

- Fourth derivatives from fossil fuel made through synthesis. Polycaprolactone (PCL); polyester amide (PEA); aliphatic co-polyester or polybutylene succinate adipate (PBSA); aromatic co-polyester, such as the polybutylene adipate-co-terephthalate (PBAT) (Babu *et al*., 2013).
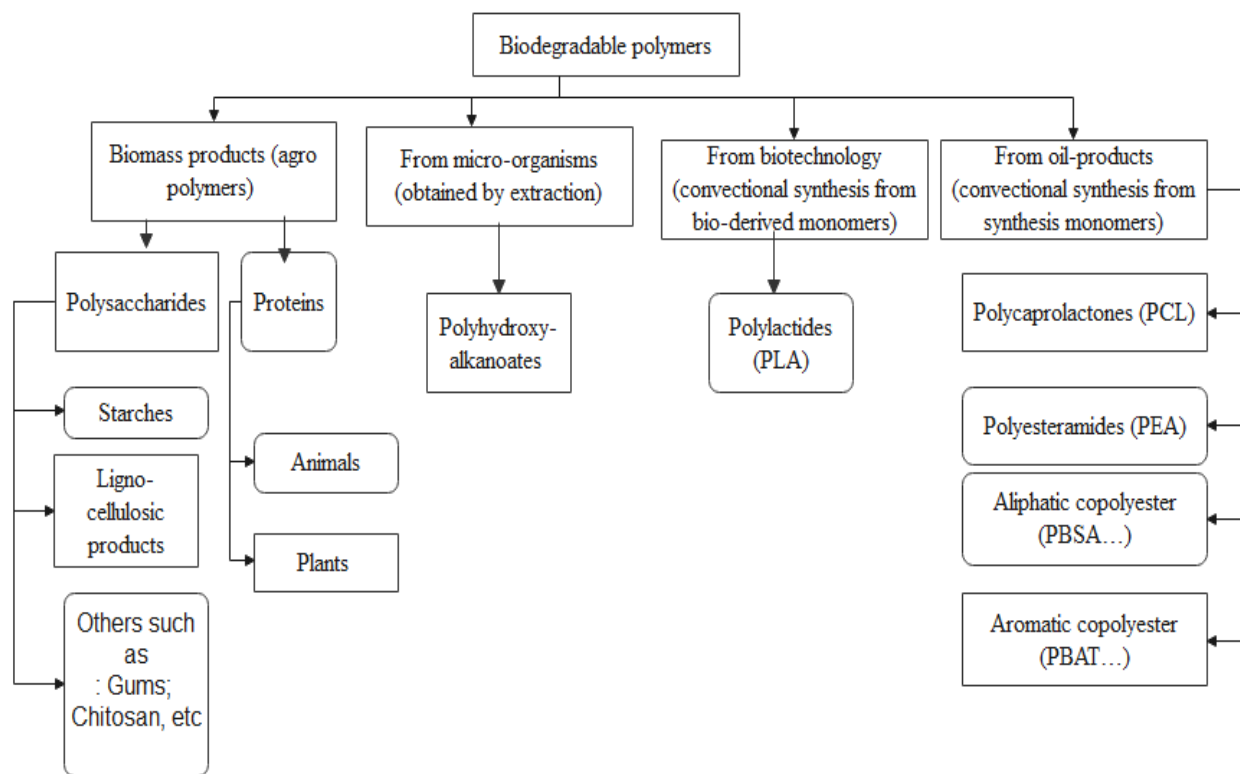
Figure 2.3: Production of biodegradable polymers (Anne, 2011).

2.13 Types of bioplastic

There are several different types of bioplastics which are originated from different classes and different parts of raw materials. One type of bioplastic varies from another by the raw materials it is manufactured from, properties, strength, biodegradability, transparency, etc. Some of the most general types of bioplastics are listed below:

2.13.1 Starch-based plastics

Thermoplastic starch most widely used bioplastic nowadays and constitutes about 50 % of the bioplastics market. Pure starch can absorb humidity and is thus a comfortable material for the manufacture of drug capsules by the pharmaceutical sector. Flexibility and plasticizers like sorbitol and glycerin can correspondingly be added so the starch can also be processed thermo-plastically. The features of the subsequent bioplastic (also called "thermoplastic starch") can be tailored to particular needs by modifying the amounts of these additives (Mehta *et al.*, 2014).

Due to the source of its raw material, starch is low-cost, abundant, and renewable. Starch-based plastics are difficult merges of starch by compostable plastics such as Polylactic acid, Polybutylene Adipate Terephthalate, Polybutylene Succinate, Polycaprolactone, and Polyhydroxyalkanoates.

These difficult merges enhance water-resistance as well as the processing and mechanical properties. Starch-based films most commonly used for packaging purposes are made mainly from starch merged with thermoplastic polyesters to yield biodegradable and compostable products. These films are seen definitely in consumer goods packaging of magazine wrappings and bubble films. For the case of food packaging, this film is used for bakery or fruit and vegetable bags. Composting bags with these films are used in selective collecting of organic waste (Avérous, L., & Pollet, 2014). The main disadvantages behind starch-based polymers exhibit poor mechanical properties and poor moisture stability.

2.13.2 Cellulose-based bioplastics

Cellulose is a glucose polymer with β-1; 4-glucosidic bonds linking the glucose groups (Luchese *et al*., 2018). It is present in the cell walls of all major plants and green algae, as well as in the membranes of most fungi. Cellulosic polymers are made from natural cellulose that has been extracted or chemically modified. Cotton fibers and wood pulp are the most popular sources of cellulosic plastic. The two forms of cellulosic plastics are organic cellulose esters and regenerated polyethylene. Organic cellulose esters are made by esterifying cellulose with organic acids. Currently, about 20 % of total chemical-grade pulp is used in the manufacture of organic cellulose esters (Eric & Luc, 2014). The organic cellulose esters cellulose acetate (CA), cellulose acetate propionate (CAP), and cellulose acetate butyrate (CAB) are the most important in the industry. Packaging film, cigarette filters, textile fabrics, pharmaceuticals, and other specialty industrial applications use organic cellulose esters. Cellulose regenerate is created by dissolving cellulose with chemicals and then re-structuring it into fibers or films (Thielen, 2014).

2.13.3 Polylactic acid-based bioplastics

The most important bioplastics on the market today are polylactic acid (PLA) and polylactide plastics (Pilla, 2011). PLA is a lactic acid-based product made primarily through the microbial fermentation of starch from maize, cassava, potato, sugarcane, and sugar beet. These PLA bioplastics should solve the problems that have been found in starch substituted bioplastics. The plant starch is first converted into lactic acid in this process. Microorganisms convert the monomer to lactic acid, which is then chemically treated to link the molecules into long chains or polymers. This PLA looks like it has the appearance of traditional petrochemical plastics and is completely biodegradable. PLA plastics are primarily used in food packaging due to their properties that are

similar to polyethylene and polypropylene. Furthermore the production of PLA plastic saves two-thirds of the energy needed for the production of fossil-fuel-based plastics. The PLA plastics also emit almost 70 percent fewer greenhouse gases than conventional plastics during the degradation in a landfill. PLA and PLA blends are currently available in the granulated form in a variety of grades for use in the production of the film, molded pieces, beverage containers, cups, bottles, and other everyday products (Andreas Künkel, 2016). PLA-based plastics are now being used in a variety of areas, including medical, clothing, cosmetic, and household applications. Furthermore, the car industry uses PLA-based plastics to make dashboards, door tread plates, and other parts (Mohanty *et al.*, 2003). The major advantages of PLA plastics are high level of rigidity, stability, transparency, thermoplasticity, and superior performance in existing equipment of the conventional plastics manufacturing industry. Disadvantages of PLA based films are, low melting point makes PLA film unsuitable for high temperature applications. PLA may even show signs of getting soft or deforming on a hot summer day. PLA has a higher permeability than other plastics. Moisture and oxygen will go through it more easily than other plastics (Andreas Künkel, 2016).

2.14 Structure and properties of starch

Starch is a polymeric carbohydrate consisting of a large number of glucose units linked by the presence in human diets and it is available in stable foods (Rajam & Parthasarathi, 2020). Starch is mainly available in nature. Starch is primarily found in plants such as corn, potatoes, and wheat. Plants, wood, corn, potatoes, and wheat are all raw materials that are renewable, biodegradable, and easily available (Bastioli, 2000). Starch is white, tasteless carbohydrate food substance that is made up of hundreds or thousands of D-glucose molecules. It does not dissolve in cold water, while at higher temperatures (e.g. heating it with extra water under pressure) starch granules collapse, and an opalescent colloid solution is obtained (gelatinization). The gelatinization temperature of the starch is affected by plant genetic and environmental factors (Hadisoewignyo, 2018). Starch contains two types of anhydroglucose polymers amylose and amylopectin. Amylose is a linear polymer in which anhydrousglucose units are abundantly connected through α-D-(l, 4) glycosidic bonds. Amylopectin is a branched polymer, containing finite branches joined with the backbones through α-D-(l, 6) glycosidic bonds. The content of amylose and amylopectin in starch is mainly depends on the starch source (Gadhave *et al.*, 2018).
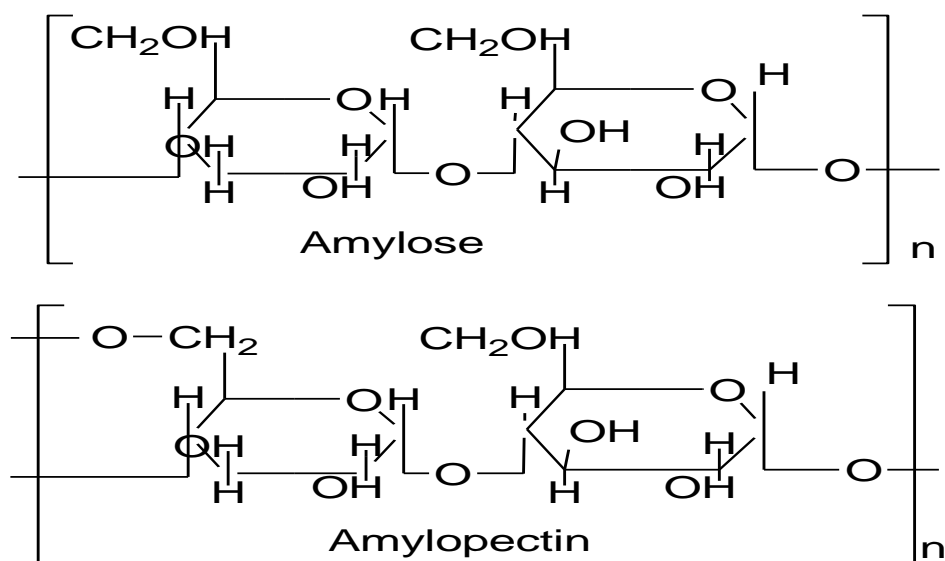
Figure 2.4: Chemical formula for starch (Lubis & Harahap, 2018).

Starch is one of the main building blocks of wheat bran. Wheat bran is a by-product from the milling process in the manufacture of refined grains and has an approximated yearly production of ∼100 – 150 million tons per year worldwide (Hell *et al*., 2014). Bran is the most outer layer of wheat grains and it contains the tissues known as aleurone, hyaline, testa, and pericarp (Prinsen *et al*., 2014). The main consistency components in the wheat bran tissues are starch (25 – 39 %) and non-starch polysaccharides including dietary fibers (40 – 47 % of which 52 – 70 % is arabinoxylan, 20 – 24 % is cellulose and ∼6 % is ß-glucan), lignin (6 – 12 %), proteins (10 – 25 %), lipids (2 – 4 %), and minerals (3 – 8 %). The outer bran layer, the pericarp, is made up of mainly insoluble dietary fibers and lignin (Apprich *et al*., 2014). In blend with other fillers, chemically improved starch from wheat bran could create constituents for biodegradable packaging materials. Starch can be used to reduce the carbon footprint of traditional resins because they can replace petroleum-based polymers with natural ones. It is also highly degradable, meaning it can be used alongside a compostable polymer without interfering with the degradation process.

2.15 Review on bioplastic production from different biomass sources

Previously different biomass sources was used to synthesis biodegradable films. A different source of starch with different fillers was also done. The technique to synthesis bioplastics at lab scale is solution cast method; which is whereby the film-forming solution is spread on a level surface and then dried to produce films (Altemimi, 2018).

2.15.1 Biodegradable plastic production from corn starch

Bioplastics were produced using a mixture of glycerol, cornstarch, vinegar, and food color (Keziah *et al*, 2018). Corn starch-based antimicrobial packaging film reinforces with plumbago zeylanica (Amira) root crude extract was done. The methanol extract of plumbago zeylanica root was used as antimicrobial agents (Muche, 2018). Bioplastics were produced from corn starch by incorporating the cellulose obtained from sugarcane bagasse. The maximum and minimum value of tensile strength (26.81 and 11.55 MPa), water absorption (39.02 % and 20.45 %) and elongation at break (25.99 % and 4.32 %) was obtained respectively. This was done by considering two factors dry oven temperature (30-500 °C) and fiber amount (5-15 w/w) (Mosisa, 2017). Starch films were prepared from starch extracted from cassava, corn, potato, and yam with and without plasticizers to evaluate the effects of the type and quantity of plasticizer on the mechanical properties of the starch films (Adeyefa, 2015).

2.15.2 Biodegradable plastic production from potato starch

For potatoes starch, which is one of the best polysaccharides, highlighting the importance of the amylose/amylopectin ratio during production and leading to improved strength and lowered strain (Priedniece *et al*., 2017). Thermoplastic Starch film was prepared from sweet potato blend with polyvinyl alcohol (PVA), at varying compositions by gelatinizing and plasticizing it with water and glycerol, the melting and glass transition temperatures of the TPS increased from 146 °C to 167 °C and 50.8 °C to 71.8 °C respectively, with the addition of PVA (Offiong & Ayodele, 2016). The potato-based bioplastic sheet was obtained the highest tensile strength percentage (4.87 Mpa) followed by a cassava-based bioplastic sheet (4.5 Mpa) and a corn-based bioplastic sheet (3.59 Mpa) (Al *et al*., 2016).

2.15.3 Biodegradable plastic production from Banana peel

Tensile strength of approximately 0.443 Mpa (0.22mm thick), 1.098 Mpa (0.15mm thick) and 1.596 Mpa (0.37 mm thick) were observed for banana peels treated with $Na_2S_2O_5$, untreated banana peel plus agar and banana peel treated with $Na_2S_2O_5$ + sorbitol composites (Mukhopadhyay *et al*., 2017). Antimicrobial packaging film also manufactured from banana peel starch via ginger oil (Zerihun *et al*., 2016).

2.15.4 Bioplastics production from cottonseed

Cotton-seed protein bioplastics from cottonseed flour were successfully prepared by hot-press molding in the presence of urea, aldehydes, and glycerol (Yue *et al*., 2014). A novel class of environmentally friendly protein-based bioplastics cottonseed protein plastic sheets (CP-sheets) was prepared by compression molding in the presence of cottonseed flour as the main raw material, aldehydes as crosslink agent and glycerol as plasticizer (Yue *et al*., 2014).

2.15.5 Bioplastics production from Cassava Starch

The objective of this study was done to production of bioplastics from cassava peel starch plasticized using sorbitol with a variation of 20; 25; 30% (wt/v of sorbitol to starch) reinforced with microcrystalline cellulose (MCC) with a range of 0 to 6 % (wt/wt of MCC to starch). The results showed improvement in tensile strength with higher MCC content up to 9.12 Mpa compared to non-reinforced bioplastics (Wahyuningtiyas & Suryanto, 2018). Bioplastic component of cassava starch, glycerol as plasticizer and nanoclay as reinforcement were also investigated, The results show that the addition of nanoclay into bioplastic results increasing the tensile strength of bioplastic also increases from 5.2 MPa to 6.3 Mpa (Wahyuningtiyas & Suryanto, 2018). Production of Biodegradable Plastic Packaging Film from Cassava Starch were also investigated, obtained result was a biodegradability of 41.27 % compared to 10.33 % and 85.99 % for polythene and paper respectively, the film also has a tensile strength of 24.87 N/mm^2 compared to 10.86 N/mm^2 and 8.29N/mm^2 for polythene and paper (Ezeoha & Ezenwanne, 2013). Mechanical properties of bioplastics cassava starch film with Zinc Oxide nanofillers as reinforcement was done, the result showed that the Tensile strength (TS) was improved significantly with the addition of zinc oxide but the elongation at break (EB %) of the composites was decreased. The maximum tensile strength obtained was 22.30 N/mm on the addition of zinc oxide by 0.6% and plasticizer by 25% (Harunsyah *et al*., 2017).

2.15.6 Bioplastics production from chitosan

Bioplastics production from starch and chitosan blends shows that the glycerin has an important role at the flexibility of the film, the acetic acid influences on the consistency, elasticity and shape, and the chitosan influences on the stiffness and thickness (Catálise *et al*., 2017). Bioplastic from chitosan and yellow pumpkin starch with castor oil as a plasticizer, the characterization of the optimum tensile strength test was obtained on the 40/60 composition of 6.787 ± 0.274 Mpa and

the fastest biodegradation test process within 5-10 days occurred in the 50/50 composition. The more chitosan content the higher the value of the tensile strength test obtained, while the fastest biodegradation rate occurred in the composition of yellow pumpkin starch and chitosan balanced 50:50 (Sarinigsh *et al*., 2018).

2.16 Chemical composition of wheat straw

Wheat straw is a by-product of agriculture that is mostly made up of cellulose, hemicellulose, and lignin. Nodes, internodes, and leaves are the basic components of WS. Chemical analysis of WS is high in carbohydrates (cellulose, hemicellulose, and lignin), proteins, minerals (calcium and phosphorus), silica, acid detergent fibers, and ash. WS is particularly high in bioactive substances and vitamins. However, the actual macro and micronutrient content can vary depending on cultivar, plant growth stage, kind of soil and fertilizer used, and climatic circumstances. The physical content demonstrated that different parts of the wheat plant, such as internodes (68.5 %), leaf sheath (20.3 %), leaf blade (5.5 %), nodes and fines (4.2 %), and grains and debris (1.5 %), have different mass percentages of WS components (Khan & Mubeen, 2017).

Table 2.2: Chemical composition of wheat straw.

Components by Percentage (%)					Reference
Cellulose	Hemicellu lose	Lignin	Ash	Extractives soluble in alcohol – acetone	
33.7 to 40	21 to 26	1 1 to 22.9	7 to 9.9	Not stated	(Khan & Mubeen, 2017)
49.78	Not stated	19.64	5.28	4.93	(Kasmani & Samariha, 2011)

Table 2.3: Chemical composition of different Sources on a dry basis

Particulars	Wheat straw	rice husk	bagasse	banana fiber	garlic straw
Cellulose	48.8	45.0	55.2	63-64	41
Hemicellulose	35.4	19.0	16.8	10	18
Lignin	17.1	19.5	25.3	5	6.3

Source**:** (Rajinipriya *et al*., 2018).

2.17 Alkali treatment of fiber

The significant adjustment done by alkaline treatment is the distraction of hydrogen bonding in the network structure, thus increasing surface roughness resulting in enhanced mechanical interlocking and the amount of cellulose exposed on the fiber surface. The addition of aqueous sodium hydroxide (NaOH) to natural fiber helps to ionize the hydroxyl group to the alkoxide. This raises the number of possible reaction sites and permits improved fiber wetting. The possible reaction happened for the fiber and NaOH which is represented as shown below (Ebisike *et al.*, 2013).

The following reaction takes place as a result of alkali treatment.

$$\text{Fiber - OH} + \text{NaOH} \rightarrow \text{Fiber - O}^-\text{Na}^+ + \text{H}_2\text{O} \qquad\qquad 2.1$$

2.18 Glycerol as a Plasticizer

Plasticizers are colorless and odorless esters, primarily phthalates, that increase a material's elasticity (V, Koester, 2015). Starch-based polymers are known for having poor mechanical properties and are notoriously brittle, necessitating the use of a plasticizer. Plasticizers' primary function is to increase polymer chain mobility by reducing intermolecular forces, which helps to increase flexibility and lower the glass transition temperature of plasticized starch materials, according to (A, Edhirej, *et al.*, 2016). Plasticizers are tiny chemicals that mix and insert into and between polymer chains, disrupting hydrogen bonding and spreading the chains apart, increasing flexibility while also increasing water vapor and gas permeability. Plasticizers improve the required mechanical qualities of bioplastic film, such as glycerol, sorbitol, and polyethylene glycol (PEG) are the most often used plasticizers in starch-based films. It's needed to combat film brittleness while also preventing chipping and breaking during future handling and storage according to (P, Jantrawut *et al.*, 2017).

Plasticizers are useful in the manufacturing of bioplastics because they increase flexibility and workability, but they also reduce hardness, as indicated by (S, Maulida, *et al.*, 2016). When a high concentration of plasticizer is used, the mechanical strength, barrier properties, and rigidity are decreased. Plasticizers that are added to film formulations decrease the film density and increase the free volume of the film matrix which, in turn, increases the permeability of the films to gases and vapors. For example, glycerol molecules interfere with starch packing, thus decreasing intermolecular attraction and increasing polymer mobility (Kuorwel et al., 2011).

Glycerol is a waste product from the biodiesel production process that has a lot of potential for usage in a variety of applications (Uliana, 2019). In commercial products, glycerol is utilized to change the properties of the film materials. Glycerol goes between the polymer chains and prevents them from forming a crystalline structure by preventing them from lining up in rows. The film becomes brittle and stiff when it crystallizes. Glycerol is a tiny molecule that gets between the polymer chains and helps them slide over one other easily, giving the film become like plastic. G lycerol lowers intermolecular interactions between starch chains, allowing film chains to move m ore freely (Gail *et al*., 2016). Table 2.4 is the physical parameters of glycerol and starch.

Table 2.4: Physical properties of starch and glycerol.

Material	Starch	Glycerol
Chemical formula	$(C_6H_{10}O_5)n$	$C_3H_8O_3$
Molecular mass (g/mol)	Variable	92.10
Melting point (°C)	Decomposes	18
Boiling point (°C)	-	290
Density (g/cm³)	1.5	1.26

Source: (Mohsen *et al*., 2017).

Glycerol $(C_3H_8O_3)$
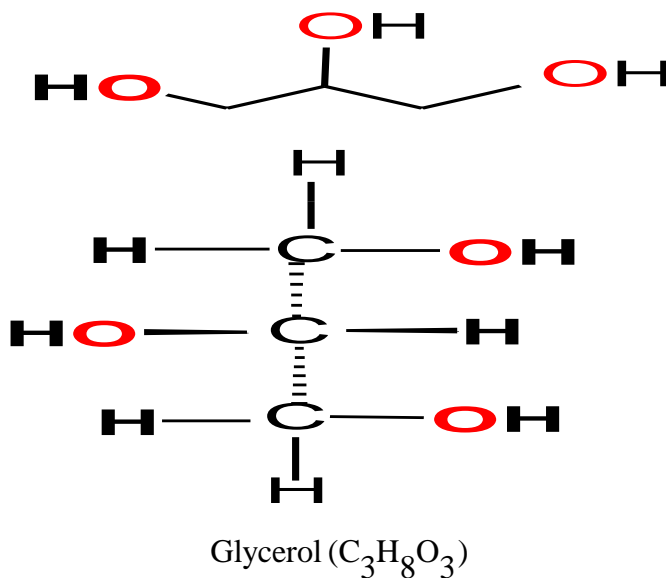
Figure 2.5: Molecular structure of glycerol

2.19 Bioplastic film production techniques

There are three most common techniques of bioplastic production (Wittaya, 2012). Those are casting extrusion and electro-hydrodynamic automatization.

1) Casting is a technique in which setting hot solutions on a surface upon cooling and drying a solution or a gel. It's a simple method for making bioplastic films with consistent thickness.

2) Extrusion, also known as the thermal pressing process, is a method for producing objects with a definite cross-sectional profile. In this instance, the material is pushed or dragged through a die of the desired cross-section. Because the material only experiences compressive and shear pressures, it is used to manufacture extremely complicated cross-sections and brittle work materials. It also produces finished products with a high-quality surface finish.

3) Electrostatic atomization is a type of electro-hydrodynamic atomization. Electro-hydrodynamic atomization is known as electrostatic atomization or electro-spraying. This is a technique in which a liquid is forced with the help of a capillary and a potential difference of the order of kilovolts has happened between the capillary and the collection electrode. In general, the solution casting technique was selected due to its effectiveness, low cost, and simplicity to conduct at the lab scale.

2.20 Bioplastic film preparation by method of casting

The bioplastic films were prepared by the solution casting method adapted from the method described by (Maulida, 2018). A film-forming dispersion was prepared by mixing the starch and distilled water. The dispersion is stirred by hand on the shaker water bath for purpose of gelatinization. Then, the different concentration of glycerol were mixed on a dry weight basis of starch for purpose of plasticity. The various concentration of cellulose fiber was added to starch to improve physio-chemical properties. Each mixture was stirred for homogeneity and to make the gelatin very strong and then allowed to cool at room temperature before being cast on a Petri dishes. Film-forming solutions were transferred into casting in Petri-dishes. Then Petri-dishes were placed in an oven at a given temperature until to dry. Then, the Petri dishes were removed from the oven and the films were peeled off, and then it was stored at room temperature in a polyethylene bag for further analysis. The most important factors for production of bioplastic films are oven drying temperature, the concentration of glycerol, and the concentration of fiber on a starch basis were studied.

2.21 Characterization of bio-plastic developed from natural resource

2.21.1 Mechanical Property

Mechanical properties of bioplastics offer an indication of the mechanical act of the materials. The tensile properties are usually measured, assessed, and used throughout the industry. Tensile testing contains tensile strength, modulus of elasticity, and elongation at break (Orezzoli *et al*., 2018). The increased mass of fiber content, tensile strength for bioplastics film increases. The addition of fiber concentration on gelatinized starch films resulted in intermolecular hydrogen bonding to the group which cause molecular bonds between amylose to be more condensed. Whereas the addition of plasticizers like glycerol would decrease the tensile strength of the film. The high tensile strength values can be recognized as the number of hydrogen bonds between the starch chains that contribute to cohesiveness and low flexibility. The elongation at break value reduced with the accumulation of fiber content. Meanwhile, the addition of plasticizers to bioplastics has the opposite effect (Maulida, 2018).

2.21.2 Water absorption properties

TPS has a low water resistance, which is a major disadvantage in many practical applications. In reality, TPS can absorb a significant amount of water from the surrounding environment, resulting in a significant reduction in mechanical qualities. Water absorption was reduced in the presence of cellulose fibers. This is mostly due to the presence of cellulose fibers, which are less hydrophilic than starch and can absorb a portion of glycerol with a decrease in TPS hydrophilic characteristics (Curvelo *et al*., 2011). Furthermore, the presence of less hydrophilic cellulose fibers reduced TPS water absorption, possibly due to the constraint exerted by the fibers at the interface on matrix swelling (Wattanakornsiri *et al.*, 2012). Furthermore, amylopectin-rich TPS is more water-absorbent than amylose-rich TPS (Curvelo *et al*., 2011).

2.21.3 X-ray diffraction (XRD)

 X-ray diffraction (XRD) techniques can be used to evaluate polymer recrystallization (crystalline or amorphous as well as semi-crystalline structure). The peaks of crystalline formations can be observed using the XRD technique. The creation of a new peak can also be used to detect recryst allization. The mechanical characteristics of TPS can be affected by changes in crystallinity and moisture content during storage. Increased crystallinity increases tensile strength and modulus of elasticity in films while lowering elongation at break. When a film is stored at a relative humidity

(RH) of less than 75 %, the moisture content rises and the film becomes highly pliable (Suppakul *et al*., 2013).

Polymers come in a variety of shapes and sizes, including highly crystalline, semi-crystalline, and amorphous, and all three can be found in a single polymer sample. The presence and relative quantity of these forms are determined by how the polymer was created and processed, and this has been shown to affect mechanical qualities like compression, tensile strength, buckling, and creep. As a result, the degree of crystallinity is a critical quality to precisely assess.

2.21.4 Functional groups

Fourier transform infrared spectroscopy (FT-IR) is a strong technique for recognizing different types of chemical bonds in polymer composites in a molecule by producing an infrared absorption spectrum that looks like a molecular fingerprint. (Wattanakornsiri *et al*., 2012) studied the FT-IR spectra of green composites, which revealed typical polysaccharide patterns. Non-reinforced TPS and green composites having 4 and 8 % wt/wt of fibers to the matrix are characterized. C-O stretching of the C-O-C group in the anhydroglucose ring and the C-O-H group is responsible for the peaks in the ranges of 1,026 - 1,027 and 1,079 - 1,155 cm^{-1}, respectively. Wave numbers between 1,414 and 1,454 cm^{-1} are intended for O-H bonding (Prachayawarakorn *et al*., 2011). The bound water contained in non-reinforced TPS and composites causes peak positions in the region of 1,638 - 1,639 cm^{-1}. The C-H stretching is connected with the 2,931 cm^{-1} bands. Furthermore, bands related to the complicated vibrational stretching associated with free, inter, and intramolecular bound hydroxyl groups exist in the range of 3,414 - 3,420 cm^{-1} for hydrogen bonded hydroxyl (O-H) groups (Galicia-Garcia, 2011).

The presence of cellulose fibers caused the bands to shift to lower wavenumbers, indicating an increase in intermolecular hydrogen bonding. When polymers are compatible, a unique interaction, such as hydrogen bonding or dipolar interaction, occurs between the chains of TPS matrix and cellulose fibers, resulting in alterations in FT-IR spectra on composites, such as band shifts and widening (Prachayawarakorn *et al*., 2011).

In general, wheat bran starch and wheat straw fiber were chosen to produce innovative natural bioplastic films in this study. The goal of this study was to use cellulose fibers as a thermoplastic matrix reinforcing ingredient. Following cellulose fiber isolation, biodegradable fiber reinforced thermoplastic composites were prepared, and their tensile strength, elongation at break, and water

absorption were assessed. The developed outcome was compared to that of a controlled film. Fourier transform infrared spectroscopy was used to study the relationship between the structure and properties of the bioplastic films.

2.21.5 Thermogravimetric analysis

Thermogravimetric analysis is a method for investigating the reaction of thermal decomposition between weight change and temperature, which is lost as a result of the material's temperature influence. The result of the thermal study is a thermogram curve. It mainly studies materials' thermal stability. Thermal decomposition is the transformation of a sample's shape into a simpler form, which is impacted by a variety of parameters including temperature, heating rate, pressure, moisture, residence time, particle size, and material composition (Slopiecka *et al.*, 2012). The weight of the polymer changes as a result of thermal breakdown. The term "thermal decomposition of the polymer" refers to an increase in temperature that has or has not experienced any chemical changes, and it is also used to identify various chemical mechanisms that are involved in underlying structural changes, polymer morphology effect, additive reaction path, and filler interaction (Kelly *et al.,* 2018).

The mechanism of the thermal decomposition of wheat straw fiber reinforced wheat bran starch-based bioplastic film has the following stages. Stage 1 is the reduction of weight caused by the release of moisture or water until 16.5 % weight loss occurred at 20 - 270 °C. Stage 2 is the process of releasing maximum removal of volatile matter that occurred due to a high level of weight loss 65 % at 270 - 402 °C. Stage 3 is the stage after the release of volatile matter in the samples occurred at the temperature of 402 - 450 °C with low (constant) weight loss. This process does not produce ash, since it has been fully decomposed in the thermal decomposition process.

3 MATERIALS AND METHODS

3.1 Experimental location

The experimental work was carried out at the school of chemical engineering, environmental engineering, and material science and engineering laboratories at Jimma Institute of Technology, Ethiopian Conformity Assessment Enterprise (ECAE), and Adama science and technology university (ASTU).

3.2 Materials

3.2.1   Raw materials and chemicals

In this research, the wheat straw (Triticum aestivum) was collected from Dawro zone Zaba Gazo woreda Gazo koysha Kebele and wheat bran from Jimma city wheat flour factory using plastic bags and used as raw materials. Chemical and reagents used in this study includes analytical grade glycerol (98.5 %) was used as a plasticizer for film production, ethanol (97 %) used as a dewaxing agent and for solubility determination, sodium hydroxide (99.8 %) for treatment of fiber, hydrogen peroxide (35 %) for bleaching agent, hydrochloric acid (36.46 %) for pH adjustment, iodine, acetic acid and amylose for determination of amylose content, potassium bromide as pellets for FTIR test. Solutions preparations were carried out using deionized and distilled water.

3.3 Methods

3.3.1   Proximate analysis of raw materials

3.3.1.1 Proximate analysis of wheat bran

i. Determination of moisture content: Moisture contents in the wheat bran were determined by following the oven drying method proposed according to (Abdul *et al*., 2019). It was carried out under a temperature of 105 ºC for $2\frac{1}{2}$ hours. The percentage of moisture was calculated using the following formula:

$$\text{Moisture content} = \frac{M_1 - M_2}{M_1} * 100\%$$

3.1

Where M_1 - is the initial mass of the sample (g) and M_2 - is the final mass of the sample (g)

ii. Determination of ash content: Ash content of the wheat bran was assessed by following the ignition method by muffle furnace suggested by described by (Abdul *et al*., 2019). 2 g of wheat

bran was placed in crucible and ignition at temperature 550 °C for $2\frac{1}{2}$ hours to obtain complete ash. The total ash content of the sample was determined by the following formula:

$$\text{Ash content} = \frac{M_1 - M_0}{M_2 - M_0} * 100\%$$

3.2

Where M_1- is the mass of ash + crucible (g), M_2 - the mass straw sample + crucible (g), and

M_0 - is the weight of the empty crucible (g)

iii. Volatile matter: The volatile matter of sample was determined by according to the methods defined in European Standard EN15148-2009. The 3 g of wheat bran were heated in a crucible at 650 °C for 10 min and allowed to cool down in a desiccator. Then, the volatile matter was calculated by using the following equation:

$$\text{Volatile matter} = \frac{M_1 - M_2}{M_1} * 100\%$$

3.3

Where M_1- is the initial mass of the sample (g) and M_2- is the final mass of the sample (g)

iv. Fixed carbon: The fixed carbon content of wheat straw is calculated by subtracting the volatile matter and the ash from the 100 following the (ASTM method D3172-07a). The fixed carbon is defined as the residue left after removing the volatile matter and the ash from the substance.

$$\text{Fixed carbon} = 100 - (\%\text{ ash content} + \%\text{ volatile matter})$$

3.4

3.3.1.2 Proximate analysis of wheat straw

i. Moisture content: The purpose of this analysis was to determine the moisture content of the wheat straw was performed by using oven drying methods. It was carried out under a temperature of 105 °C for 3 hours following the ASTM E871 – 82 (2013) standards. Moisture was calculated using the following equation:

$$\text{Moisture content} = \frac{M_1 - M_2}{M_1} * 100\%$$

3.5

Where M_1 – is the initial mass of the sample (g) and M_2 - is the final mass of the sample (g)

ii. Ash content: The ash content of wheat straw was performed method described by ASTM D 1102 – 82 (2013). In a muffle furnace, 3 g of straw was placed in a pre-weighed crucible and burnt at 550 °C for 2 hours to obtain ash. The crucible was then placed in desiccators to cool the product, and then estimated by the following equation:

$$\text{Ash content} = \frac{M_1 - M_2}{M_0} *100\%$$

3.6

Where M_1 – is the mass of crucible with wheat bran sample (g), M_2 – is the mass of crucible with ash sample (g), and M_0 – is the mass of bran (g)

iii. Volatile matter: The volatile matter of wheat straw was determined by the method used according to ASTM E872 – 82 (2013). 3 g of wheat straw samples were burned in a crucible at 600 °C for 8 minutes and permitted to cool down in a desiccator. Based on a dry basis the volatile matter content was calculated by using the following equation:

$$\text{Volatile matter} = \frac{M_1 - M_2}{M_1} *100\%$$

3.7

Where M_1 - is the initial mass of the sample (g) and M_2 - is the final mass of the sample (g)

iv. Fixed carbon: The fixed carbon content of wheat straw is calculated by subtracting the volatile matter and the ash from the 100 following the ASTM D 1102 - 84 (2013). The fixed carbon is defined as the residue left after removing the volatile matter and the ash from the substance.

$$\text{Fixed carbon} = 100 - \left(\%\ \text{ash content} + \%\ \text{volatile matter}\right)$$

3.8

3.3.2 Extraction of Starch from wheat bran

The extraction of starch from wheat bran was conducted according to the methodology proposed by (Hadisoewignyo, 2018) with some modifications. In this method, 100 g of the wheat brain was soaked with 500 ml ethanol (97 %) at room temperature for 10 hrs. Then, the treated wheat bran with liquid residue was ground in a laboratory blender. The ground slurry was filtered through 150 µm then 75 μm nylon cloth where it was left and washed thoroughly with 150 ml distilled water. Then, the solution was subjected to centrifugation at 4000 rpm for 10 minutes. The sediment was remained by removing and discarding the upper dark brown mucilage layer with a spatula. Then added 150 ml of NaOH and stirred with a magnetic stirrer with agitating speed of 5 minutes for 1

hr and centrifuge as above. Sediment was separated and added 75 ml of distilled water, stirred for 10 min, and neutralized by adding 0.75 M HCl and centrifuged as above. Thereafter, 50 ml of distilled water, stirred for 30 min, and centrifuge as above, and eventually oven-dried for 6 hrs, and the starch was extracted. Then the starch in dried form was triturated with the help of a motor pestle to obtain the starch in powder.
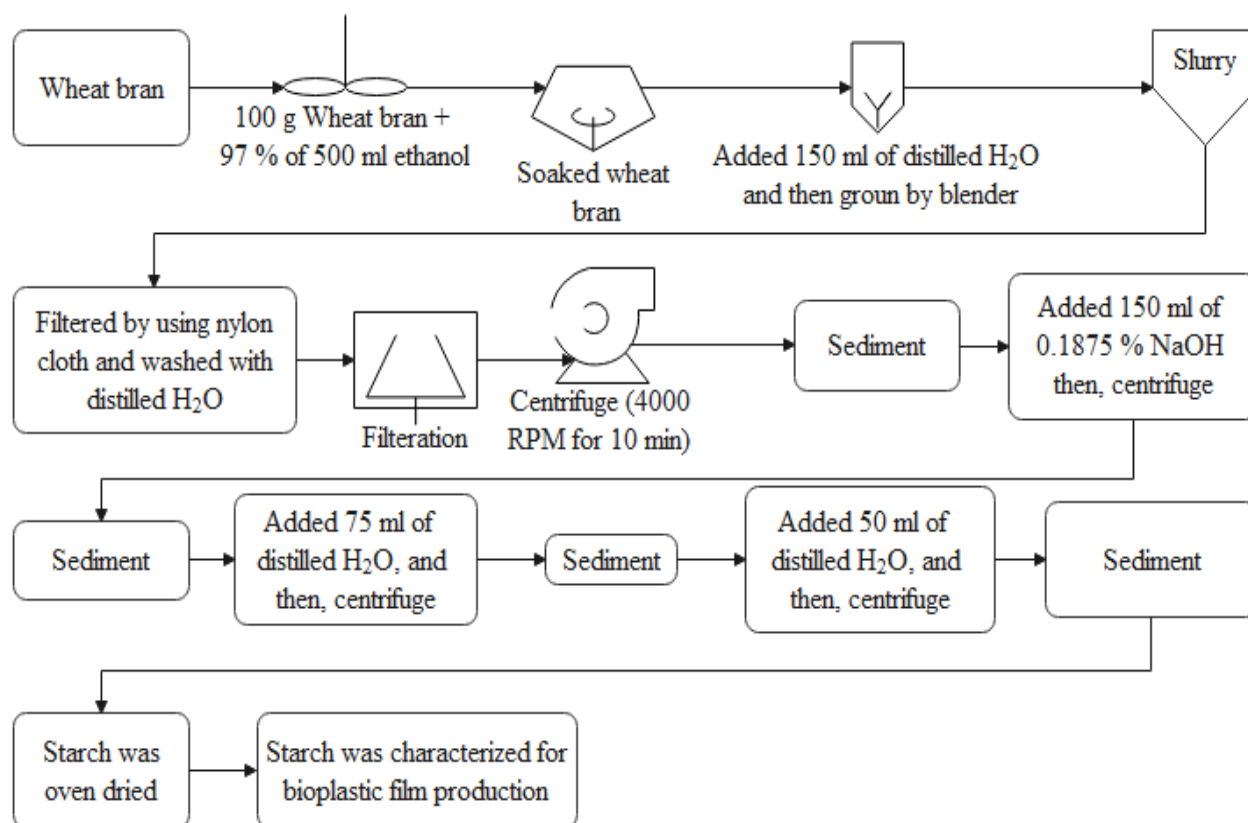
Figure 3.1: Flow chart for isolation and purification of wheat bran starch.

Figure 3.2: A. wheat bran, B. ethanol dewaxed wheat bran, and C. pH value of starch.

3.3.3 Characterization of wheat bran starch

a. The presence of starch: One gram of starch powder was transferred to the test tube and 4 drops of iodine solution were added to it then, any color change was noted (Zaini, 2012).

b. PH value determination: The pH of the starch slurry was investigated based on the method of (Magu, 2017). Three grams of starch was mixed with 15 ml of CO_2-free distilled water and is mixed carefully for 15 min. The pH value was subsequently measured using a pH meter.

c. Solubility of Starch: The solubility of the starch was tested in water and ethanol at 30 ^oC. The 0.5 g of extracted starch was added to 10 ml of each solvent and stirred for 10 minutes. The solubility was observed as the solute gradually mixed with the solvent (Yehuala *et al.*, 2013).

d. Moisture content determination: Two grams of starch were placed into a crucible and inserted in an oven at a temperature of 105 ^oC and dried for 24 hours to constant weight. Moisture content in the dried starch was determined by keeping the measured amount of sample in a thermostat-controlled oven at 105 ^oC for 24 hours. The dry weight of each sample was taken on a weighing balance (Oladayo *et al*., 2016). The percentage of the moisture content and dry matter was then calculated by the formula as presented below:

$$\text{Moisture content}\,(\%) = \frac{M_1 - M_2}{M_1} * 100\,\%$$

3.9

Where M_1 - initial weight of the sample (g) and M_2 - final weight of the sample (g)

e. Determination of ash content: The sample was heated at a temperature of 550 ^oC for 5 hrs as such that the organic compound and its derivatives were damaged and vaporized, producing mineral elements and the organic compound according to (Hadisoewignyo, 2018). The ash content was calculated using the following formula:

$$\text{Ash content}\,(\%) = \frac{M_1 - M_2}{M_0} * 100\,\%$$

3.10

Where M_1 - mass of crucible and ash sample (g), M_0 - mass of starch (g) and M_2 - mass of crucible (g)

f. Determination of amylose content: 50 mg of amylose was dispersed into 1 ml of 97 % ethanol, and 9 ml of 1M NaOH was added to the solution. The solution was positioned in a boiling water bath for 10 min with frequent shaking to obtain a clear solution and then cooled it for a few

minutes; then the entire volume was adjusted to 100 mL using distilled water to obtain the standard stock solution. Then, added different volume of acetic acid (0.25, 0.50, 0.75, 1.00 and 1.25 ml), iodine solution of 1.25 ml and amylose stock solution (1, 2, 3, 4 and 5 ml) in a concentrated amylose. This solution was mixed and placed at room temperature for 30 min, after which it was scanned using a spectrophotometer at the 620 nm wavelengths. Finally, draw absorbance versus amylose concentration curve. For the determination of amylose content, 0.125 g of wheat bran starch was dispersed into 1 ml of 97 % ethanol, and 9 ml of 1 M NaOH was added to the solution. The solution was positioned in a boiling water bath for 10 min with frequent shaking to obtain a clear solution and then cool. Next transferred 5 ml of starch solution into measuring flask and added 50 ml of distilled water, 2 ml of iodine solution, and distilled water to make the final solution 100 ml, after which it was scanned using a spectrophotometer at 620 nm wavelengths (Ma & Deng, 2017). By relating the amylose standard calibration curve and absorbance of the starch solution shown in (appendix G), the maximum value of the amylose that is found in wheat bran starch was determined using the following formula.

$$\text{Amylose content} (\%) = 105.25 * \text{absorbance} - 0.1555 \qquad \qquad 3.11$$

$$\text{Amylopectin content} (\%) = 100 - \text{amylose content} (\%) \qquad \qquad 3.12$$

g. The yield of wheat bran starch: The yield of wheat bran starch was calculated by dividing the mass of extracted starch to mass of wheat bran used for extraction of starch times 100 %.

$$\text{Yield of starch} (\%) = \frac{\text{Mass of extracted starch}}{\text{Mass of wheat bran used}} * 100 \% \qquad \qquad 3.13$$

3.3.3.1 X-ray diffraction (XRD) analysis of wheat bran starch

The crystalline structure of starches of the starch samples was obtained using a diffractometer (XDS 2000, Scintag Inc, CA) with copper K-alpha emission radiation. The X-ray source was operated at 25 mA and 30 kV. Two theta scans with an angular range from 5° to 45° at a scan speed of 0.02 deg/min (Hadisoewignyo, 2018). The crystallinity (%) was calculated by the following equation:

$$\text{Crystallinity} (\%) = \frac{A_c}{A_c + A_a} * 100 \% \qquad \qquad 3.14$$

Where A_c - is the crystalline area on the X-ray diffractogram and A_a - is the amorphous area.

3.3.3.2 Fourier Transform Infrared (FTIR) analysis of the wheat bran starch

FTIR spectra were recorded using a Perkin-Elmer Spectrum Frontier FT-IR/NIR (Perkin-Elmer Corp. Norwalk, CT). The sample holder was used a potassium bromide powder in appropriate ratios to make a pellet for FT-IR spectroscopy analysis. These measurements were executed and the spectra were collected in the range of (4000 - 500 cm^{-1}) according to (Ascheri *et al*., 2010).

3.3.4 Extraction of cellulose from wheat straw

According to the method of (M. S *et al*., 2013), the wheat straw was washed, sun-dried, milled by scissors. Then it was dewaxed using ethanol (0.1 % w/v, biomass/ethanol; 1:10 g/mL) for 4 hours. Then the treated wheat straw sample was carefully washed with too much water to discard unwanted particles and oven-dried to remove moisture content. At first, Alkaline Hydrogen Peroxide (AHP) solution preparation was taking place. AHP Solution was prepared by mixing 1 % alkaline solution (1 %; $NaOH/H_2O$; 1 g/100 mL) into 20 % hydrogen peroxide solution (20 %; H_2O_2/H_2O; 33.36 g/166.7 mL). 10 g of dewaxed wheat straw was dispersed in a 120 mL solution of alkaline hydrogen peroxide in a stainless steel autoclave at 121 °C for 30 minutes. After a certain time, the residue, DWSAHP (white color), was washed thoroughly with distilled water till it became free from chemicals and attained neutral PH. The residue was then filtered by using filter paper and then dried by an oven at 75 °C and size reduced by mortar and pestle for bioplastic production.

```
                                        ┌──────────┐
                                        │ Ethanol  │
                                        └────┬─────┘
                                             │
                                             ▼
┌──────────┐   ┌────────────────────┐   ┌────────────┐   ┌─────────────────┐
│  Wheat   │──▶│ Washed with        │──▶│ Immersed   │──▶│ Washed with     │
│  straw   │   │ distilled H₂O, cut │   │ into       │   │ distilled H₂O   │
│          │   │ into small pieces  │   │ ethanol    │   │ and oven dried  │
│          │   │ and dried          │   │            │   │                 │
└──────────┘   └────────────────────┘   └────────────┘   └─────────────────┘
                                                                   │
┌──────────┐   ┌────────────────────┐   ┌────────────┐   ┌─────────────────┐
│Disperssed│◀──│ Washed with        │◀──│ Filtered by│◀──│ Product was     │
│into AHP  │   │ distilled H₂O until│   │ filter     │   │ oven dried      │
│solution  │   │ it became neutral  │   │ paper      │   │                 │
└──────────┘   └────────────────────┘   └────────────┘   └─────────────────┘
     │
┌──────────┐   ┌────────────────────┐
│Cellulose │──▶│ Product            │
│was ground│   │ characterization   │
│mortal    │   │                    │
│with pestle│  │                    │
└──────────┘   └────────────────────┘
```
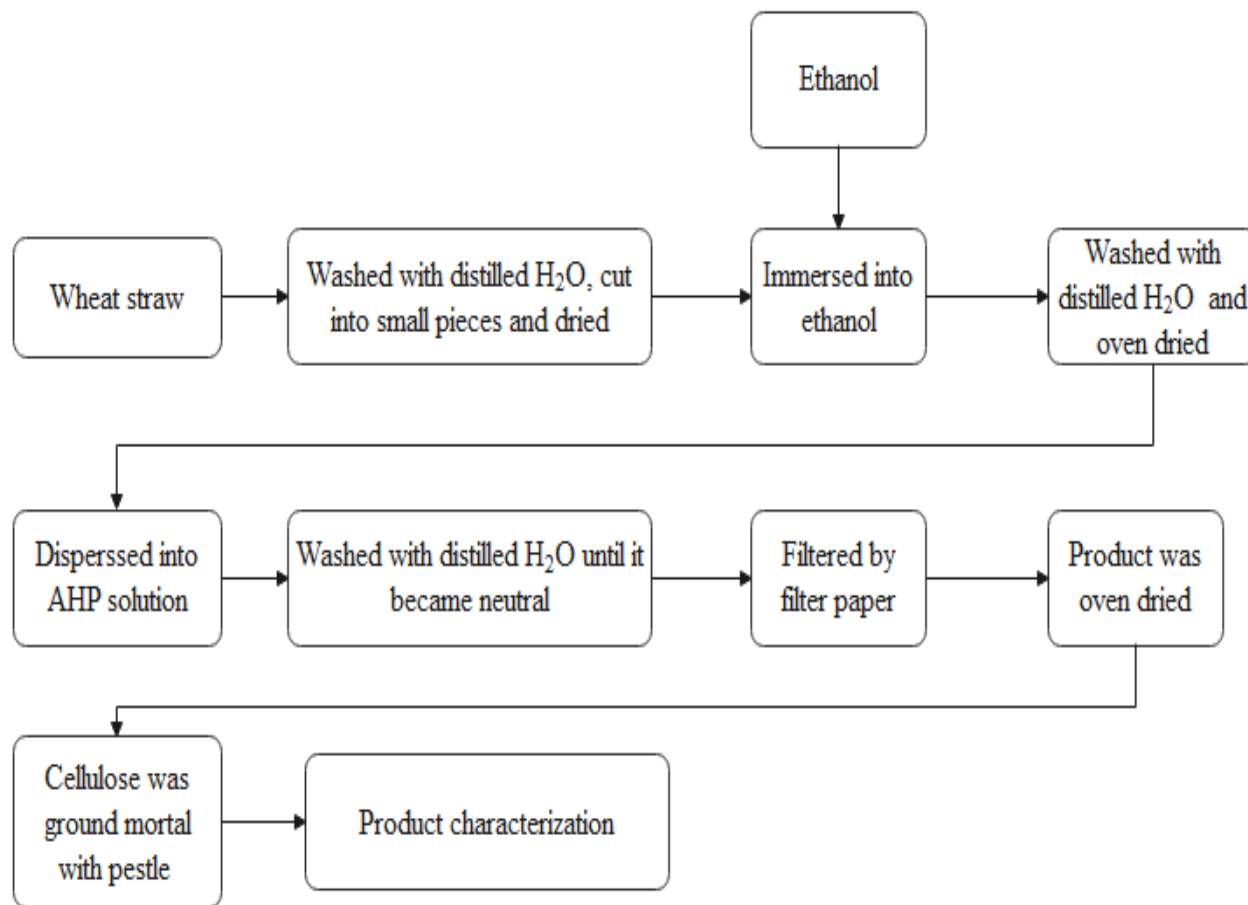
Figure 3.3: Flow chart for extraction of cellulose through Alkaline Hydrogen Peroxide (AHP) Treatment.

Figure 3.4: A. WS sample and B. washed and size reduced WS

3.3.5 Characterization of wheat straw cellulose

a. Moisture Content: The fiber moisture content was determined by the difference between the mass of fiber before dried and after dried. The process was done by drying the wet fiber it becomes constant weight, the reduction in the fiber weight can be calculated in the following formula (Ebisike *et al.*, 2013).

$$\text{Moisture content}\,(\%) = \frac{M_1 - M_2}{M_1} * 100\,\%$$

3.15

Where M_1 - initial mass of sample (g) and M_2 - final mass of sample (g)

b. Water Absorption of wheat straw cellulose: A water absorption test was done by soaking the dried fiber with water for 24 hours and at the end, the soaked fiber was measured. After immersion, the surplus water on the surface of the fiber was removed by using a filter cloth and the final weight of the samples was then taken. The water absorption of the fiber was calculated by the following equation according to (Ebisike *et al.*, 2013).

$$\text{Fiber water absorption}\,(\%) = \frac{M_1 - M_2}{M_2} * 100\,\%$$

3.16

Where M_1 - water soaked mass of sample (g) and M_2 - filtered mass of sample (g)

c. The density of extracted wheat straw cellulose: The density of extracted fiber was calculated using the Archimedes method (Amiri, 2017). The mass of extracted fiber was measured and immersed in a measured volume of the water. Again volume of fiber can be calculated by the volume difference of water after immersion and before immersion of the fiber. And density was calculated with a mass over volume formula.

$$\text{Density} = \frac{\text{Mass (g)}}{\text{Volume (ml)}}$$

3.17

d. Cellulose Content: The cellulose content of wheat straw fiber was determined based on the method proposed by (Yussuf *et al.*, 2010). Cellulose in wheat straw fiber has been used for further processing; it is enough to know cellulose content and non-cellulose content. The cellulose content of raw wheat straw fiber was analyzed by soaking the 1g of fiber in a 10 ml of 0.3 M sodium hydroxide solution for 1 hour at a temperature of 90 °C. After the process, the soluble components were removed, and the fiber was washed in distilled water until it reached a neutral state, then

dried. By using gravimetric analysis to calculate the cellulose and non-cellulose content of raw fiber before and after soaking, the cellulose content of the fiber was calculated.

$$Cellulose\,(\%) = \frac{M_1 - M_2}{M_1} * 100\,\%$$

3.18

Where M_1 - Mass of the sample before soaking (g) and M_2 - Mass of the sample after soaking (g)

e. The yield of wheat straw cellulose: The yield of fiber present in the wheat straw was calculated by dividing the mass of extracted cellulosic fiber by the mass of wheat straw used for extraction of fiber times 100 %.

$$Yield\,of\,fiber\,(\%) = \frac{Mass\,of\,extracted\,fiber}{Mass\,of\,wheat\,straw\,\,used} * 100\,\%$$

3.19

3.3.5.1 X-ray diffractometer (XRD) analysis of wheat straw fiber

An X-ray diffractometer was used to evaluate the phase behavior of raw and treated wheat straw. Instrument conditions were set at 1.540˚ A wavelength (CuKα radiation), with a scan speed of 2deg/sec and a 2θ range of 5–80° (Qasim *et al.*, 2020).

3.3.5.2 Fourier Transform Infrared (FTIR) analysis of wheat straw fiber

FTIR spectra were recorded using a Perkin-Elmer Spectrum Frontier FT-IR/NIR (Perkin-Elmer Corp. Norwalk, CT) equipped with a deuterated triglycine sulfate (DTGS). By using potassium bromide background spectrum for identification. Then the FTIR spectrum was permitted to pass through the prepared sample and the spectrum responses were recorded. Finally, the peak plot of wavenumber (4000 - 400 cm^{-1}) versus Transmittance (%) was plotted using origin software to identify the functional groups.

3.3.5.3 Thermogravimetric analysis (TGA) for wheat straw fiber

The TGA is used to measure the thermal stability of the produced wheat straw fiber and was performed on the Shimadzu TGA Q500 equipment under nitrogen atmosphere, the flow rate of 60 mL/min, a heating rate of 10 °C/min, and temperature range of 30 to 500 °C.

3.3.6   Bioplastic film preparation from wheat bran starch and wheat straw fiber

The bioplastic films were prepared by the solution casting method adapted from the method described by (Maulida, 2018). A film-forming dispersion was prepared by mixing the 5 g starch extracted from wheat bran and 100 ml of distilled water. The dispersion is stirred by hand on the

shaker water bath set at 75 °C for 15 minutes while stirring at the same rate till it becomes gelatinized. The 30 %, 35 %, and 40 % of glycerol were mixed on a dry weight basis of starch. The concentration of cellulose fiber was added to starch by 5 %, 10 %, and 15 % based on a starch weight basis of the gelatinized suspension. Each mixture was stirred for homogeneity and to make the gelatin very strong and then allowed to cool at room temperature before being cast on a Petri dishes. Film-forming solutions (40 mL) were transferred into casting in Petri-dishes having 10 cm diameter. Then Petri-dishes were placed in an oven at temperature of about 35 °C, 45 °C, and 55 °C until dry. Subsequently, the Petri-dishes were removed from the oven and the films were peeled off, and then it was stored at room temperature in a polyethylene bag for characterization.

i) Measuring cylinder: For liquid measurement   viii) Water bath: For heating starch solution
ii) Distilled H_2O ix) volumetric flask: For holding for gelatinized solution
iii) Sample holder: For solute sample   x) Gelatinized solution
iv) Balance: For measuring each starch and cellulose   xi) cooler: For cooling down solution
v) volumetric flask: For holding starch solution   xii) Petri-dish: used for casting gelatinized solution
vi) Starch solution   xiii) Oven: for product drying
vii) Stirrer: For mixing solution uniformly   xiv) End product (bioplastic)

Figure 3.5: Experimental setup for bioplastic production.
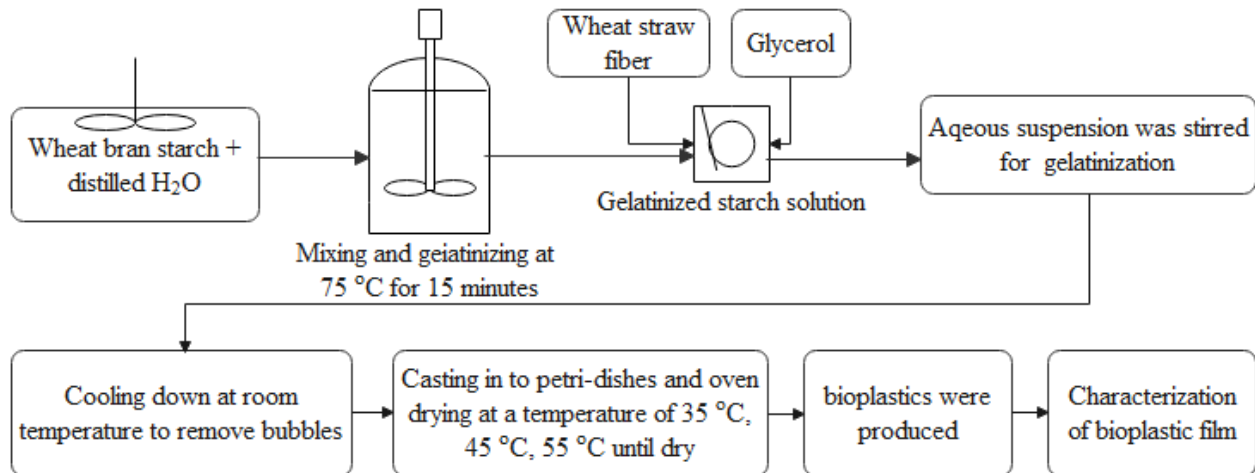
Figure 3.6: The block flow diagram for production of bioplastic from wheat bran starch and wheat straw cellulose fiber.

3.3.7 Characterization of produced bioplastic film

Mechanical properties of produced bioplastic film include tensile strength and elongation at break, water absorption, thickness, solubility, transparency, moisture content, and density, and biodegra dability for the synthesized plastic film, and characterize the best film by using FTIR, XRD, and TGA test was analyzed.

a. Water solubility: The film's solubility in water was determined according to the method reported by (Yehuala *et al.*, 2013). Disks of the film were cut into 2 x 2 cm and measured as the mass of M_1 and immersed in a beaker containing 50 ml of distilled water. After 24 hours of immersion at 25 °C with a slow agitation, the pieces of the sample were taken out and dried to the constant mass of M_2 in an air circulated oven set at a specified temperature for 24 hours.

$$\text{Water solubility} = \frac{M_1 - M_2}{M_1} * 100\,\%$$

3.20

Where M_1 - initial mass of the sample (g), and M_2 - final mass of the sample (g)

b. Moisture content: The film was prepared with a size of 2 x 2 cm and oven dried 24 hrs at 90 °C. Film moisture content was obtained by the following equation according (Khazaei *et al.*, 2014).

$$\text{Moisture content}\,(\%) = \frac{M_1 - M_2}{M_1} * 100\,\%$$

3.21

Where M_1 - final mass (g) and M_2 - initial mass (g)

c. Density (D): It was obtained by dividing the mass (M) per unit volume (V) of the produced plastic sample. The mass of the produced bioplastic film was measured using an analytical balance. The film was prepared with a size of 2 x 2 cm and weighted (g) before immersing it in distilled water. The measuring cylinder was filled with 30 ml of distilled water kept for 4 hrs. The amount of liquid displaced after immersing film into the liquid was recorded as (V) was operated to calculate the film density (ρ).

$$Density = \frac{Mass\,(g)}{Volume\,(ml)}$$
3.22

d. Transparency of produced bioplastics: The transparencies of the films were measured by using a spectrophotometer (UV 7804C). The transmittance of films was measured at 620 nm as described by (Yehuala *et al.*, 2013). The film samples were cut into rectangles and made as a solution form, then put into the internal side of the spectrophotometer cell.

$$Transparency\,(\%\,T) = \frac{-\log T620\,nm}{x}$$
3.23

Where T600 = is the transmittance at 620nm and X is the film thickness (mm).

e. Thickness of Film: The film thickness was measured using digital micrometers and measurement was made in at least, three random locations: two at edge regions and one within the central area. Three separate measurements were recorded according to (Naela *et al.*, 2021).

$$Average\,thickness = \frac{point_1 + point_2 + point_3}{3}$$
3.24

f. Tensile strength: Tensile strength can define as the strength of a produced bioplastic film in terms of force per unit area of cross-section whereas applying force in a linear direction.

$$Tensile\,strength\,at\,yield\,(Mpa) = \frac{Force\,(N)}{Area\,(mm)} * 100$$
3.25

g. Elongation at break: It can be defined as in terms of increase in length divided by the original length.

$$\%\,Elongation\,at\,break = \frac{increase\,in\,length\,(mm)}{original\,length\,(mm)}$$
3.26

h. Water absorption: Water uptake was investigated by cutting bioplastic film into 2 x 2 and then weighing the mass. The film was placed into a container full of distilled water for 24 hours. After

water immersion, the film was removed from the water and weighed to measure the wet weight according to (Ebisike *et al.*, 2013). Water uptake was calculated as follows.

$$\text{Water absorption}\,(\%) = \frac{M_2 - M_1}{M_1} * 100\,\%$$

3.27

Where M_1 - wet mass after immersing into water (g) and M_2 - dried mass (g)

i. Biodegradability: Bioplastic biodegradability was measured using a soil burial degradation test, in which bioplastics were buried in the soil and destroyed its mass after some time (Ardiansyah, 2011). Degradation testing is used to detect the extent to which bioplastics have been damaged. Bioplastics were cut into 2 x 2 cm^2. Then, they were buried into the ground at 8-cm depth; the burial duration varied (4, 8, 12, and 16 days). Before burial, the initial mass of degradation was determined. The final mass of degradation of the bioplastics was measured afterward. Any changes in mechanical properties due to the degradation process were observed and when the bioplastics were completely degraded, the biodegradability was measured (Wahyuningtiyas, N. E., & Suryanto, H. 2017).

$$M\,(\%) = \frac{M_1 - M_2}{M_1} * 100\,\%$$

3.28

Where M_1 - is the weight of the bioplastic sample before being buried in soil (g), M_2 - is the weight of bioplastic sample after buried in soil (g) and M (%) is the weight loss.

3.3.7.1 X-ray diffraction (XRD) analysis of bioplastic film

An X-Ray Diffractometer (Drawell XRD 7000) measurement was described by Bergo and Sobral (2007). XRD was used to measure the crystalline and amorphous characteristics of the film. Each sample was cut into 2 x 2 cm^2 and mounted onto a glass slide before placement in the diffractometer chamber for measurement. The diffracted intensity of CuKα radiation ($\lambda = 1.54$Å) was noted between 5° and 80° at 40 kV and 30 mA.

3.3.7.2 Fourier Transform Infrared (FTIR) analysis of the bioplastic film

The FTIR is used to identify the functional groups (chemical bonds) of produced bioplastic film. FTIR spectra were recorded using a Perkin-Elmer Spectrum Frontier FT-IR/NIR (Perkin-Elmer Corp. Norwalk, CT. By using potassium bromide background spectrum for identification. Then the FTIR spectrum was permitted to pass through the prepared sample and the spectrum responses

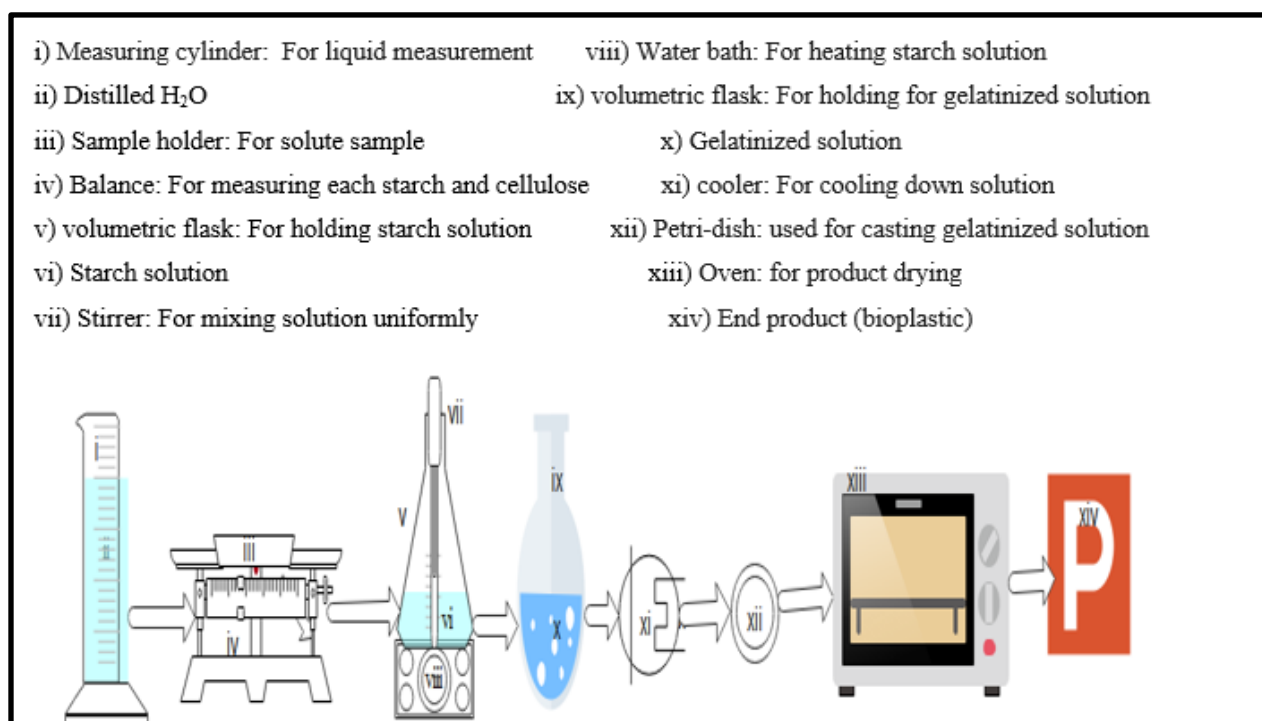were recorded. Finally, the peak plot of wavenumber (4000 - 400 cm⁻¹) versus Transmittance (%) was plotted using origin software.

3.3.7.3 Thermogravimetric analysis (TGA) of bioplastic film

The TGA is used to measure the thermal stability of the produced bioplastic film and was performed on the Shimadzu TGA-50 equipment under nitrogen atmosphere, a flow rate of 50 mL/min, a heating rate of 20 °C/min, and temperature range of 20 to 450 °C.

3.4 Experimental design and statistical analysis

The experimental design is used to optimize the process parameters of the bioplastic production and at the same time to generate a mathematical model by considering the individual and interactive effects of the process parameters. Analysis of experimental data was carried out by using Design Expert version 11 software (Stat-Ease Inc., Minneapolis, USA). In this study, optimization was considered to determine optimum conditions that can give the best bioplastic film production from the performed experiments using central composite design (CCD). To determine the optimum conditions for bioplastic production using three independent process variables were investigated; oven drying temperature (28 – 62 °C), concentration of glycerol (26.6 - 43.4 %), concentration of fiber (1.6 - 18.4 %) and the variables range was selected based on (Nanang Eko *et al*, 2019). The optimization of the bioplastic production was carried out using a five-level three-factor central composite design, requiring a total of 20 experimental runs including 8 factorial points, 6 axial points and 6 points at the center.

$$2^k + 2k + k_c = 2^3 + 2*3 + 6 = 20 \qquad\qquad 3.29$$

Where k is the number of independent parameters and k_c is the number of center points.

While the dependent variables (response variables) such as tensile strength, elongation at break, and water absorption of the bioplastic film were investigated. Each response was used to develop an empirical model that correlated the response to the three independent process variables using a second-degree polynomial equation.

$$Y = \beta_O + \sum_{i=1}^{k} \beta_i x_i + \sum_{i=1}^{k} \beta_{ii} x_i^2 + \sum_{i=1}^{k} \sum_{j=i+1}^{k} \beta_{ij} x_i x_j \qquad\qquad 3.30$$

Where Y_i is the predicted response, β_o the offset term, β_i the linear effect, β_{ii} the square effect, and β_{ij} is the interaction effect. It is a polynomial regression model in one variable and is called

the second-order model or quadratic model. The following second-order polynomial models were used analogically to describe the relationship between the three independent variables and the three response variables:

$$TS = a_0 + a_1A + a_2B + a_3C + a_{12}AB + a_{13}AC + a_{23}BC + a_{11}A^2 + a_{22}B^2 + a_{33}C^2 \qquad 3.31$$

$$EA = b_0 + b_1A + b_2B + b_3C + b_{12}AB + b_{13}AC + b_{23}BC + b_{11}A^2 + b_{22}B^2 + b_{33}C^2 \qquad 3.32$$

$$WA = c_0 + c_1A + c_2B + c_3C + c_{12}AB + c_{13}AC + c_{23}BC + c_{11}A^2 + c_{22}B^2 + c_{33}C^2 \qquad 3.33$$

Where TS, EA and WA are the predicted response which indicates tensile strength, elongation and water absorption respectively; a_o, b_o and c_o are an intercepts; [a_1, a_2 , a_3] , [b_1, b_2 , b_3] and[c_1, c_2 , c_3] were the estimated linear effects; [a_{11}, a_{22} , a_{33}], [b_{11}, b_{22} , b_{33}] and [c_{11}, c_{22} , c_{33}] were quadratic effects; and [a_{12}, a_{13}, a_{23}], [b_{12}, b_{13}, b_{23}] and [c_{12}, c_{13} , c_{23}] were interaction effects of independent variables which were ''A'' (oven drying temperature), ''B''(concentration of glycerol) and ''C'' (concentration of fiber) .

The general formula for experimental design for three factors with three levels

Table 3.1: The experimental ranges and levels of the independent variables

Independent variables	Factor coding	Units	Coded levels				
			$-\alpha$	-1	0	1	α
Oven drying temperature	A	ºC	28	35	45	55	62
Concentration of glycerol	B	%	26.6	30	35	40	43.4
Concentration of fiber	C	%	1.6	5	10	15	18.4

4   RESULTS AND DISCUSSIONS

4.1 Proximate Analysis of Raw Materials

4.1.1   Proximate analysis of wheat bran

i. Moisture Content: Two samples of wheat straw were employed to determine the moisture content, and two different values were collected. The moisture content of the sample was then determined using equation (3.1), yielding a mean value of 12.3 %. As a result, the moisture content of wheat bran is close to (14.14 $\pm$ 0.65 %) (Abdul *et al*., 2019).

ii. Ash Content: The ash content of the two samples was determined using the standard method indicated in equation (3.2), and the results were recorded. This experiment yielded a mean ash content of 11.3 %, which is slightly lower than the result (18.02$\pm$ 4.18 %) stated by (Abdul *et al*., 2019). The high ash content may lead to reduced purity and quality of starch.

iii. Volatile Matter: Two samples of wheat bran were engaged to measure the moisture content, and two different data were recorded according to the procedure outlined in equation (3.3). The average value of volatile matter obtained was found to be 65.5 %.

iv. Fixed Carbon: According to equation (3.4) fixed carbon content was calculated, and the value of the two samples was noticed as 10.9 %.

4.1.2   Proximate analysis of wheat straw

i. Moisture Content: To determine the moisture content of the wheat straw two samples were used and two different data were recorded. Then, the moisture content for the sample was calculated according to equation (3.5) and the mean value was found to be 7.54 %. Different authors reported that the moisture content of the wheat straw from different regions on a dry basis ranged from (5.58 - 11.1 %) (Montero *et al*., 2016).

ii. Ash Content: The ash content was determined according to the standard method described in equation (3.6) and the values of the two samples were recorded. Then, the ash content for the sample was calculated and the mean value was found to be 6.67 %. As different literature shows, the ash content of wheat straw from different region ranges between (4.57-17.04 %), which is in the normal range with literature (Montero *et al*., 2016). The high ash content may lead to reduced purity of cellulose yield.

iii. Volatile Matter: Two samples of wheat straw were utilized to measure the moisture content, and two distinct data were recorded according to the procedure outlined in equation (3.7). The volatile matter determined with an average value of 76.5 %. The volatile matter of wheat straw has been recorded in several locations with values ranging from (68.23 - 84.04 %) by different authors. Wheat straw, with high volatile content, shows its reactivity.

iv. Fixed Carbon: According to equation (3.8) fixed carbon content was calculated, and the mean value of the two samples was recorded as 16.83 %. The reported values for fixed carbon in wheat straw from diverse locations range from (11.38 - 18.2 %).

Table 4.1: Proximate analysis of wheat straw from different regions.

Moisture content (%)	Fixed carbon (%)	Volatile matter (%)	Ash content (%)	Region	Reference
7.70	18.20	76.00	5.30	Spain	(García *R, et al*., 2014)
6.00	11.38	84.04	4.57	UK	(Chufo *et al.,* 2015)
5.58	14.72	68.23	17.04	Mexico	(Montero *et al*., 2016)
7.54	16.83	76.5	6.67	Ethiopia	This study

4.2 Characterization of starch extracted from wheat bran

a. The presence of starch: Wheat bran starch with bluish violet color was observed, which shows the presence of iodine in starch. The bluish violet color indicates the linkage between amylopectin bonded with iodine as reported by (Hadisoewignyo, 2018).

b. PH determination: The pH of the starch obtained was found to be 6.78, therefore, the result was acceptable ranges of (4 - 7) reported by (Alcázar *et al*., 2015).

c. Solubility of starch: The result analysis that starch was quickly soluble in ethanol because alcohols have a high power to break the bond between starches.

d. Moisture content: The moisture content of wheat bran starch in this study was found to be 12.5 %. The obtained result was comparable with 14 % as reported by (Oladayo *et al*., 2016) and 12 % according to the African Organization for Standardization of cassava starch. The higher the moisture content, the lower the number of dry solids in the starch. Higher values of moisture in starch cause caking of the starch affects its texture and encourage the growth of microorganisms which cause odors and off-flavor (Oladayo *et al*., 2016).

e. Ash content: The ash content obtained in this study was found to be 0.75 %. As different literature shows that the ash content of the starch was falls below 1 %. The results was acceptable range with those reported by (Alcázar *et al*., 2015) and (Hadisoewignyo, 2018). Low ash content indicates high quality and purity of starch yields.

f. Amylose Determination: A standard amylose calibration curve, as shown in the mathematical tool that gives a set of reference points against which an unknown sample concentration can be evaluated. The curve can also be used to find the concentration of the sample once all other numbers related to techniques like linear regression, the correlation coefficient (R^2) have been determined, the curve can also be used to determine the concentration of a sample that was unknown. It was calibrated using spectrophotometry that the absorbance of the sample at 620 nm wavelength was obtained 0.235 and the unknown sample concentration (using the slope and the intercept from the standard calibration equation) was also determined which is within the range of the standard absorbance and it implies that the unknown solution certainly contains amylose which was a found to be 24.6 % and amylopectin 75.4 % based on the calibration curve in the (appendi x G) and from equation (3.11 and 3.12) in materials and methods section. The amylose content was 24.6 %, which was greater than previous estimates those published by (Hadisoewingyo, 201 8) for maize starches (16.9 - 21.3 %), but significantly lower than those reported by (Chavan *et a l*., 2010) for horse gram starches (34.00 - 36.30 %).

The amount of amylose and amylopectin in starch affects mechanical properties of the starch. Be cause there are fewer branching structures in high amylose starch than in high amylopectin starch, it has higher stiffness and hardness (Tanetrungroj *et al.,* 2015).

g. Starch yield: In the this study, the yield of starch was 18.25 %, which was ranged with previous work of (6.08 - 19.47) (Hadisoewignyo, 2018)

.

Table 4.2: The result of wheat bran starch and comparisons with other starches

Types of test	Form	Color	Odor	Taste	pH	Moisture content (%)	Ash content (%)	Amylose (%)	References
	Powder	White	Odorless	Tasteless	4 - 7	<20	<1	(17-25)	(Alcázar *et al*., 2015)
	Powder	Brownish white	Odorless	Tasteless	6.15 ±0.35	6.06±0.83	0.98±0.27	39.57 ±1.65	(Hadisoewignyo, 2018)
	Powder	Bluish violet	Odorless	Tasteless	6.78	12.2	0.75	24.6	This study

4.2.1   X-ray diffraction (XRD) of wheat bran starch

X-ray diffraction is a technique used to determine whether a material is crystalline or amorphous. In this study, the main peaks for wheat bran starch were observed at $2\theta = 5.39°$, $12.86°$, $20.21°$, and $25.34°$ shown in Figure 4.1. A broad peak with low intensity is observed between $18.6°$ and $21.2°$. Results reported were approachable with (Munoz *et al*., 2015) for four natural starches, wheat, potato, cassava and corn. They have found a broad XRD signal between $15°$ and $23°$ with peaks at $18.3°$ and $21.5°$. XRD studies was comparable with results reported by (Kaur and Singh, 2016) for wheat and barley starch. The slight difference between this study and the previous one is due to the ratio amylose and amylopectin. As a result, the crystallinity (degree of crystallization) of wheat bran starch was calculated to be 32.5 %. As different journalists described the starch from wheat bran obtained in this work had a good crystallinity and in acceptable range with literature.
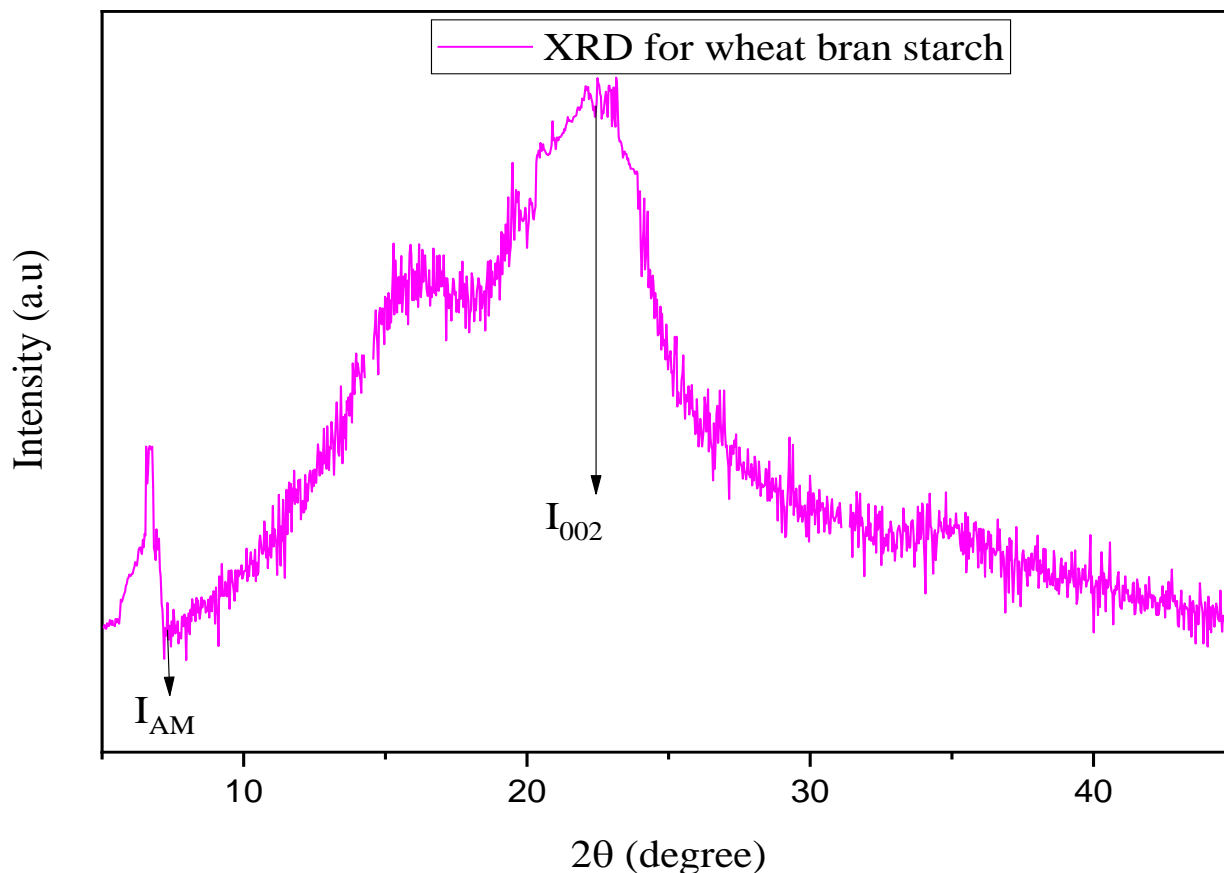
Figure 4.1: XRD patterns for the wheat bran starch.

4.2.2 Infrared spectra of wheat (FTIR) analysis of wheat bran starch

Functional groups and surface structure were characterized by Fourier transform infrared spectroscopy. The result from the FT-IR spectrum showed that there were different functional groups present on the surface of the wheat bran starch as shown in Figure 4.2. The broad spectrum peaks in the band of 3670 cm^{-1} were attributed to the –OH functional groups. The absorption wave number at 2934 and 1726 cm^{-1} indicates to the C-H and the C=O stretching vibrations functional group respectively, which were similar to those reported by (Nakason *et al*, 2010) . The 1436 - 500 cm^{-1} regions can be divided into two sub-regions. The peak between 1436 and 1313 cm^{-1}, which corresponds to the normal modes of C-H in-plane bend, and another between 1313 and 500 cm^{-1}, which corresponds to the normal modes of C-O and C-C stretch in a D glucose ring. As a result of the connection of C-C and C-O stretches, they are a vibrational network in which all atoms in a macromolecule's chain vibrate in phase and normal modes (Zhang *et al*., 2009).
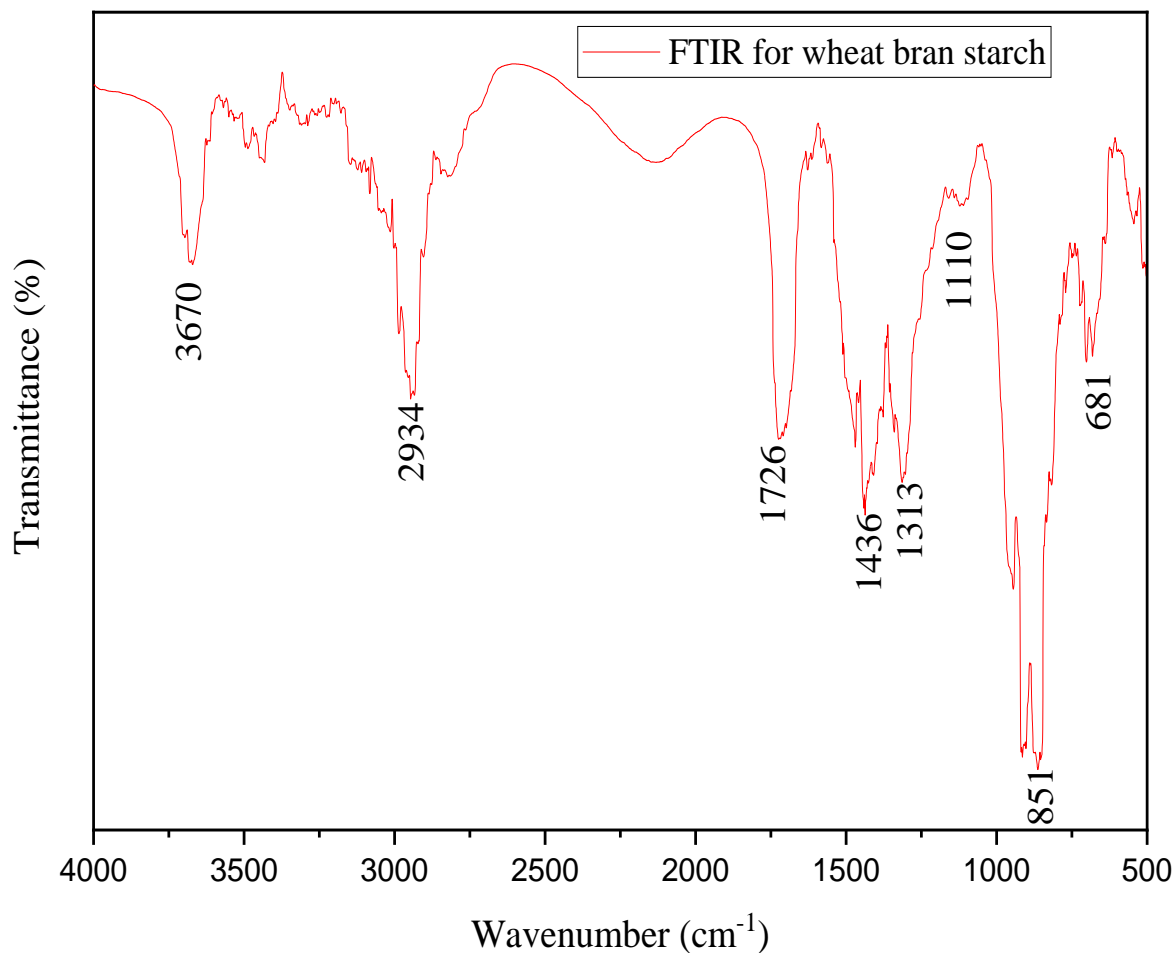
Figure 4.2: FT-IR spectra of the wheat bran starch.

4.3 Characterization of wheat straw fiber

a. Moisture content of the fiber: The moisture content obtained was found to be 73.7 %, which was lower than the values of 90 % for banana fiber reported (Ebisike *et al*., 2013). This shows that banana fiber has high water uptake capacity than wheat straw fiber.

b. Water Absorption of the fiber: The water absorption capacity of fiber obtained in this study was 3.6 %. Alkaline treatment is one of the strategies for reducing water absorption in natural fibers (Kalia *et al.*, 2009).

c. The density of the fiber: The result obtained in this study was found to be 1.62 gm/cm^3. The density of the fiber increased as it was treated more because more polymerization leads to hi gher molecular groupings (Amiri, 2017).

d. Cellulose Content of the extracted fiber: The percentage of cellulose content of wheat straw in this study was found to be 49.25 %, which was greater than (33.7 to 40 %) reported by (Khan & Mubeen, 2017) and less than (49.78 %) reported by (Kasmani & Samariha, 2011). Since the cellulose part of a wheat straw fiber has been used for further processing. Therefore, the result is fit for film production.

e. Yield for wheat straw fiber: The obtained yield for wheat straw fiber was found to be 81.75 %. Therefore, the result was comparable or certainly agreable with 79 % reported by (Qasim *et al*., 2020).

Table 4.3: The result of WS fiber and comparisons with other fibers

Types of test	Yield (%)	Density (g/cm^3)	Moisture content (%)	Water Absorption (%)	Cellulose content (%)	Reference
	28.85	1.34±0.027	-	3.62±0.18	68.54±0.72	(Njoku, C. E. *et al*., 2020)
	81.75	1.62	73.7	3.6	49.25	This study

4.3.1 X-ray diffractometer (XRD) analysis of wheat straw fiber

XRD wheat straw cellulose was shown in Figure 4.3. Cellulosic fibers were a combination of lignin and hemicellulose (amorphous region) and cellulose (crystalline region). The AHP treated fibers, showed the peak of high intensity at 22.46°. This high-intensity peak defined the crystallinity of the substance. The crystallinity of WS fiber in this study was 69.45 %. The increment of crystallinity is due to the efficient removal of non-cellulosic components (Qasim *et al*., 2020).
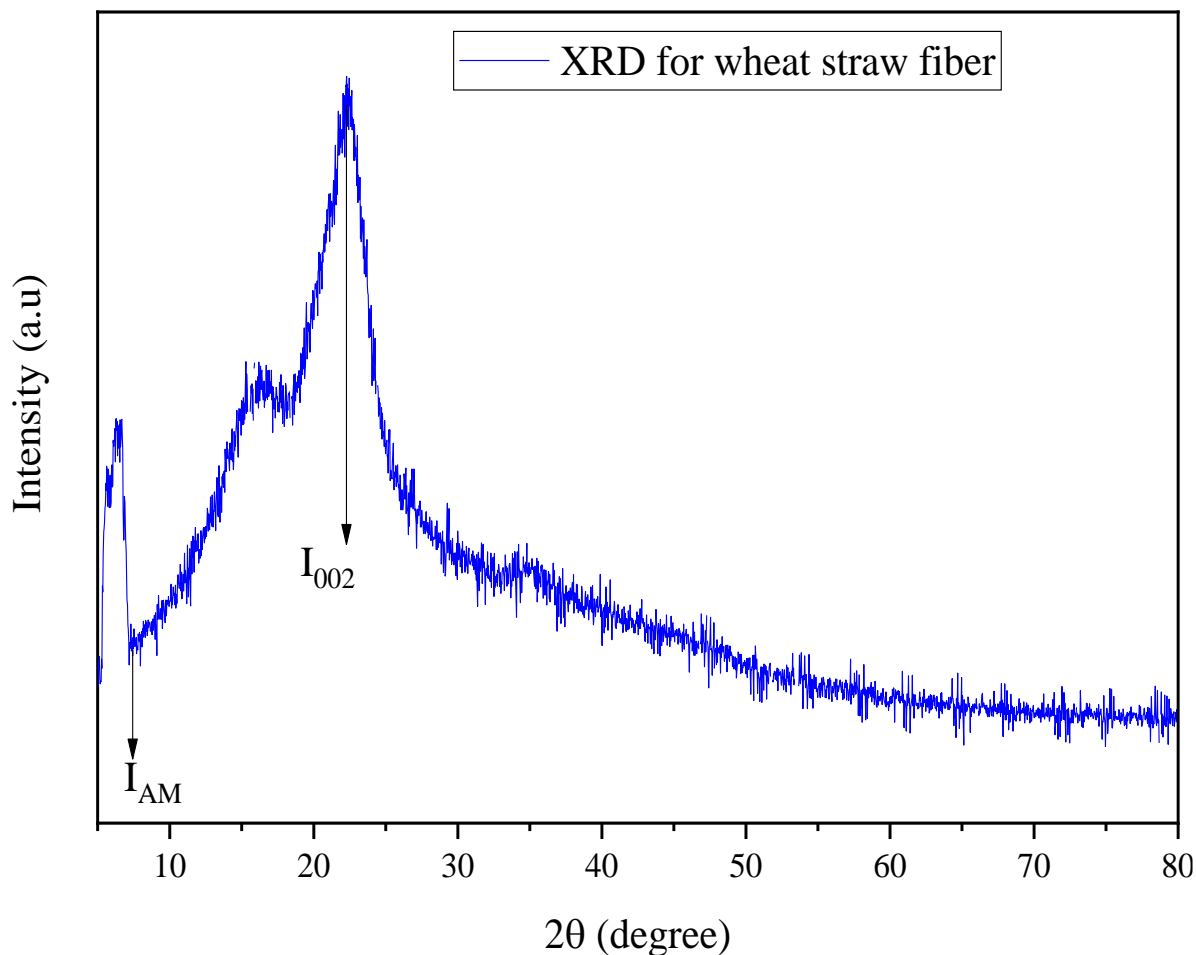
Figure 4.3: XRD patterns of the wheat straw fiber

4.3.2 Fourier Transform Infrared (FTIR) analysis of the wheat straw fiber

FTIR was used to investigate the functional characteristics of wheat straw cellulose as shown in Figure 4.4. The O-H stretching of intramolecular hydrogen bonds for cellulose was thus responsible for the signal at 3657.6 cm^{-1}. C-H stretching produces the FTIR peak at 2934.8 cm^{-1}. The absorption peak at 1702.1 cm^{-1} indicates the carbonyl C=O (carbonyl group) linkage of stretching vibration of carboxylic acid in lignin or ester group in hemicellulose. Furthermore, the peaks at 1492, 1412.3, and 1315 cm^{-1} are related to bending vibrations of –CH$_2$, C-H, and C-O of cellulose was agreeable with results reported according to (Liu *et al*., 2004). Due to the aryl group in lignin, the spectra at 955 cm^{-1} revealed the signature of CO out of plane stretching. Moreover, the absorption around 882.2 and 662 cm^{-1} refers to the cellulose component's C-O stretching and C-H vibration according to (Joha *et al*., 2012).
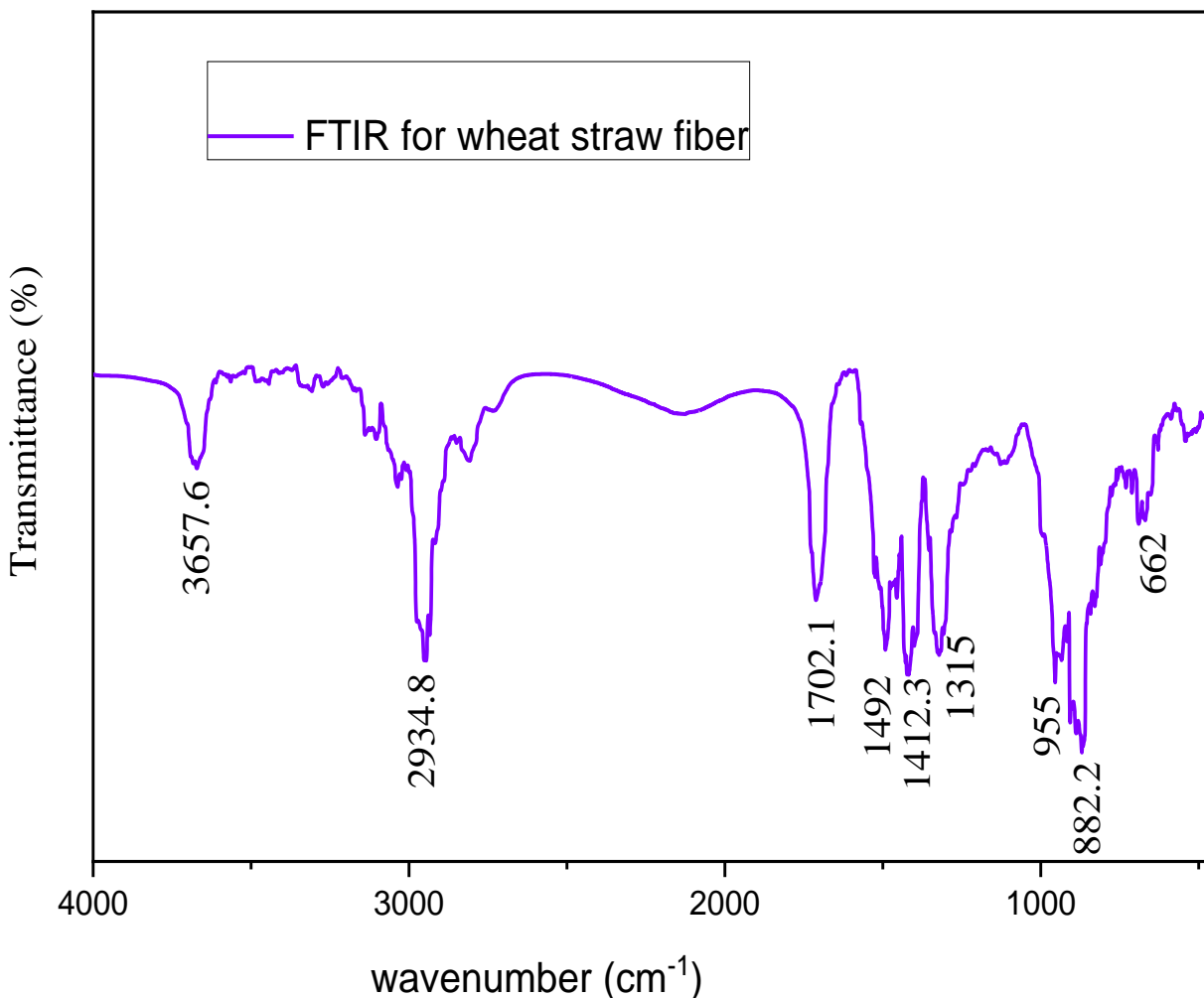
Figure 4.4: FT-IR spectra of the wheat straw fiber.

4.3.3 Thermogravimetric analysis (TGA) for wheat straw fiber

The thermal stability of cellulose derived from wheat straw was assessed by thermal gravimetric analysis Figure 4.5. The thermal analysis showed that fibers falls in four phases, with the first phase 16.12 % weight loss of the TGA curve below 114 °C was due to the evaporation and dehydration of adsorbed and surface water from the synthesized WS cellulose. The second stage from 279 to 310 °C, which accounts for the total loss of 42.5 % could be due to the interference or overlap between cellulose and lignin and elimination of non-cellulosic components (lignin and hemicelluloses) as well as a high degree of structural arrangement achieved after treatments. At the third stage, the temperature from 310 to 402 ºC, accounts for the total weight loss of 12.3 %, which indicates a higher residue amount of WS fibers. At the fourth stage, the TGA curve remained almost constant and there was no more weight loss observed from the curve which shows cellulose

was only present and is stable above 490 °C, this is caused by hemicellulose and cellulose degradation. The results obtained were comparable to those reported by (Kaushik, A., & Singh, 2011, & Nuruddin *et al*., 2013)
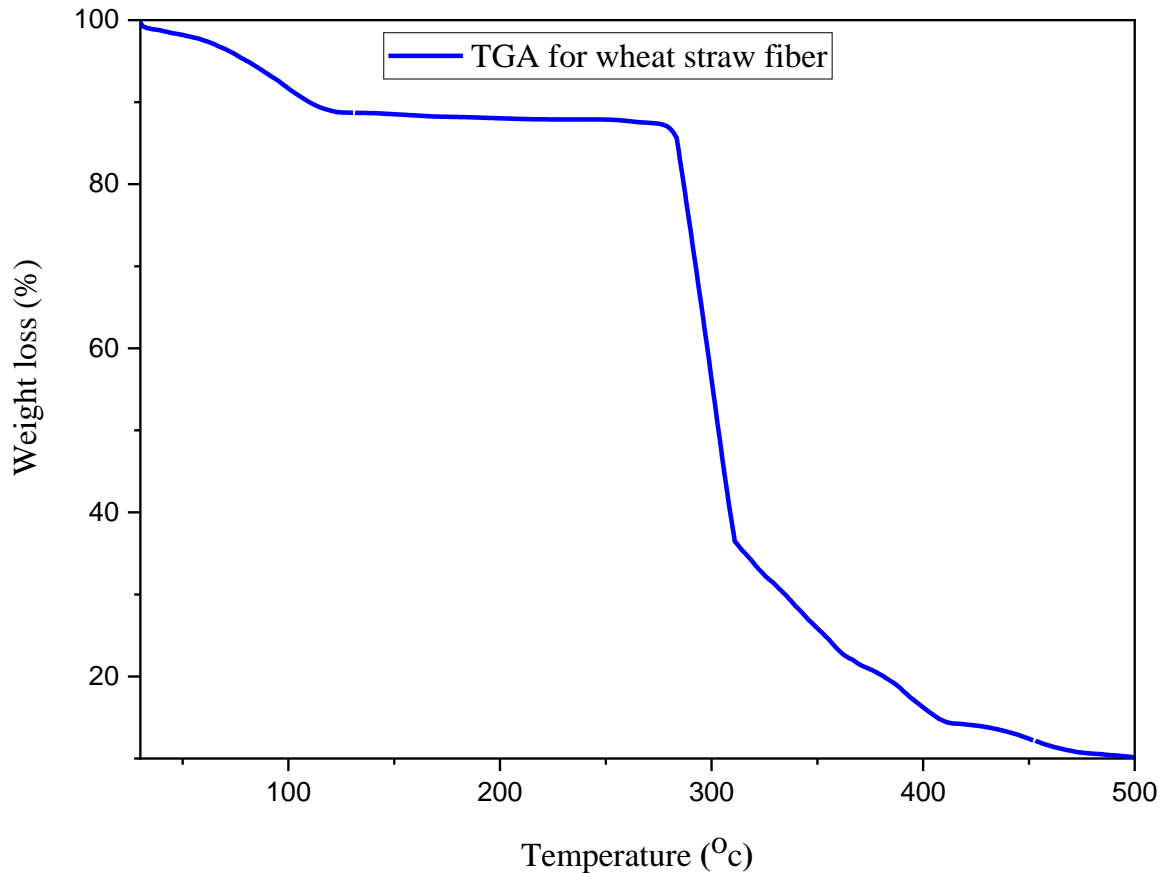
Figure 4.5: TGA curves for wheat straw fiber

4.4 Experimental design and statistical analysis of tensile strength, elongation at the break, and water absorption of bioplastics

By applying multiple regression analysis on the experimental data, second-order polynomial equations were developed for the responses (tensile strength, elongation at break, and water absorption) which can express the relationship between process variables (oven-drying temperature, concentration of glycerol, and concentration of fiber) and the responses.

Table 4.4: Values of the three response variables associated with the three factors

Std	Run	A: Oven dry.Temp. (°C)	B: Conc. of glycerol (%)	C: Con. of fiber (%)	TS (Mpa)	EA (%)	WA (%)
10	1	62	35	10	17.9	8.8	18.8
3	2	35	40	5	12	17	26.5
7	3	35	40	15	12.3	14	23.7
16	4	45	35	10	19.8	11	21.3
13	5	45	35	1.6	12.8	14.5	25.5
19	6	45	35	10	19.6	11.1	21.3
8	7	55	40	15	17.5	9.7	19.8
6	8	55	30	15	20	8.1	19.7
12	9	45	43.4	10	14	14.7	24
11	10	45	26.6	10	16.5	8.5	20.9
5	11	35	30	15	14.2	10.4	20.7
4	12	55	40	5	13.7	12.9	22.9
18	13	45	35	10	19.4	10.8	21.4
14	14	45	35	18.4	17.2	9.8	21.3
9	15	28	35	10	11.5	15.5	22.9
17	16	45	35	10	19.3	10.7	21.4
1	17	35	30	5	13	12.7	23.1
2	18	55	30	5	14.7	9.4	22.1
20	19	45	35	10	19.7	10.9	21.2
15	20	45	35	10	19.1	10.6	21.3

4.4.1   Statistical analysis of factors affecting the response variables

The experimental results obtained from the tensile strength, elongation at break, and water absorption based on CCD are presented in (Table 4.4). The main effects (linear, interaction, and quadratic) of the independent process variables on the responses (TS, EA, and WA) were determined using analysis of variance (ANOVA). The constraints used to choose the right model are the lowest standard deviation, the highest R-square, the highest Adjusted R-Square, the highest Predicted R-Square, and the lowest PRESS value. The suggested RSM model based on Summary

Statistics Model is quadratic. The final equations obtained in terms of coded factors after excluding the insignificant terms were given in equations 4.1, 4.2, and 4.3 respectively.

4.4.1.1 Analysis of variance for tensile strength

The ANOVA of the quadratic regression model was a significant model, from the evidence of Fisher"s "F" test with a very low probability value P-value is 0.0001. From Table 4.5 it was observed that the P-values less than 0.0500 indicate model terms were significant. The results showed that A, B, C, AC, BC, A², B², and C² had a significant effect on tensile strength, whereas AB had no significant effect presented in Table 4.5.

Table 4.5: Analysis of variance for the quadratic model on the tensile strength.

Source	Sum of Squares	Df	Mean Square	F-value	p-value	
Model	178.78	9	19.86	450.68	< 0.0001	Significant
A-Oven dry. Temp.	46.38	1	46.38	1052.22	< 0.0001	
B-Con. of glycerol	8.23	1	8.23	186.83	< 0.0001	
C-Con. of fiber	23.72	1	23.72	538.26	< 0.0001	
AB	0.0450	1	0.0450	1.02	0.3361	
AC	7.22	1	7.22	163.81	< 0.0001	
BC	0.7200	1	0.7200	16.34	0.0024	
A²	41.51	1	41.51	941.79	< 0.0001	
B²	32.88	1	32.88	746.01	< 0.0001	
C²	36.84	1	36.84	835.87	< 0.0001	
Residual	0.4408	10	0.0441			
Lack of Fit	0.0924	5	0.0185	0.2653	0.9142	not significant
Pure Error	0.3483	5	0.0697			
Cor Total	179.22	19				

The Model F-value of 450.68 implies the model is significant. There is only a 0.01 % chance that an F-value this large could occur due to noise**.** The Lack of Fit F-value of 0.2653 implies the Lack of Fit is not significant relative to the pure error. There is a 91.42 % chance that a Lack of Fit F-value this large could occur due to noise. A non-significant lack of fit is good because it shows that the model is well fitted and as it was obtained by the model.

4.4.1.2 Analysis of Variance Elongation at break

The ANOVA of the quadratic regression model was a significant model, from evident of Fisher"s "F" test with a very low probability value P-value is 0.0001. From Table 4.6 it was observed that the P-values less than 0.0500 indicate model terms were significant. The results showed that A, B, C, AB, BC, A², B², and C² had a significant effect on elongation at break, whereas AC had no significant effect presented in Table 4.6.

Table 4.6: Analysis of variance for the quadratic model on the Elongation at the break.

Source	Sum of Squares	Df	Mean Square	F-value	p-value	
Model	116.41	9	12.93	131.75	< 0.0001	Significant
A-Oven dry. Temp.	46.78	1	46.78	476.54	< 0.0001	
B-Con. of glycerol	40.18	1	40.18	409.34	< 0.0001	
C-Con. of fiber	22.95	1	22.95	233.78	< 0.0001	
AB	0.9800	1	0.9800	9.98	0.0102	
AC	0.0800	1	0.0800	0.8149	0.3879	
BC	0.8450	1	0.8450	8.61	0.0149	
A²	2.37	1	2.37	24.18	0.0006	
B²	0.6475	1	0.6475	6.60	0.0280	
C²	2.38	1	2.38	24.25	0.0006	
Residual	0.9817	10	0.0982			
Lack of Fit	0.8067	5	0.1613	4.61	0.0595	not significant
Pure Error	0.1750	5	0.0350			
Cor Total	117.39	19				

The Model F-value of 131.75 implies the model is significant. There is only a 0.01 % chance that an F-value this large could occur due to noise. The Lack of Fit F-value of 4.61 implies there is a 5.95 % chance that a Lack of Fit F-value this large could occur due to noise. A non-significant lack of fit shows the model is well fitted and is very nearer to the perfect fitness as it was obtained by the model.

4.4.1.3 Analysis of variance for water absorption

The ANOVA of the quadratic regression model was a significant model, from evident of Fisher"s "F" test with a very low probability value P-value is 0.0001. From Table 4.7 it was observed that the P-values less than 0.0500 indicate model terms were significant. The results showed that A, B, C, AB, BC, A², B², and C² had a significant effect on water absorption, whereas AC had no significant effect presented in Table 4.7.

Table 4.7: Analysis of variance for the quadratic model on the water absorption.

Source	Sum of Squares	df	Mean Square	F-value	p-value	
Model	68.75	9	7.64	1133.49	< 0.0001	Significant
A-Oven dry. Temp.	19.69	1	19.69	2920.93	< 0.0001	
B-Con. of glycerol	11.47	1	11.47	1701.34	< 0.0001	
C-Con. of fiber	23.11	1	23.11	3428.52	< 0.0001	
AB	3.78	1	3.78	561.07	< 0.0001	
AC	0.0112	1	0.0112	1.67	0.2254	
BC	0.1512	1	0.1512	22.44	0.0008	
A²	0.3719	1	0.3719	55.18	< 0.0001	
B²	2.36	1	2.36	349.78	< 0.0001	
C²	7.90	1	7.90	1172.03	< 0.0001	
Residual	0.0674	10	0.0067			
Lack of Fit	0.0391	5	0.0078	1.38	0.3666	not significant
Pure Error	0.0283	5	0.0057			
Cor Total	68.82	19				

The Model F-value of 1133.49 implies the model is significant. There is only a 0.01 % chance that an F-value this large could occur due to noise. The Lack of Fit F-value of 1.38 implies the Lack of Fit is not significant relative to the pure error. There is a 36.66 % chance that a Lack of Fit F-value this large could occur due to noise. A non-significant lack of fit is good because it shows that the model is well fitted and as it was obtained by the model.

4.4.2 Adequacy check for the developed response surface quadratic models

Model adequacy can be realized considering the regression coefficients R^2. Therefore, the regression coefficient (R^2) was used to decide the relationship between the experimental and the predicted responses. The R^2 of 0.9975, 0.9916 and 0.9990 shows the predicted R^2 of 0.9929, 0.9433, and 0.9949 is in reasonable agreement with the adjusted R^2 of 0.9953, 0.9841, and 0.9981 for tensile strength, elongation at break, and water absorption respectively. The values of R^2 should be between 1 and 0. The closer the value of R^2 (correlation coefficient) to 1, the better is the correlation between the experimental and predicted values, as a result showing the adequacy of the model (Li *et al*., 2018). The Predicted R^2 is in reasonable agreement with the Adjusted R^2 that means the difference is less than 0.2 for all responses. Adeq precision measures the signal-to-noise ratio and a ratio greater than 4 is appropriate. The ratio of (56.6572, 43.8324, and 132.2709 for tensile strength, elongation at the break, and water absorption) respectively, indicates a satisfactory signal which could be used to navigate the design space. The coefficient of variation (CV) indicates the degree of precision with which the experiments are compared. Generally, the higher the value of the CV is, the lower the reliability of the experiment. Here a lower value of CV (1.30, 2.71, and 0.3733 for tensile strength, elongation at the break, and water absorption) respectively, indicates greater reliability of the experiments performed.

Table 4.8: ANOVA results for response variables

	(TS)	(EA)	(WA)		(TS)	(EA)	(WA)
Std. Dev.	0.2099	0.3133	0.0821	R^2	0.9975	0.9916	0.9990
Mean	16.21	11.55	21.99	Adjusted R^2	0.9953	0.9841	0.9981
C.V. %	1.30	2.71	0.3733	Predicted R^2	0.9929	0.9433	0.9949
				Adeq Precision	56.6572	43.8324	132.2709

4.4.3 Model diagnostic plot

A diagnostic plot indicates a graphical representation of the model that can be used to interpret the chance variation of the values.

The normal probability plot as shown Figure 4.6 indicates that the residuals succeed by the normal % probability distribution. Residual is the difference between the actual value from the experiments and the predicted value from the software. In the instance of this experimental data,

the points in the plots show fitted to the straight line in Figure 4.6. Therefore, the quadratic polynomial model fulfills the analysis of the assumptions of variance for all responses.
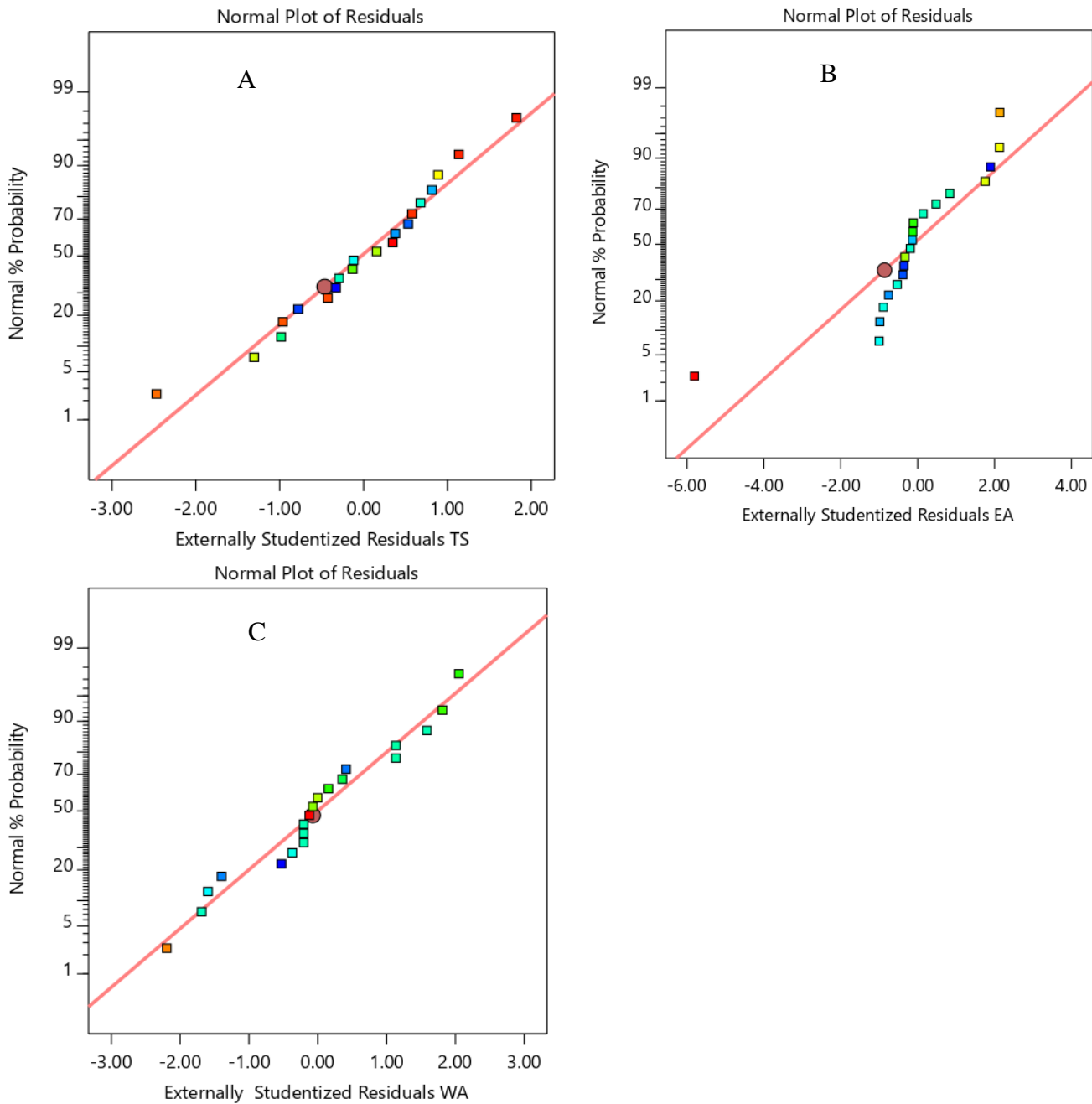
Figure 4.6: Normal Probability Plots of A (TS), B (EA), and C (WA) of bioplastic film.

Similarly, the Adequacy of the model is further shown from the predicted versus actual plots as shown in Figure 4.7. The data points on the plot of the responses (TS, EA, and WA) were reasonably distributed near the straight line, indicating a good relationship between the

experimental and predicted values of the response, and that the underlying assumptions of the above analysis were appropriate.
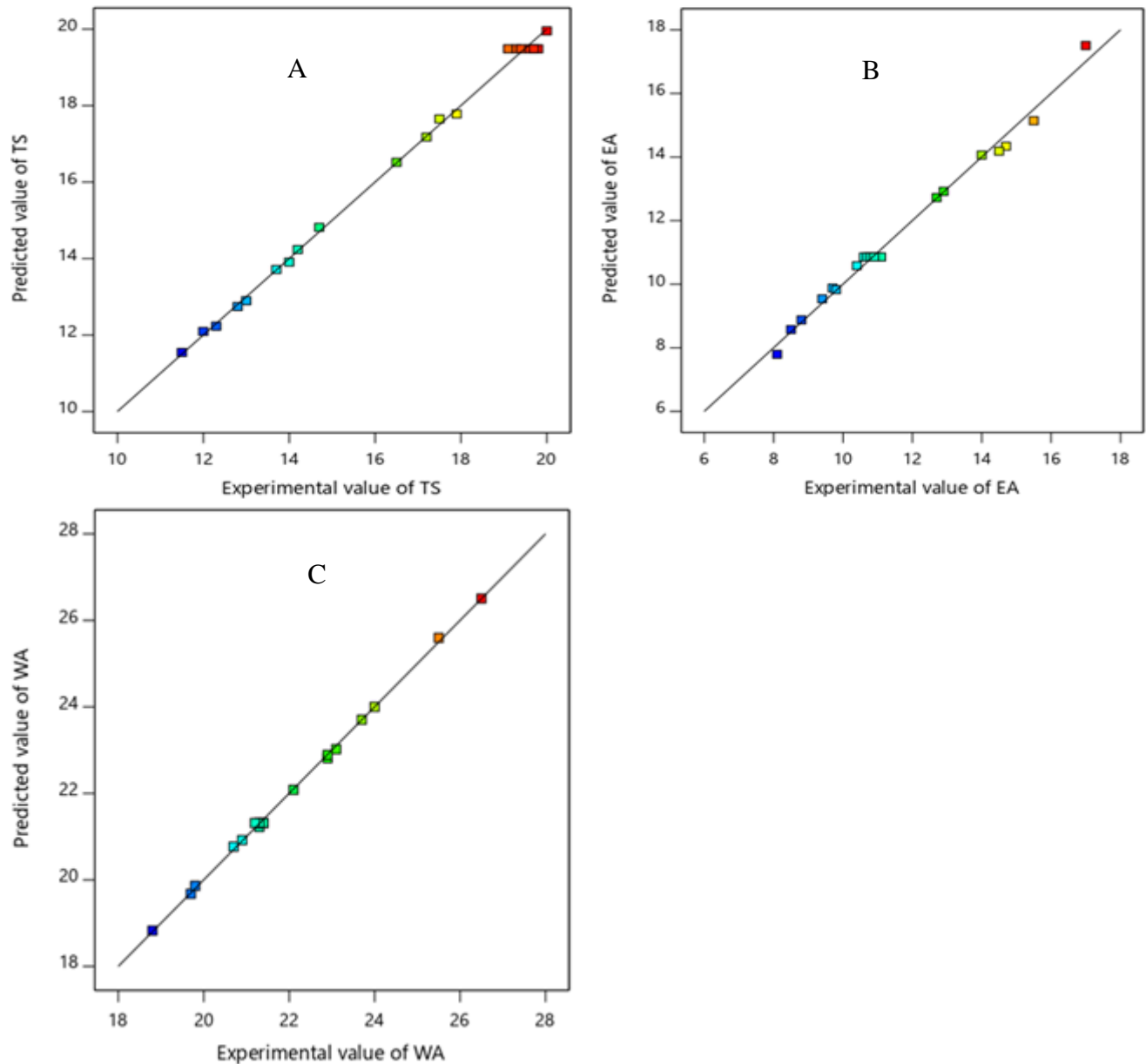
Figure 4.7: Experimental versus the predicted value of A (TS), B (EA), and C (WA) of bioplastic film.

From the above Figures 4.7, the plots represent the line of a perfect fit with points corresponding to zero error between predicted and actual values and demonstrated that the regression model equation provided an accurate description of the experimental data for all responses, in which all the points are close to the line of a perfect fit.

Data have been collected in a randomized run order or some other order that is not increasing or decreasing in any of the predictor variables used in the model to emphasize in experimental design. Hence it is better to check whether the data collection method has an influence on the capability of the model by the graphical method as shown (Figure 4.8).
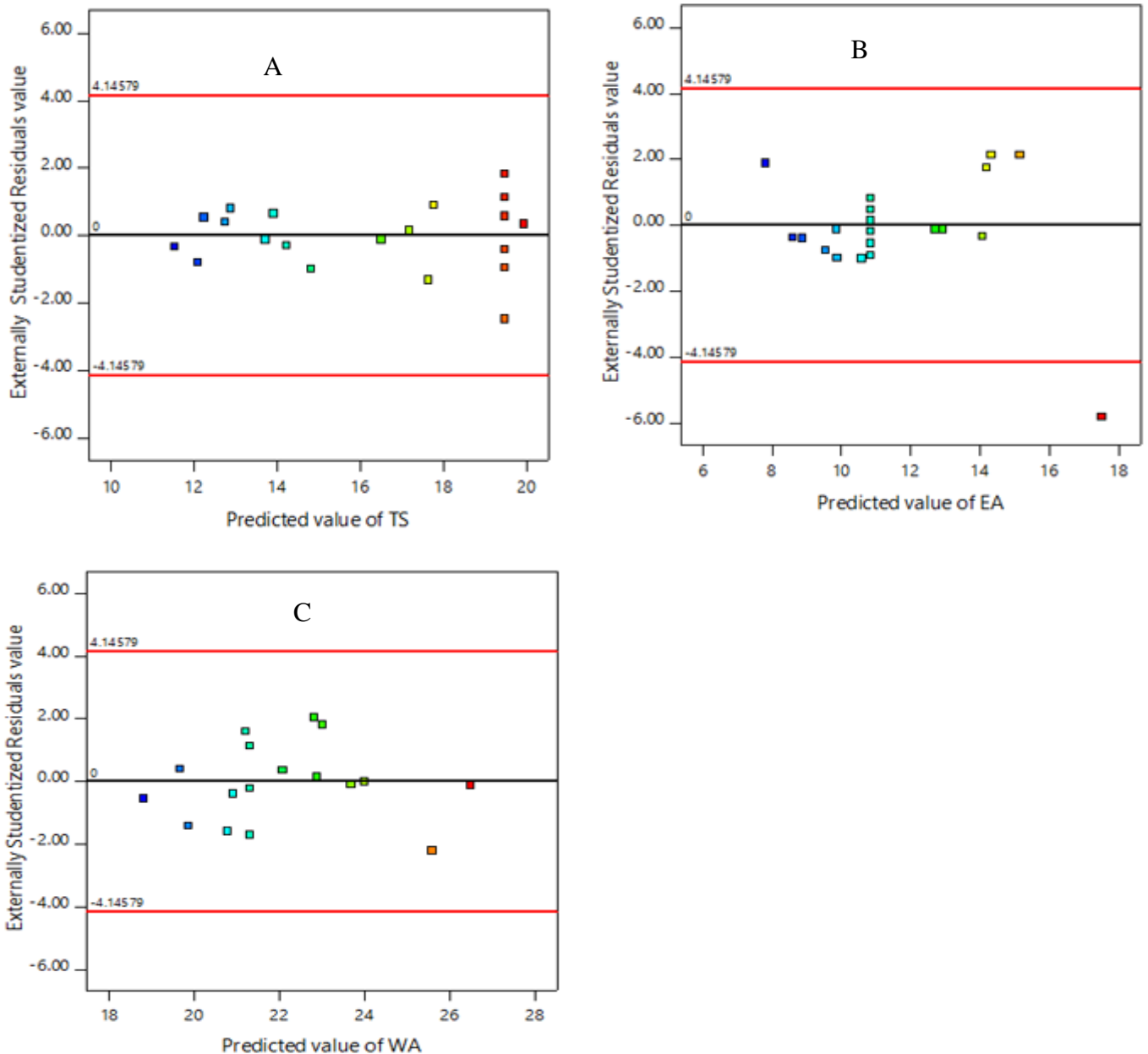
Figure 4.8: Residual versus Run Number of A (TS), B (EA), and C (WA) of bioplastic film.

Leverage: it is one of the influence plots. The leverage of a point varies from 0 to 1 and indicates how much an individual design point influences the model's predicted values. A leverage of 1

means the predicted value at that particular case will exactly equal the observed value of the experiment, i.e., the residual will be 0. The sum of leverage values across all cases equals the number of coefficients (including the constant) fit by the model. The maximum leverage an experiment can have is $1/k$, where k is the number of times the experiment is replicated. (Figure 4.9) is leverage vs. the run.
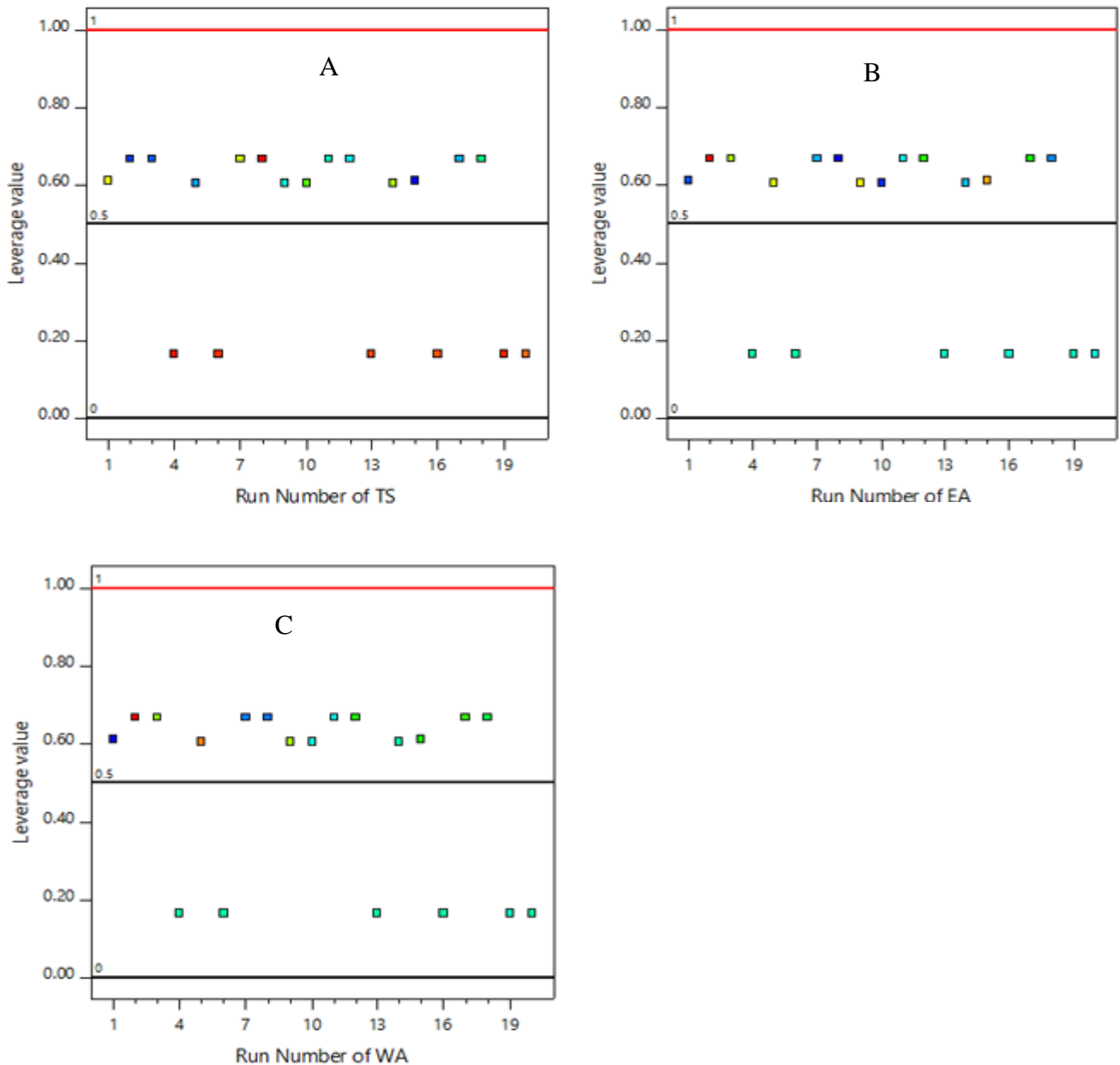
Figure 4.9: leverage versus Run Number of A (TS), B (EA), and C (WA) of bioplastic film.

4.4.4 Development of Regression Model Equation

The mathematical models were expressed in terms of coded variables. Comparing the factor coefficients of the coded equation was useful for identifying the relative impact of the factors. The mathematical relationship between the responses and the independent variables such as oven drying temperature (A), the concentration of glycerol (B), and concentration of fiber (C) in terms of coded factors can be determined by response surface methodology (RSM). The model equations developed in terms of coded values of the variable are shown in equations (4.1, 4.2, and 4.3) for TS, EA, and WA respectively. Table 4.4, the second-order polynomial function representing TS, EA, and WA can be expressed as a function of the three operating parameters of bioplastic film synthesizes, such as oven drying temperature (A), the concentration of glycerol (B), and concentration of fiber (C) after rejecting the insignificant terms:

$$TS = +19.49 + 1.79A - 0.7769B + 1.32C + 0.9500AC - 0.3000BC - 1.67A^2 - 1.51B^2 - 1.60C^2 \qquad 4.1$$

$$EA = +10.86 - 1.84A + 1.72B - 1.30C - 0.3500AB - 0.3250BC + 0.3989A^2 + 0.2124B^2 + 0.4073C^2 \quad 4.2$$

$$WA = +21.32 - 1.20A + 0.9167B - 1.30C - 0.68750AB - 0.1375BC - 0.1579A^2 + 0.4053B^2 + 0.7419C^2 \quad 4.3$$

Equations (4.1, 4.2, and 4.3) show the relationship between the percentage of TS, EA, WA, and operating parameters respectively. Linear factor shows the effect of a specific factor, while the mutual quantities of two factors show the impact of the interaction between two variables. The positive signs in the models suggest the synergetic effects of a factor, while the negative sign indicates the aggressive effect. Results showed that increasing TS resulted in the increasing oven drying temperature and concentration of fiber, whereas the decreasing concentration of glycerol due to its magnitude of the coefficient. The negative coefficient of oven drying temperature and concentration of fiber indicates a decrease in the EA and WA, but concentration of glycerol increases the EA and WA. Individual or combined values of factors represent the significant impact of the variables on the response parameters.

4.4.5 Effects of individual process variables

The effect of oven drying temperature, the concentration of glycerol, and the concentration of fiber on tensile strength, elongation, and water absorption were studied and evaluated for the best bioplastic film synthesis conditions. Based on the ANOVA, plastic synthesis was significantly affected by linear, interactive, and quadratic effects between the process variables.

4.4.5.1 Effect of process variables on the tensile strength

The effect of oven drying temperature on the physical and mechanical properties of bioplastic film is quite essential. In fact, temperature has to be adjusted in this work to achieve the desired range of values, and it has a substantial impact on the properties of the manufactured bioplastic film. As shown in Figure 4.10 (A), the acquired tensile strength for bioplastic film is low at low oven drying temperature, and the quality of bioplastic film made improves as the oven drying temperature rises. Its impact on tensile strength is more obvious, and tensile strength increases as a result. In addition to that the graphical representation, from the model equation 4.1, the coefficient of oven drying temperature is positive which indicates the TS of the bioplastic film increase with increasing oven drying temperature.

As shown in Table 4.4 the minimum tensile strength was obtained at 28 ^{o}C oven drying temperature, which is 11.5 Mpa, and the maximum tensile strength was 20 Mpa at 55 ^{o}C oven drying temperature. Despite the fact that tensile strength improves as temperature rises until it approaches the brittle-ductile transition temperature, it is better to choose the optimal temperature owing to economic considerations and to minimize side effects such as a breakable and malleable fracture. The glucosidic bonds between monomers in amylose are then broken by further heating. As the heating temperature rises, the amylose chain depolymerizes, the straight-chain amylose falters and gets shorter, lowering the amylose content (Halley, 2016).

The effects of concentration of glycerol and concentration of cellulose extracted from wheat straw on tensile strength of bioplastic film are shown in Figure 4.10 (B and C). The concentration of glycerol varies from 26.6-43.4 % w/v of starch basis. Figure 4.10 (B) as shown in Table 4.4 the minimum tensile strength was obtained at 35 % concentration of glycerol and 10 % concentration of fiber which is 11.5 Mpa and the maximum tensile strength was 20 Mpa at 30 % concentration of glycerol and 15 % concentration of fiber.

The high tensile strength values can be recognized as the number of hydrogen bonds between the starch chains that contribute to cohesiveness and low flexibility. When glycerol was incorporated into the starch polymer, competition for the formation of hydrogen bonding started. As a result of the hydrogen bond formation with glycerol, direct interfaces between starch chains were partly removed, allowing the polymer chains to move more freely (Bertuzzi, 2012).

Therefore, increasing the volume of glycerol reduces the intermolecular interaction between the amounts of starch molecules in the wheat bran which results in the reduction of tensile strength. These results agree with the previous works on cassava starch by (Tegangan, S., & Air, 2011).
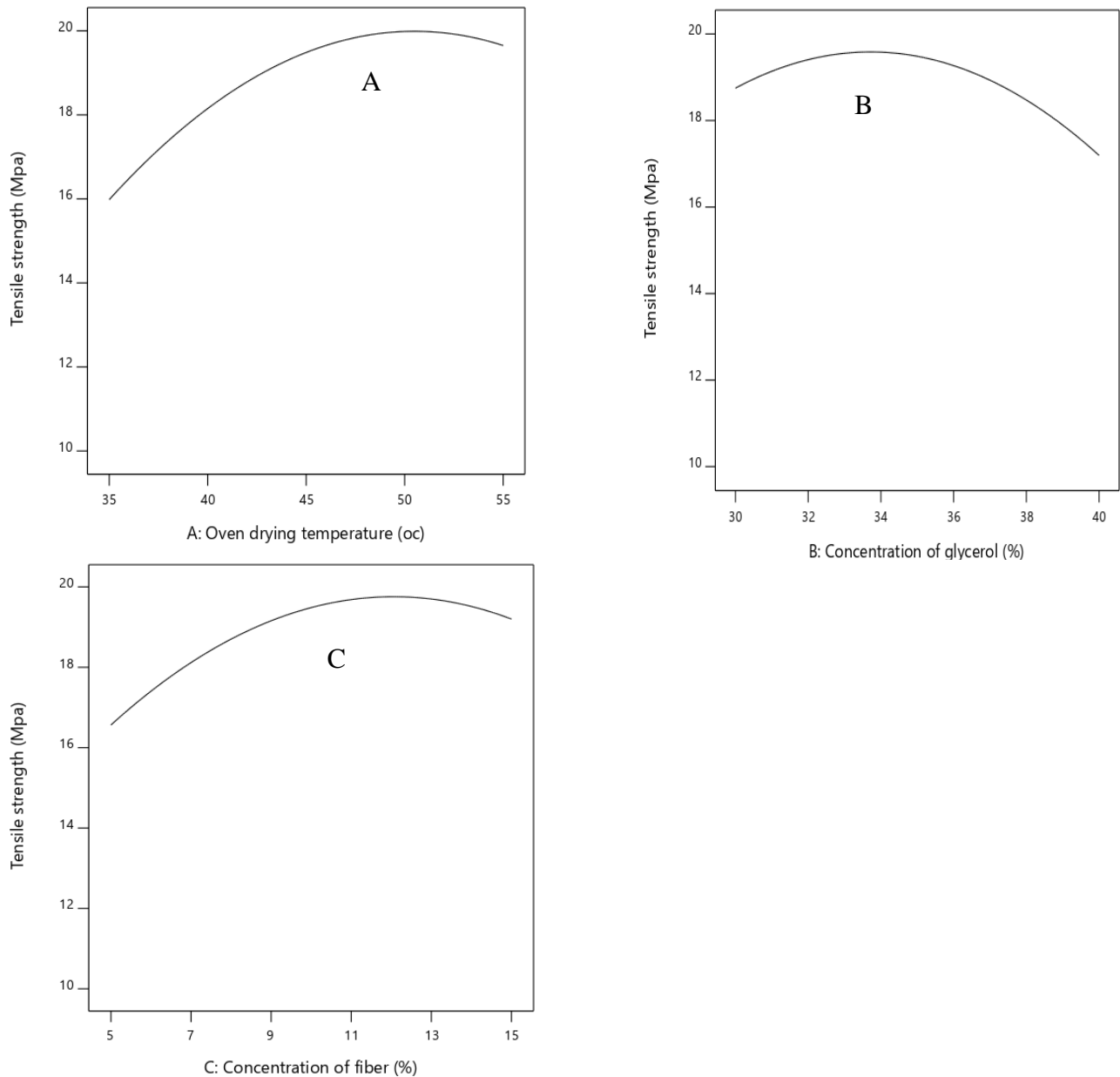
Figure 4.10: Effects of oven drying temperature (A), the concentration of glycerol (B), and concentration of fiber (C) on tensile strength of bioplastic film.

4.4.5.2 Effect of process variables on the elongation at break

The individual effects of oven drying temperature on the EA of bioplastic film was investigated by keeping other processes variables held as constant. As shown in Table 4.4 the minimum

elongation at break was obtained at 55 $^{\circ}$C oven drying temperature which is 8.1 % and the maximum elongation at break was 17 % at 35 $^{\circ}$C oven drying temperature. The increase in the oven drying temperature decrease elongation at break from 17 % to 8.1 % as shown from the Figure 4.11 (A). This is because the heat increases the kinetic energy of the molecules, causing them to vibrate and produce a free volume, allowing for bigger molecular chain rotation (Wojciechowska, 2014).

The effect of concentration of glycerol on EA of bioplastic film was examined by keeping other processes variables held as constant was shown in Figure 4.11 (B). The results obtained demonstrates that increasing concentration of glycerol resulted in increased elongation at break of bioplastic film. This is due to the intermolecular bonds between amylose, amylopectin, and amylose-amylopectin in the starch matrix is being replaced by hydrogen bonds produced between plasticizer and starch molecules, resulting in increased elongation at break in the film. By allowing for increased chain flexibility, such interruptions and reconstructions in starch molecular chains reduce stiffness and increase film flexibility (Wang *et al*., 2014).

As shown in Figure 4.11 (C), the effect of concentration of fiber on EA was studied. As shown in Table 4.4 the minimum elongation at break was obtained at 30 % concentration of glycerol and 15 % concentration of fiber which is 8.1 % and the maximum elongation at break was 17 % at 40 % concentration of glycerol and 5 % concentration of fiber. Thus, the addition of fiber to bioplastics film has the reverse effect on elongation at break. In bioplastic film, the addition of fiber tends to collaborate more with hydrogen and other monomers. Approximate results were described by (Wang *et al*., 2014). This study suggest that adding the right quantity of cellulose to a starch solution promotes ductility.
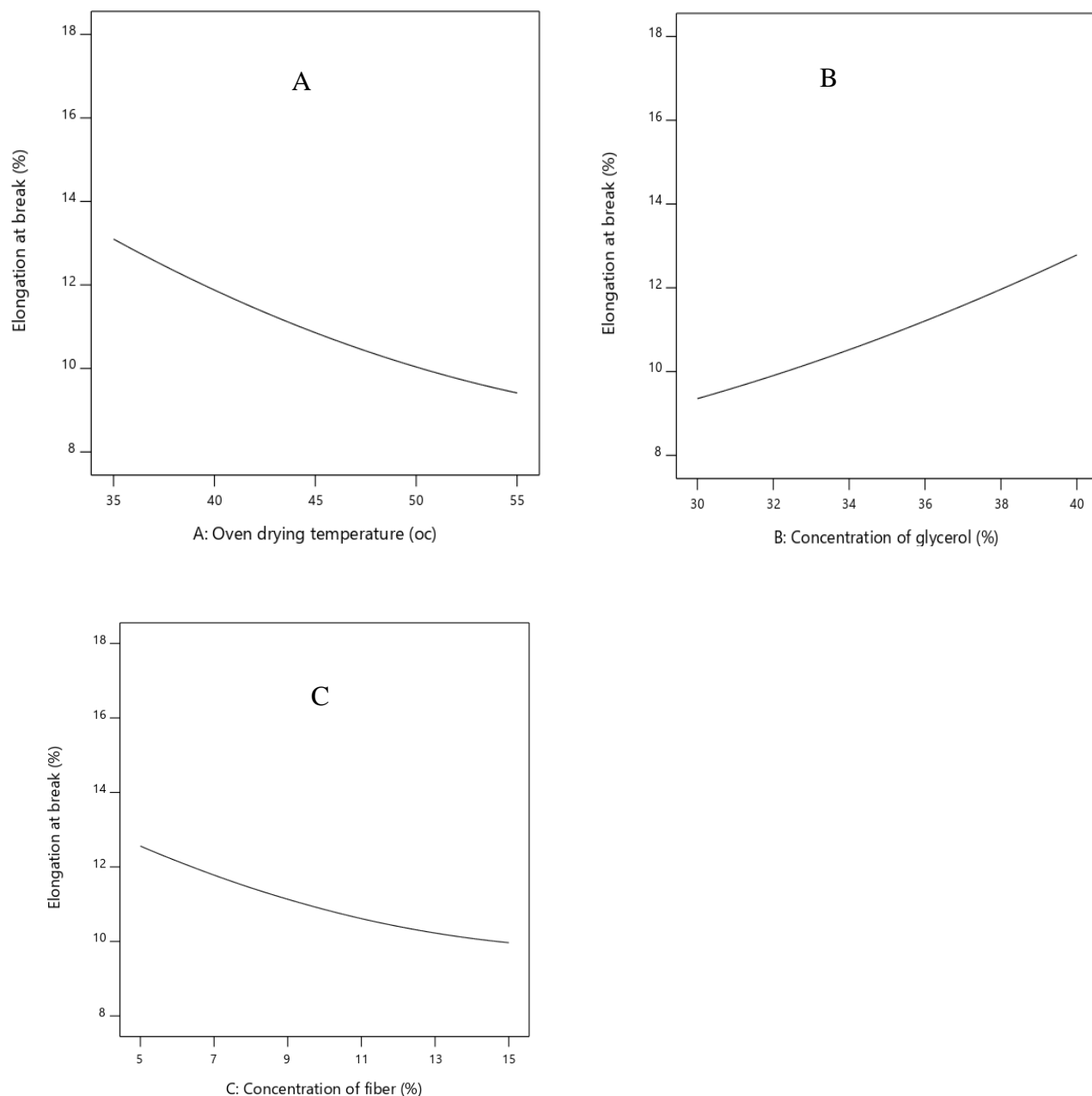
Figure 4.11: Effects of oven drying temperature (A), the concentration of glycerol (B), and concentration of fiber (C) on elongation at break of bioplastic film.

4.4.5.3 Effect of independent factors on Water absorption

The effects of oven drying temperature on WA of bioplastic film was investigated by keeping other processes variables helds at fixed point was shown in Figure 4.12 (A). As shown in Table 4.4 the minimum water absorption was obtained at 62 °C oven drying temperature, which is 18.8 % and the maximum water absorption, was 26.5 % at 35 °C oven drying temperature. As oven drying temperature increases, the exposure of bioplastic to heat increases and usually results in rigid,

cross-linked starch molecules, with stronger tensile strength and narrow free volume spaces in which the water molecules would have been diffused (Nathiqoh, A. U. 2013). Therefore, the diffusion of the water molecules into micro voids free volume space of the bioplastic was inhibited by the rigid structure created at higher temperatures.

The effects of concentration of glycerol on WA of bioplastic film was examined by keeping other processes variables helds as constant. As shown in Table 4.4 the minimum water absorption was obtained at 35 % concentration of glycerol which is 18.8 % and the maximum water absorption was 26.5 % at 40 % concentration of glycerol. From Figure 4.12 it is obvious to state that changes in water absorption of bioplastics varied depending on the variations in the concentration of glycerol. The more the glycerol is, the higher the water-swelling ratio will be. It is related to the hydrophilic properties of glycerol and starch. These properties increase the attraction between glycerol and water, therefore, increases of water absorption. The fact that wheat bran starch contains a hydroxyl (OH), carbonyl (CO), and ester (COOH) indicates that the concentration of hydrophilic properties in the bioplastics is high; high concentrations of hydrophilic starch and glycerol cause faster degradation in the soil (Nathiqoh, A. U. 2013).

As shown in Table 4.4 the minimum water absorption was obtained at 10 % concentration of fiber which is 18.8 % and the maximum water absorption was 26.5 % at 5 % concentration of fiber. This water absorption reduction in bioplastic film can be attributed to stronger hydrogen bonds between the starch matrix and the reinforced material. The incorporation of fibers in thermoplastics is an alternative for reducing water uptake in bio-composite exposed to high humidity environments, but the ratio of fiber to starch should be considered (Wittaya, 2012).
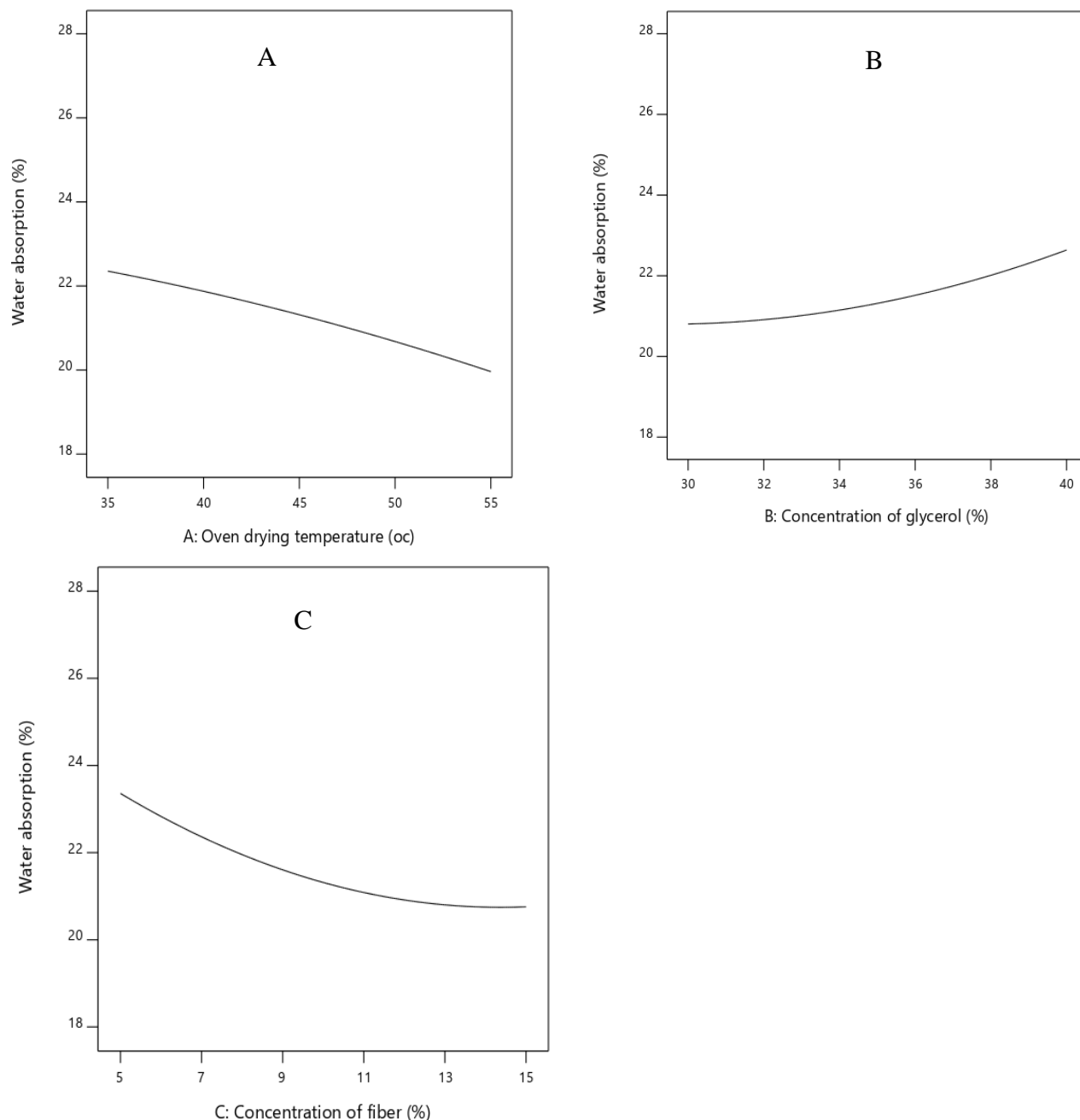
Figure 4.12: Effects of oven drying temperature (A), the concentration of glycerol (B), and concentration of fiber (C) on water absorption of bioplastic film.

4.4.6 The interaction effect between process variables and responses

The response surface methodology was utilized to analyze the interactive influence of variables on tensile strength, elongation at break, and water absorption were drawn on a 3D surface. Response surface plots as a function of two factors at the same time, with one factor, held constant, are more useful in understanding the interactions between these factors. As seen from the model

equation 4.1, 4.2 and 4.3 the interaction effects on tensile strength, elongation at break, and water absorption can be easily understood by the coefficients. There are three interactions (oven drying temperature and concentration of glycerol (AB), oven drying temperature and concentration of fiber (AC), and concentration of glycerol and concentration of fiber (BC)). Among these three interaction factors, the one which consists of higher coefficients of the regression models is the most significant interaction factor for the response. The interaction coefficient with positive signs have a positive effect on the responses, whereas, negative signs have negative effect on the response variables.

4.4.6.1 Interaction effect of process variables on tensile strength

In this study, it was found that the combined effect of oven drying temperature and concentration of fiber, and concentration of glycerol and concentration of fiber have a significant effect on tensile strength of bioplastic film.

Figure 4.13 (A) indicates the interaction effect of oven drying temperature (A) and concentration of fiber (C) on tensile strength of bioplastic film. The interaction effects between oven drying temperature and the concentration of fiber have most significant effect on tensile strength. The highest tensile strength value was 20 Mpa was observed at a 15 % concentration of fiber and 55 $^\circ$C oven drying temperature. Therefore, as oven drying temperature and concentration of fiber increases the tensile strength increases up to the optimum point, finally it decreases. In addition, AC with positive coefficient from model equation for tensile strength shows that AC positively affects the tensile strength of the film.

As shown in Figure 4.13 the interaction effects of concentration of glycerol (B) with the concentration of fiber (C) and their mutual interaction on the tensile strength of bioplastic film at constant oven drying temperature (45 $^\circ$C). As the concentration of glycerol increases and the concentration of fiber decreases, the tensile strength of bioplastic film became decreased. Probably this effect is due to increasing the molecular mobility and resulting in less rigid and high flexible materials; the concentration of glycerol dominates the concentration of fiber.
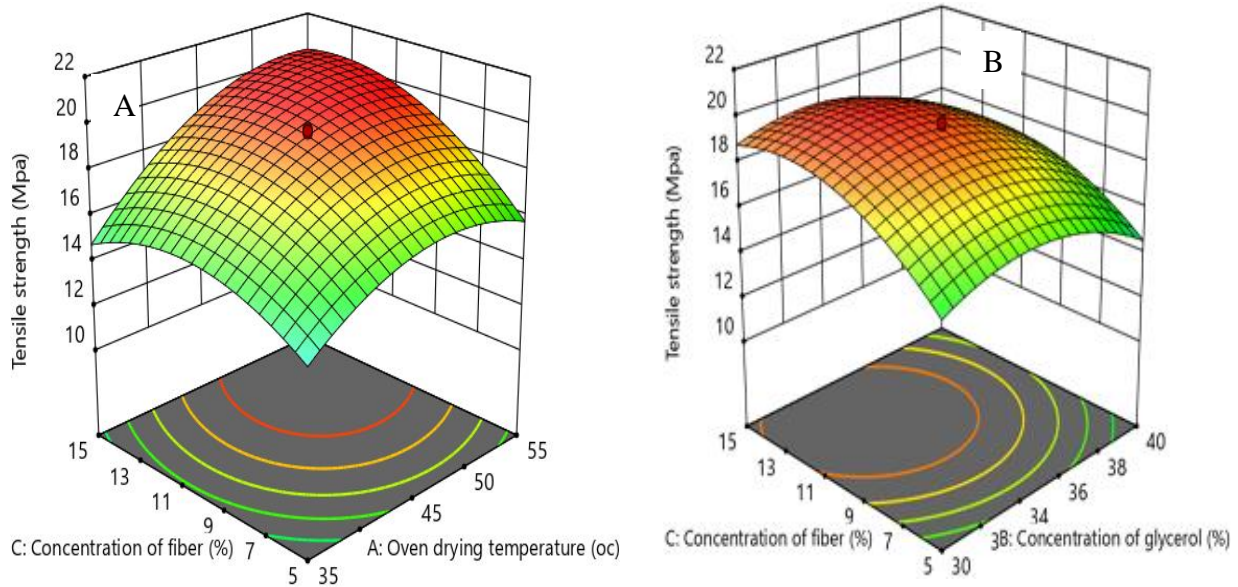
Figure 4.13: 3D plot for the combined effect of A (oven drying temperature and concentration of fiber), and B (concentration of glycerol and concentration of fiber) on TS of bioplastic film.

4.4.6.2 Interaction effect of process variables on elongation at break

The interaction of oven drying temperature (A) and concentration of glycerol (B) has a significant effect on the elongation at break of bioplastic film. It was detected that by increasing oven drying temperature (A) and decreasing concentration of glycerol (B) the elongation at break value was decreased (Figure 4.14) (A). This could be mainly the higher mobility of the polymer due to increase glycerol, enables the film to absorb moisture over time which is likely due to the hydrophilic nature of glycerol (Gujar *et al.*, 2014).

The interaction of concentration of glycerol (B) and concentration of fiber (C) has a significant effect on the elongation at break of bioplastic film. From Figure 4.14 (B) it was showed that the increased concentration of glycerol (B) and decreased concentration of fiber (C) resulted in improved elongation at break value.

Figure 4.14: 3D plot for the combined effect of A (oven drying temperature and concentration of glycerol), and B (concentration of glycerol and concentration of fiber) on EA of bioplastic film.

4.4.6.3 Interaction effect of process variables on water absorption

The interaction of oven drying temperature (A) and concentration of glycerol (B) has a significant effect on the water absorption of bioplastic film. It was noticed that as oven drying temperature (A) increases and concentration of glycerol (B) decreases the resulted water absorption value was reduced Figure 4.14 (A). This is due to the fact that as temperature increases, the water vaporizes more rapidly.

The interaction effect of the concentration of glycerol (B) and concentration of fiber (C) has a significant effect on the water absorption of bioplastic film is also shown in Figures 4.15 (B). From the result shown in Table 4.4, it indicates that water absorption was increased with increasing concentration of glycerol and was decreased beyond optimum point. The water absorption of bioplastic film was decreased with increasing concentration of fiber (C) and after optimum point water absorption of film was increased.
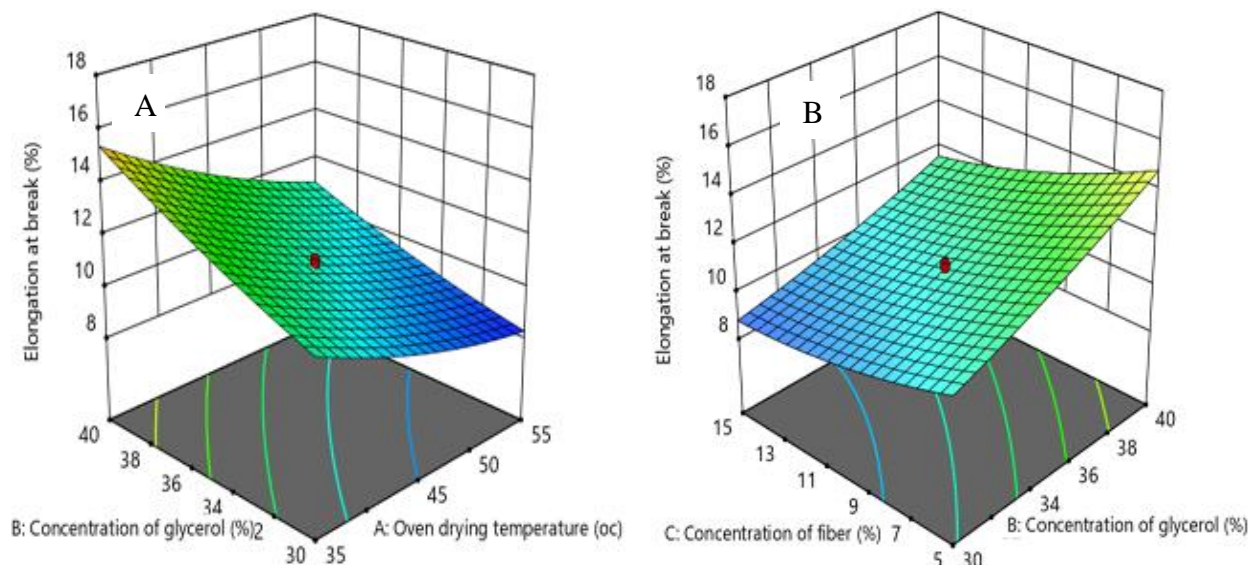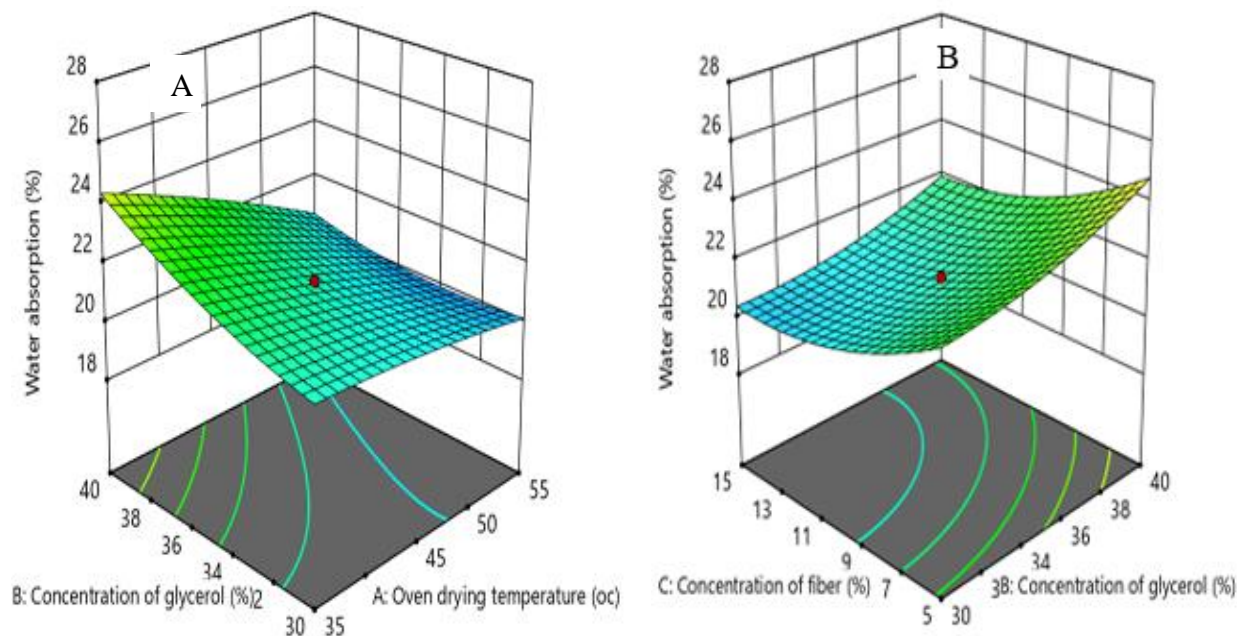
Figure 4.15: 3D plot for the combined effect of A (oven drying temperature and concentration of glycerol), and B (concentration of glycerol and concentration of fiber) on WA of bioplastic film.

4.4.7 Process factors and response variables optimization

Optimization is the process of identifying conditions that yield a function's maximum or minimum values. The act of optimizing is the process of obtaining the best feasible result under given conditions. The numerical response optimization technique was decided to determine the optimum workable conditions for wheat bran starch via wheat straw fiber-based bioplastic film was optimized by RSM using CCD. The main criterion for constrained optimization was maximum possible tensile strength, minimum possible elongation at break, and minimum possible water absorption by keeping the factor values in range oven drying temperature (35 - 55 $^{\circ}$C), the concentration of glycerol (30 - 40 %), and concentration of fiber (5 - 15 %). Table 4.12 shows the model validation for the optimum conditions of TS, EA, and WA of bioplastic film. This result is then repeated three times and the results are not too far from the repetition. The optimum conditions of TS, EA, and WA of bioplastic film were accomplished at a 55 $^{\circ}$C oven drying temperature, 31.97 % concentration of glycerol, and 14.40 % concentration of fiber. The 20.528 Mpa, 8.1 %, and 19.44 % for TS, EA, and WA of bioplastic film respectively were obtained. Model desirability (0.971) approaching unity and with a low error value describes the applicability of the model toward the responses. The TS, EA, and WA of bioplastic film in optimized conditions were

compared by different bioplastic films used in previous studies. The results shown in the literature indicate the synthesized wheat straw fiber incorporated wheat bran starch-based bioplastic film has a good performance compared to other bioplastic films presented in previous studies. Therefore, the present study showed that wheat bran starch is a potential source for bioplastic production and the result was in the acceptable range with previous studies.

Table 4.9: Summary of constraints and goals of optimizations

Name	Goal	Lower Limit	Upper Limit	Importance
Oven drying temperature	In range	35	55	3
Concentration of glycerol	In range	30	40	3
Concentration of fiber	In range	5	15	3
Tensile strength	Maximize	11.5	20	3
Elongation at break	Minimize	8.1	17	3
Water absorption	Minimize	18.8	26.5	3

Table 4.10: Comparison of mechanical properties for different types of films.

Bioplastic type	TS	EA	WA	Reference
Corn starch reinforced corn husk	11.7164 Mpa	-	-	(D Amalia, 2020)
Corn starch reinforced soybean fiber	6.71 N	-	-	(Paper *et al.*, 2017)
Avocado seed starch reinforced sugar palm fiber	2.74 Mpa	3.16 %	-	(Harahap & Ginting, 2018).
Banana peel starch	0.1445 N/mm^2	-	18.18 %	(Bejena, 2019)
Mango peel starch reinforced with clay	5.657 Mpa	43.431 %	-	(Maulida, 2018)
Cassava peel starch with shrimp shell	27.41 Kgf/cm^2	-	-	(Dasumiati & N Saridewi, 2019)
Cassava starch with clay nanoparticle	24.18 Mpa	-	-	(Harunsyah, 2018)
Wheat bran starch reinforced with wheat straw fiber	20.528 Mpa	8.1 %	19.44 %	This study

Table 4.11: Optimum possible conditions for TS, EA, and WA for bioplastic film

Number	Oven dry.Temp.	Con. of glycerol	Con. of fiber	TS	EA	WA	Desirability	
1	55.000	32.052	14.640	20.517	8.100	19.441	0.971	
2	55.000	32.040	14.599	20.520	8.100	19.441	0.971	
3	55.000	32.059	14.663	20.516	8.100	19.441	0.971	
4	55.000	32.035	14.583	20.521	8.100	19.441	0.971	
5	55.000	32.013	14.516	20.524	8.100	19.441	0.971	
6	55.000	32.086	14.751	20.509	8.100	19.441	0.971	
7	55.000	32.093	14.779	20.506	8.100	19.441	0.971	
8	**55.000**	**31.975**	**14.403**	**20.528**	**8.100**	**19.442**	**0.971**	**Selected**
9	55.000	32.122	14.884	20.496	8.100	19.443	0.971	
10	55.000	32.133	14.923	20.492	8.100	19.444	0.971	
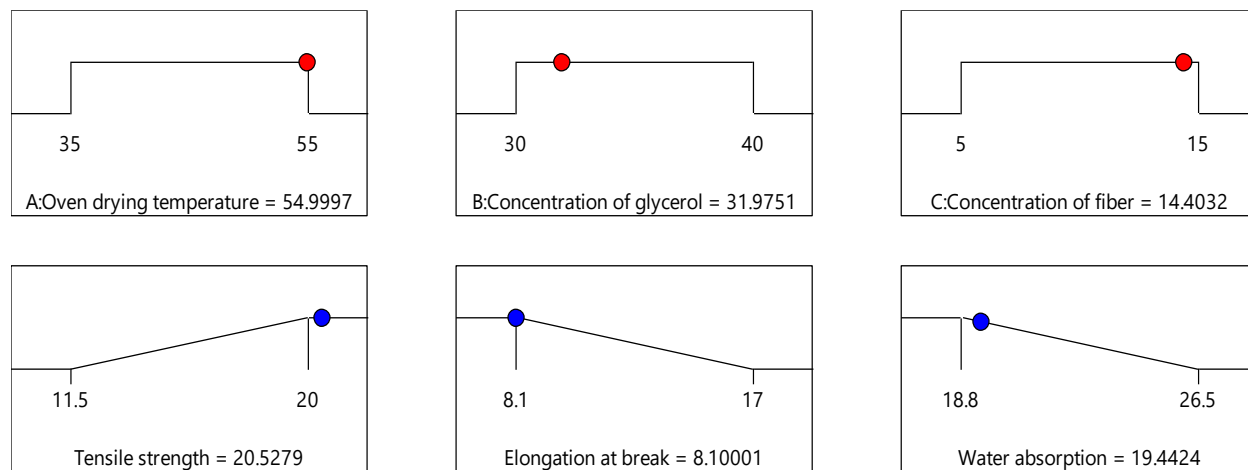
Desirability = 0.971
Solution 8 out of 10

Figure 4.16: Desirability ramp for the optimization of the response and the parameters

4.4.8 Model Validation

To confirm the developed model, the actual validation experiment was carried out at optimum conditions that were obtained by a design expert. These optimum points were oven drying

temperature of 55 °C, the concentration of glycerol of 31.97 %, and the concentration of fiber of 14.40 %. For validation, the actual experimental value, predicted value, and the percentage of error are required and listed in Table 4.12. As observed from the confirmation result in (Table 4.12), the percentage accuracy was 99 %, 99.4 %, and 98.6 % for TS, EA, and WA respectively. Because the deviation value is less than 5 %, the model that has been obtained by RSM can be accepted and carefully valid.

Table 4.12: Model validation for optimization of response variables

	Oven drying temperature	Concentration of glycerol	Concentration of fiber	Actual value	Predicted value	% error	% Accuracy
	55.00	31.97	14.40				
TS				20.32	20.528	1.02	99
EA				8.05	8.1	0.6	99.4
WA				19.17	19.44	1.4	98.1

4.5 Physicochemical characterization of the bioplastic film at optimum point

a. Water solubility: The result demonstrates that the controlled film has a solubility of 35 %, whereas the fiber incorporated film has a solubility of 30 %. When fiber is added to starch, the solubility decreases. Because starch is a hydrophilic polymer, it has a strong affinity for water. As a result, the starch film absorbs water and swells when they are hydrated. In generally, it can be recommended that films having a low solubility are favorable for the packaging purpose.

b. Moisture content: The result implements that the moisture content obtained for controlled film was found to be 16.66 %, whereas the fiber-reinforced film found to be 10.5 %. The obtained result shows that pure starch film has higher moisture content than the fiber-reinforced film, this is due to hydrophilic properties of starch.

c. Density: In this study, the density of both controlled and fiber reinforced film was evaluated. The control film yielded 1.54 g/ml, while the blended film yielded 1.62 g/ml. The increasing density by reinforcing fiber was due to the fiber's compatibility.

d. Transparency of produced bioplastics: The controlled film had a transmittance of 5.6 while the blended film had a transmittance of 4.8. The pure starch film had a higher percentage of transmittance than the fiber incorporated film. The addition of fiber to starch-based films resulted in a

drop in transparency and increased cloudiness. When utilized as packaging materials, the transparency of the films is important in particular cases (Yehuala, G. A., & Emire, 2013).

e. Film thickness: The result obtained for thickness of controlled film was found to be 0.47 mm, whereas, fiber blended film was 0.51 mm, this is due to the film thickness increases with increasing concentration of fiber. The result of film thickness obtained was greater than 0.334 mm reported by (Ibrahim *et al*., 2019) for corn starch-based film. Film thickness depends on the concentration of individual biopolymers used for the fabrication of film. The blended film cannot evaporate quickly and so it becomes thick (Abugoch *et al*., 2011).

Table 4.13: Results on comparison of physicochemical properties of films.

Types of bioplastic	Solubility (%)	Moisture (%)	Density (g/ml)	Transparency (%)	Thickness (mm)	Reference
Corn starch film	90.67 ± 0.17	0.02786 ± 0.19	5.454 ± 0.09	-	0.334 ± 0.025.4	(Ibrahim *et al*., 2019)
chitosan–nanocellulose biocomposites	56.52	17.60	-	90.78	0.23	(Danial *et al*., 2014)
Wheat bran starch film	35	16.66	1.54	5.6	0.47	This study
WS fiber-reinforced Wheat bran starch film	30	10.85	1.62	4.8	0.51	

f. Biodegradability: In this study, biodegradability testing was done to measure the rate of decomposition of bioplastic films were shown in Figure 4.17. The mass reduction in bioplastic film was performed for 4, 8, 12, and 16 days concerning the concentration of glycerol and fiber. Therefore, the maximum biodegradation of bioplastic film obtained was found to be 86.7 % at a period of 16 days. The high concentration of glycerol in bioplastic films resulted in a rapid bulk loss and decompose more quickly, due to the hydrophilic character of glycerol making them an environmentally acceptable packaging material, whereas, cellulose fiber is hydrophobic so it prevents mass losses of bioplastic films in a short period.

The rate of deterioration of a compound is determined not only by the molecule's durability, but also by the pH, temperature, humidity, and oxygen content of the surrounding environment (Gómez *et al*, 2013).

Table 4.14: Results for biodegradation of bioplastic film.

Glycerol concentration (ml)	Degradation of bioplastics (%)											
	Concentration of fiber (g)											
	4 Days			8 Days			12 Days			16 Days		
	5	10	15	5	10	15	5	10	15	5	10	15
30 %	19.5	-	16	35.3	-	32.75	48.6	-	44.3	65.6	-	63.6
35 %	-	22.9	-	-	41.5	-	-	54.2	-	-	73.1	-
40 %	31.5	-	28.7	54.8	-	51.8	67.2	-	65.21	86.7	-	81.35
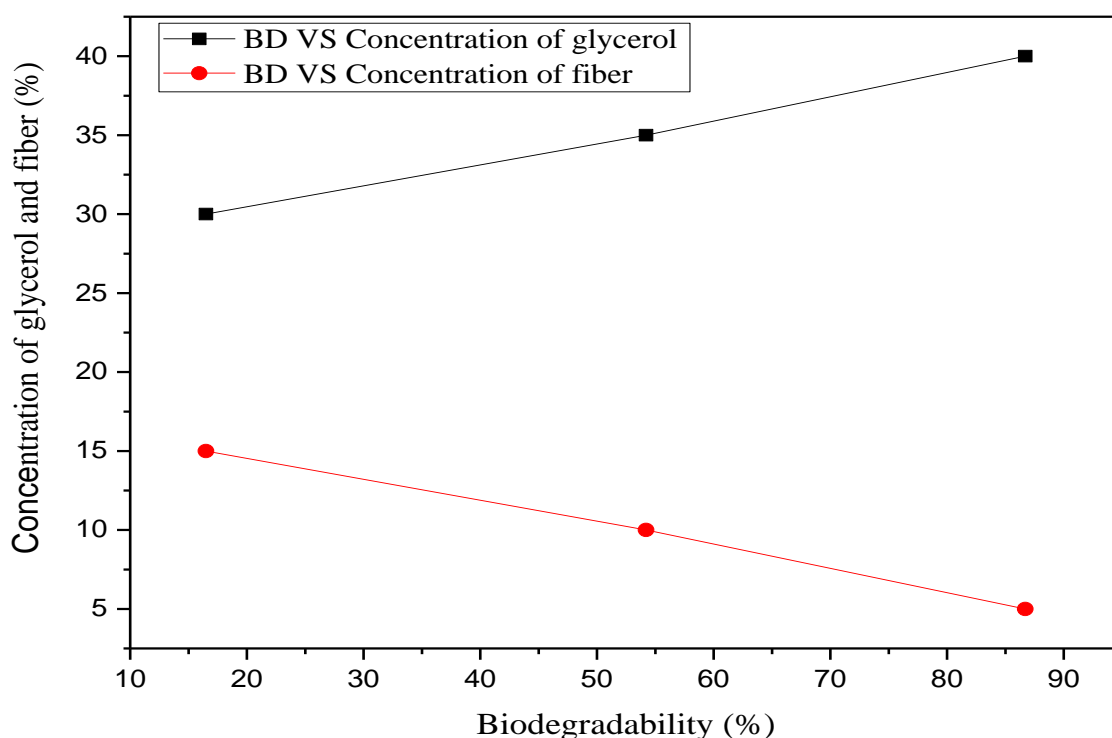
Figure 4.17: biodegradability of bioplastic as a function of the concentration of glycerol and fiber.

4.5.1 X-ray diffraction (XRD) analysis of bioplastic film

Figure 4.18 shows the XRD of both fiber-reinforced and controlled film. It can be realized that the characteristic diffraction peaks at 2θ of 5.7^o, 15.6^o, $20.3^{o,}$ and d-spacing were about 15.5, 5.67, and 4.37 for fiber-reinforced wheat bran starch-based bioplastic film, whereas 12.1^o and 25° and d-spacing were about 14.6 and 3.56 for the controlled film. The crystallinity of fiber-reinforced film was 35.4, whereas the controlled film was 29.2. The increase in the width of the peaks also indicates the reduced crystalline size and the low crystallinity of bioplastic film. It was discovered

that when wheat straw fiber was added to the starch-based film, the areas of crystallinity was increased due to high peak.
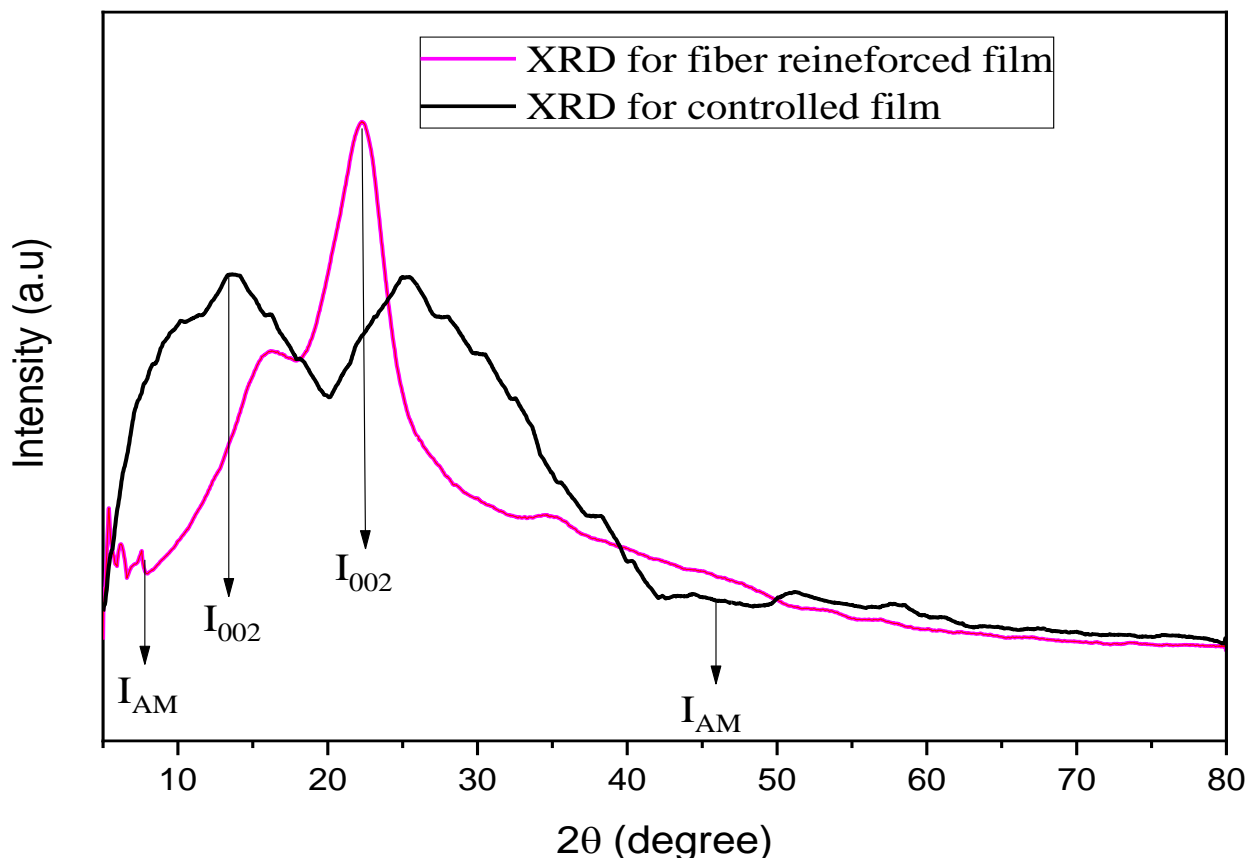
Figure 4.18: XRD pattern of the bioplastic film.

4.5.2 Fourier Transform Infrared (FTIR) analysis of the bioplastic film

FT-IR spectra of wheat bran starch-glycerol-based films with cellulosic fiber and non-cellulosic were in the range from (4000 - 400 cm^{-1}) region are shown in Figure 4.19. Based on (Figure 4.19), the FTIR spectra showed peak absorptions around the wavenumbers 3754 - 3542, 3050 - 2939, 2140, 1750, 1610, 1430, and 915 cm^{-1} for both films. There is a peak of the wavenumber 3754 - 3542 cm^{-1}, which was assigned to hydrogen-bonded hydroxyl groups or the stretching vibration of O-H (type of phenol compound, hydrogen bonding alcohol). This behavior might be due to hydrogen bond formation occurring after the addition of fiber. To confirm the increase in intermolecular hydrogen bonding, it can be observed that the band was slightly broadened after the addition of wheat straw cellulose fiber. The peak with the wavenumbers of 3050 - 2939 cm^{-1} could be attributed to the stretching of the C-H bond (type alkane compound) in CH$_2$. Peak with wave numbers 2140 cm^{-1} corresponds to the absorption caused by the triple bonds of C≡C stretch

(alkyne type compounds). At the peak with the wavenumbers 1750 cm^{-1} and 1610 cm^{-1}, corresponding to the absorption caused by the bonding C = O (a type of aldehyde, ketone, carboxylic acid, esters) and C=C (a type of alkene compound) respectively. At the peak with wavenumbers of 1430 cm^{-1} and 915 cm^{-1}, corresponds to absorption caused by the C-H bend (alkane type compound), and C-O (a type of alcohol, carboxylic acid, ester). Most probably absorption peaks between the 1400 - 600 cm^{-1} in the range are named as the fingerprint region. In general, wheat bran starch-based bioplastic with glycerol and with and without fiber reinforcement has a functional group which is a combination of specific functional groups contained in its constituent components such as C-H, O-H, C-O, C≡C, C = O, and C = C. The wavenumber of the functional group OH in wheat straw fiber-reinforced differs from the wheat bran starch-based bioplastic film. Additionally, wheat straw fiber consists of polysaccharide compounds (cellulose, hemicellulose) and macromolecule polyphenolic compound (lignin). The treatment of wheat straw fiber removes hemicellulose, lignin, waxes, and oil. The only difference is wheat straw fiber has a rough surface due to the fiber aggregation which can be removed by NaOH (Arbanah *et al*, 2018).
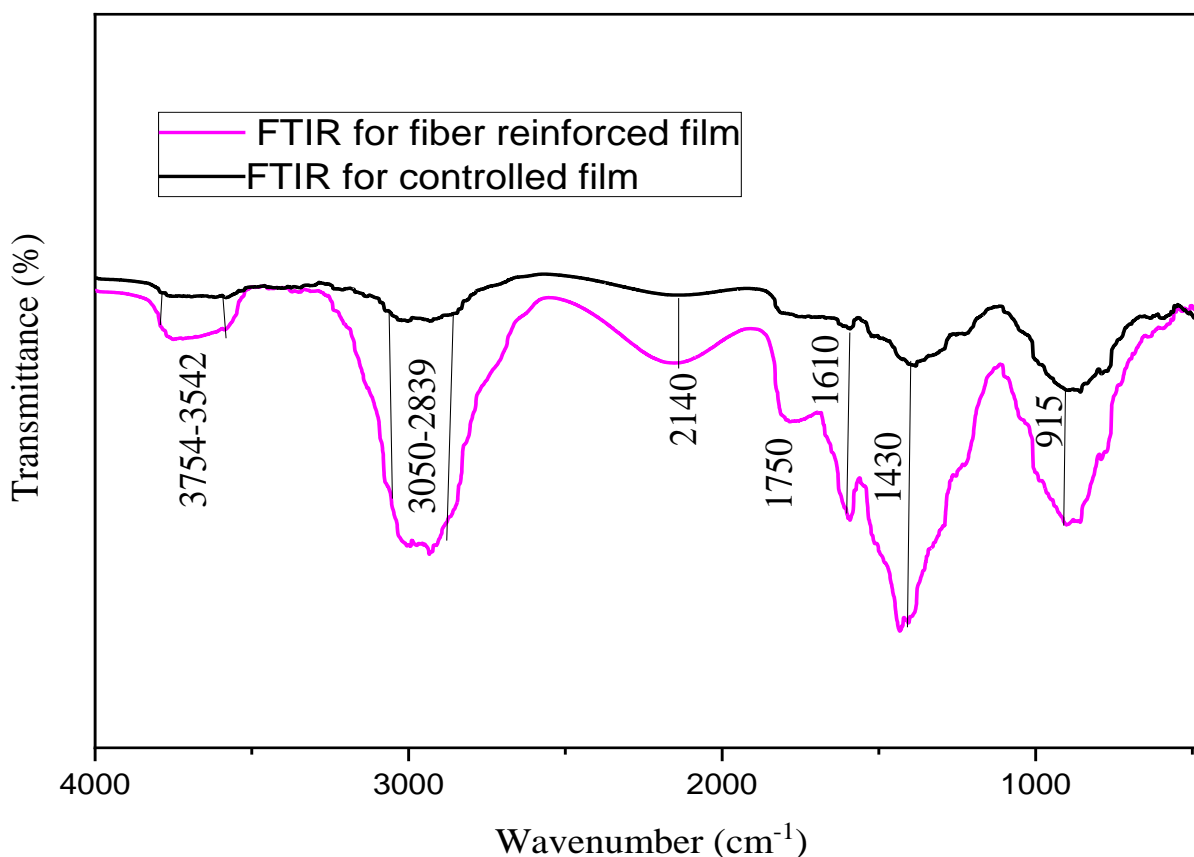
Figure 4.19: FT-IR spectra of the bioplastic film.

4.5.3 Thermogravimetric analysis (TGA) of bioplastic film

Thermal degradation can be studied through TGA. It is a technique for measuring the variation in mass as a function of time or temperature when a sample is a temperature scanned in a controlled, inert, or oxidative atmosphere. A three-step process is involved in the heat degradation of the bioplastic film in a nitrogen atmosphere. The TGA curves of the starch-based bioplastic film with and without wheat straw reinforcement and glycerol plasticized were shown in (Figure 4.20). There is 16.5 % occurred at 20 °C to 270 °C for reinforced film and 14.8 % occurred at 20 to 174 °C for the controlled film. Weight loss at this stage is caused by moisture or water evaporation from the material, according to (Azwa *et al*., 2013).

The second stage is the process of releasing volatile matter that occurred at 270 to 402 °C for reinforced film and 174 °C to 404.5 °C for the controlled film. There is 65 % weight loss for reinforced film and 67.2 % for the controlled film. The process of this stage causes quick thermal decomposition with a large mass loss and runs quickly due to the considerable amount of oxygen.

The third stage is the stage after the release of volatile matter which leaves or forms carbon in the samples occurred at the temperature of 402 to 450 °C for reinforced and 405 to 450 °C for controlled film. The fixed carbon content of bioplastic was relatively low, i.e., 12.5 %. In this stage, the charcoal is flammable as it is surrounded by volatile matter and oxygen is diffused on the surface of the charcoal, which burns the charcoal and volatile matter simultaneously (Wahyuningtiyas *et al*., 2017). This shows that the incorporation of highly thermal resistant cellulosic fiber which is extracted from the wheat straw is the highest option to advance the thermal stability of the film. Since starch is more hydrophilic than fiber initially, low volatile components are vaporized in the controlled film rapidly than the reinforced film. In general, as shown from (Figure 4.20) the weight loss for the controlled film rises more quickly than the reinforced bioplastic film.
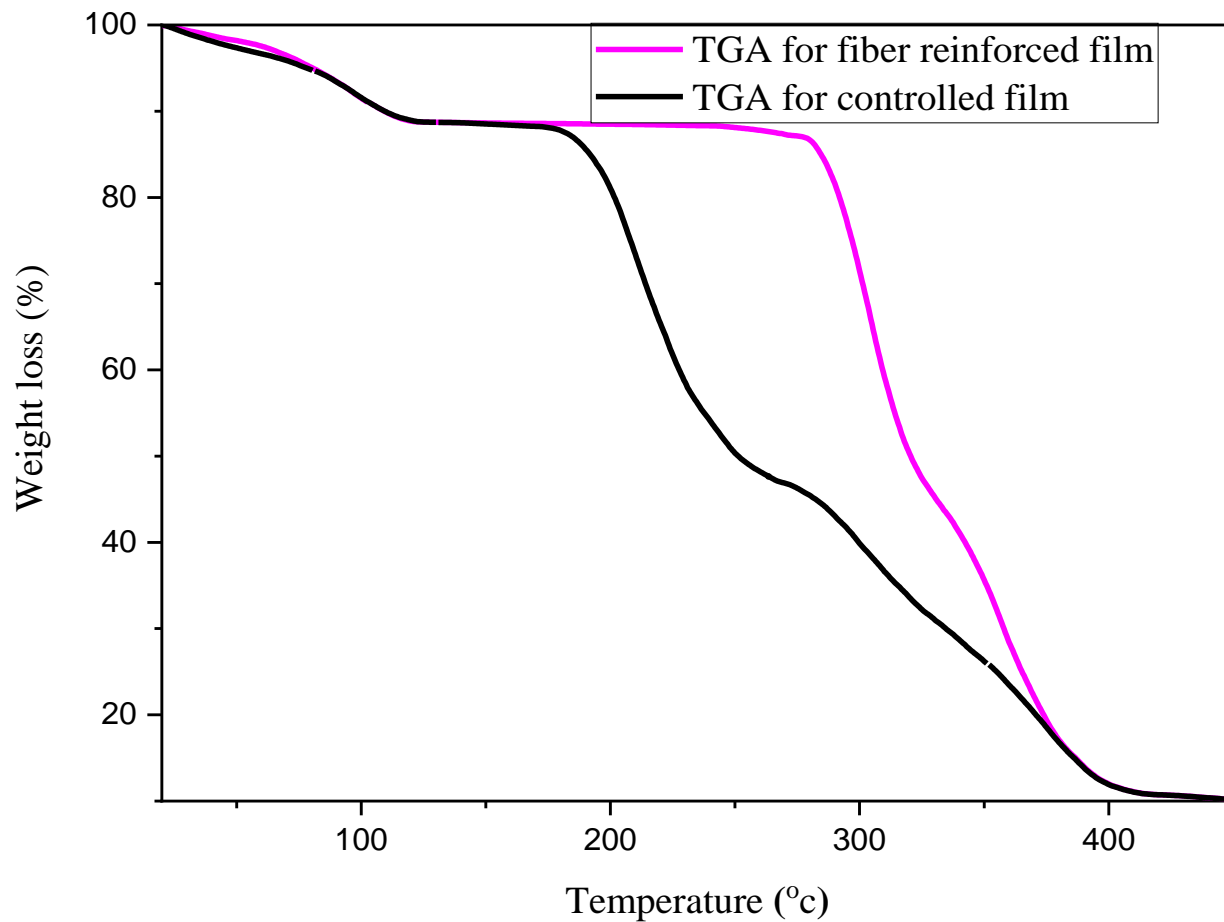
Figure 4.20: TGA curve for the bioplastic film.

5   CONCLUSION AND RECOMMENDATION

5.1 Conclusion

In this research, the bioplastic film from wheat bran starch and wheat straw fiber was successfully developed by using glycerol as a plasticizer. The proximate analysis of wheat bran and wheat straw was performed. Bioplastics made from only starch have high water sensitivity, poor mechanical and thermal properties, which can be improved by adding cellulosic fillers. The physicochemical characteristics of the prepared starch and fiber samples were examined using analytical methods.

During the synthesis of bioplastics films, the effects of independent variables (oven drying temperature, concentration of glycerol, and concentration of fiber) on tensile strength, elongation at break, and water absorption were studied using response surface methodology. From the conducted experiment, the recorded result shows that the maximum tensile strength, minimum elongation at break, and minimum water absorption were chosen by using numerical optimization.

The optimum conditions of tensile strength, elongation at break, and water absorption were obtained at an oven drying temperature, concentration of glycerol, and concentration of fiber of 55 $^{\circ}$C, 31.97 %, and 14.40 %, respectively, with the desirability of 0.971. Under these conditions, the maximum tensile strength, minimum elongation at break, and water absorption of 20.528 Mpa, 8.1 %, and 19.44 %, respectively, were obtained. The validation of the model with the error rate of tensile strength, elongation at break, and water absorption was 1.02 %, 0.6 %, and 1.4 % respectively. Thus, the results of this study can be declared valid (error $<$5 %). The physicochemical properties of bioplastic film were studied at the optimum point such as density (1.54 g/ml), moisture content (16.66 %), solubility (35 %), transparency (5.6 %), and thickness (0.47 mm). The crystallinity, functional group, and thermal stability of film were studied by using XRD, FTIR, and TGA respectively. The duration of bioplastic degradation (86.7 %) produced from the optimum value is 16 days. The finding of the study shows that wheat bran starch and wheat straw fiber can be explored as promising alternative feedstocks for the commercial production of bioplastic film.

5.1 Recommendation

In this study, for bioplastic film production, only the effects of three independent factors were explored. Further investigation needed for the selection of several factors for bioplastic production in lab scale such as the particle size of wheat bran starch and wheat straw fiber, stirring speed, gelatinization temperature, and the use of different plasticizers (sorbitol and polyvinyl alcohol) on the quality, mechanical and physicochemical property of bioplastic film. However, the wheat bran and wheat straw collected from different parts of our country, and the mineral concentration of the soil will affect the composition, as well as the production of starch and fiber. As a result, collecting wheat bran and wheat straw from particular parts of our country to explore the impacts is recommended. In addition, extensive research is required on the permeability (water vapor and gas transmission rates), barrier properties, and the effect of hydrophobic plasticizers, and the effectiveness of this bioplastic film on a different application. This research area needs consideration from communities, researchers, universities, and governments because it is unindustrialized area in our country. Additionally, the characterization of bioplastic films by other characterization methods that were not used in this work due to unavailability, such as scanning electron microscope (SEM) needs further investigation.

References

Abdul, M., Bhuyain, B., Hossain, I., & Jewel, A. (2019). Determination of the Proximate Composition of Available Fish Feed Ingredients in Bangladesh. 1 (January), 2013–2014.

Abioye, O. P., Abioye, A. A., Afolalu, S. A., & Ongbali, S. O. (2018). A review of biodegradable plastics in Nigeria. *International Journal of Mechanical Engineering and Technology (IJMET)*, *9*(10).

Abugoch, L. E., Tapia, C., Villamán, M. C., Yazdani-Pedram, M., & Díaz-Dosque, M. (2011). Characterization of quinoa protein–chitosan blend edible films. *Food Hydrocolloids*, *25*(5), 879-886.

Adeyefa, O. S. (2015).Biodegradable starch film from cassava, corn, potato, and yam. Chemistry and Materials Research, 7(12), 15–24.

Alcázar-Alay, S. C., & Meireles, M. A. A. (2015). Physicochemical properties, modifications, and applications of starches from different botanical sources. *Food Science and Technology*, *35*(2), 215-236.

Al, R., Sujuthi, F. M., & Liew, K. C. (2016). Properties of bioplastic sheets made from different types of starch incorporated with recycled newspaper pulp. Journal of Food Technology, 3, 257–264.

Al-Enizi, A. M., Zagho, M. M., & Elzatahry, A. A. (2018). Polymer-based electrospun nanofibers for biomedical applications. *Nanomaterials*, *8*(4), 259.

Ali, A., Yu, L., Liu, H., Khalid, S., Meng, L., & Chen, L. (2017). Preparation and characterization of starch-based composite films reinforced by corn and wheat hulls. *Journal of Applied Polymer Science*, *134*(32), 45159.

Altemimi, A. B. (2018). Extraction and optimization of potato starch and its application as a stabilizer in yogurt manufacturing. Journal of Food Science, 1-11.

Amri, A., Ekawati, L., Agustin, Y. E., Padmawijaya, K. S., & Kartika, T. (2018). Mechanical properties of bioplastics cassava starch film with Zinc Oxide nanofiller as reinforcement.IOP Conf. Series: Materials Science and Engineering 210 (2018) 012015

Amiri, A., Triplett, Z., Moreira, A., Brezinka, N., Alcock, M., & Ulven, C. A. (2017). Standard density measurement method development for flax fiber. *Industrial crops and products*, *96*, 196-202.

Andreas Künkel, J. B. (2016, September 29). "Polymers, Biodegradable". *Ultimate Encyclopedia of industrial chemistry*, pp. 1-29.

Anne, B. (2011). Environmental-friendly biodegradable polymers and composites. *Integrated waste management*, 341-364.

Anteneh, A., & Asrat, D. (2020). Wheat production and marketing in Ethiopia: Review study. *Cogent Food & Agriculture*, *6*(1), 1778893.

Apprich, S., Tirpanalan, Ö., Hell, J., Reisinger, M., Böhmdorfer, S., Siebenhandl-Ehn, S., ... & Kneifel, W. (2014). Wheat bran-based biorefinery 2: Valorization of products. *LWT-Food Science and Technology*, *56*(2), 222-231.

Arbanah Muhammad, Ahmad Ramli Rashidi, M. M. H. S. B., &Material. (2018). *Effect of Coconut Fiber Reinforcement on Mechanical Properties of Corn Effect of Coconut Fiber Reinforcement on Mechanical Properties of Corn Starch Bioplastics*. *October*.

Ardiansyah, R. (2011). Pemanfaatan Pati Umbi Garut untuk Pembuatan Plastik Biodegradable. *D epok: Universitas Indonesia*.

Arikan, E. B., & Bilgen, H. D. (2019). Production of bioplastic from potato peel waste and investigation of its biodegradability. *International Advanced Researches and Engineering Journal*, *3*(2), 93-97.

Arikan, E. B., & Ozsoy, H. D. (2015). A review: investigation of bioplastics. *J. Civ. Eng. Arch*, *9*, 188-192.

Ascheri, D. P. R., MOURA, W. D. S., Ascheri, J. L. R., & de Carvalho, C. W. P. (2010). Caracterização física e físico-química de rizomas e amido do lírio-do-brejo (Hedychium coronarium). *Embrapa Agroindústria de Alimentos-Artigo em periódico indexado (ALICE)*.

Avérous, L., & Pollet, E. (2014). Nanocomposites based on plasticized starch. In *Starch Polymers* (pp. 211-239). Elsevier.

Aviles Trujillo, L. (2017). Characterization of a biomaterial composed of agricultural waste for application as a thermal insulator (Master's thesis, University of Sciences and Arts of Chiapas).

Azwa, Z. N., Yousif, B. F., Manalo, A. C., & Karunasena, W. (2013). A review on the degradabi lity of polymeric composites based on natural fibres. *Materials & Design*, *47*, 424-442.

Babu, R. P., O'Connor, K., & Seeram, R. (2013). Current progress on bio-based polymers and their future trends. *Progress in Biomaterials*, 2(8).

Balaji, A. N., & Nagarajan, K. J. (2017). Characterization of alkali treated and untreated new cellulosic fiber from Saharan aloe vera cactus leaves. *Carbohydrate Polymers*, 174, 200-208.

Bejena, B. D. (2019). Synthesis and Experimental Study of Production Bioplastic from Banana Peels. October.

Bertuzzi, M. A., Gottifredi, J. C., & Armada, M. (2012). Mechanical properties of a high amylose content corn starch based film, gelatinized at low temperature. *Brazilian Journal of Food Technology*, *15*, 219-227.

Brazel, C. S., & Rosen, S. L. (2012). Fundamental principles of polymeric materials. John Wiley & Sons.

Cafer, A. M., & Rikoon, J. S. (2018). Adoption of new technologies by smallholder farmers: the contributions of extension, research institutes, cooperatives, and access to cash for improving tef production in Ethiopia. *Agriculture and human values*, *35*(3), 685-699.

Catálise, L. De, Universidade, A., & Avenida, F. (2017). Bioplastics production from starch and chitosan blends.Journal of polymers, 9, 46–53.

Chavan, U. D., Shinde, B. G., Kadam, S. S., & Amarowicz, R. (2010). Isolation and characterization of starch from horse gram. *African Journal of Food Science and Technology*, *1*(3), 64-67.

Chufo, Akiber, Hairong Yuan, Dexun Zou, Yunzhi Pang, and Xiujin Li. 2015. ―Biomethane Production and Physicochemical Characterization of Anaerobically Digested Teff (Eragrostis Tef) Straw Pretreated by Sodium Hydroxide.‖ *Bioresource Technology* 181 (April): 214–19. https://doi.org/10.1016/j.biortech.2015.01.054.

Civancik-uslu, D., Ferrer, L., Puig, R., & Fullana-i-palmer, P. (2018). Science of the Total Environment Are functional fillers improving the environmental behavior of plastics ? A review on LCA studies. *Science of the Total Environment*, *626*, 927–940.

Curvelo, A.A.S., Carvalho, A.J.F.D. and Angelli, J. A. M. . (2011). Thermoplastic starch-cellulosic fibers composites: preliminary results. . 2001: *Carbohydrate Polymers*. 45, 183- 188.

CSA, (2017). Agriculture Sample Survey 2015/16.

Amalia, D., Saleh, D., & Djonaedi, E. (2020). Synthesis of biodegradable plastics using corn starch and corn husk as the fillers as well as chitosan and sorbitol. In *Journal of Physics: Conference Series* (Vol. 1442, No. 1, p. 012007). IOP Publishing.

Dehnad, D., Emam-Djomeh, Z., Mirzaei, H., Jafari, S. M., & Dadashi, S. (2014). Optimization of physical and mechanical properties for chitosan–nanocellulose biocomposites. *Carbohydrate Polymers*, *105*, 222-228.

DiGregorio, B. E. (2009). Biobased performance bioplastic: Mirel. *Chemistry & Biology*, *16*(1), 1-2.

Ebisike, K., AttahDaniel, B. E., Babatope, B., & Olusunle, S. O. O. (2013). Studies on the extraction of naturally-occurring banana fibers. *Int J Eng Sci*, *2*(9), 9.

Edhirej, A., Sapuan, S. M., Jawaid, M., & Zahari, N. I. (2017). Effect of various plasticizers and concentration on the physical, thermal, mechanical, and structural properties of cassava-starch-based films. *Starch‐Stärke*, *69*(1-2), 1500366.

Emadian, S. M., Onay, T. T., & Demirel, B. (2017). Biodegradation of bioplastics in natural environments. *Waste management*, *59*, 526-536.

Eric, P., & Luc, A. (2014, January 1). "Nanobiocomposites Based on Plasticized Starch". In L. A. Pollet, *Starch Polymers* (pp. Pp 211-239). France: ELSEVIER.

Ezeoha, S. L., & Ezenwanne, J. N. (2013). Production of Biodegradable Plastic Packaging Film from Cassava Starch, *3*(10), 14–20.

Gadhave, R. V, Das, A., Mahanwar, P. A., & Gadekar, P. T. (2018). Starch-Based Bio-Plastics : *The Future of Sustainable Packaging*. 21–33.

Gail, M., C, P. G., & G, A. L. (2016). Extraction of starch from banana (Musa sapientum) peel to produce bioplastic. *Proceedings of 146th The IIER International Conference, Hong Kong (December).*

Galicia-Garcia, T. M.-B.-A.-G.-M.-D. (2011). Thermal and microstructural characterization of biodegradable films prepared by the extrusion-calendering process. *Carbohydrate polymers. 83, 354-361.*

García R, Pizarro C, Lavín A, B. J. (2014). Spanish biofuels heating value estimation. Part II: proximate analysis data. *Fuel, 117:1139-47.*

Gaspar, M., Benkő, Z., Dogossy, G., Reczey, K., & Czigany, T. (2005). Reducing water absorption in compostable starch-based plastics. *Polymer Degradation and Stability, 90(3), 563-569.*

Gebreselassie, Samuel; Haile, Mekbib G.; Kalkuhl, M. W. (2017). The wheat sector in Ethiopia: Current status and key challenges for future value chain development.

Gertz, J. E. (2016). The Earth Is Becoming a Plastic Planet. Retrieved November 8, 2017, from http://www.takepart.com/article/2016/01/29/earth-becoming-plastic-planet

Geyer, R., Jambeck, J. R., & Law, K. L. (2017). Production, use, and the fate of all plastics ever made. *Science advances*, *3*(7), e1700782.

Glenn, G. M., Orts, W., Imam, S., Chiou, B. S., & Wood, D. F. (2014). Starch plastic packaging and agriculture applications. *In Starch Polymers (pp. 421-452). Elsevier.*

Gómez, E. F., & Michel Jr, F. C. (2013). Biodegradability of conventional and bio-based plastics and natural fiber composites during composting, anaerobic digestion, and long-term soil

incubation. *Polymer Degradation and Stability*, *98*(12), 2583-2591.

Gozan, M., & Noviasari, C. (2018). The effect of glycerol addition as a plasticizer in bioplastics. *67,11–14.*

Gujar, S., Pandel, B., & Jethoo, A. S. (2014). Effect of plasticizer on mechanical and moisture absorption properties. *An International Quarterly Scientific Journal.13(2), 425-428.*

Habte, E., Alemu, D., Amsalu, B., & Yirga, C. (2018). Production and marketing of major lowland pulses in Ethiopia: Review of developments, trends, and prospects. *Ethiopian Journal of Crop Science*, *6*(3), 435-465.*in Oromia National and Regional State*.

Habte, Z., Legesse, B., Haji, J., & Jeleta, M. (2016). Supply analysis in the wheat industry : contributions of value chain analysis in Ethiopia *: Cases from Arsi and East Shewa Zones*

Hadisoewignyo, L. (2018). Isolation and characterization of Agung banana peel starch from East Java Isolation and characterization of Agung banana peel starch from East Java Indonesia. January 2017.

Halley, P. and M. C. F. F. (2016). The future of plastics - Curious.

Hammer, J., M.H.S. Kraak, and J. R. P. (2012). Plastics in the marine environment: the dark side of a modern gift. 8*Reviews of environmental contamination and toxicology*, 1-44.

Harahap, M. B., & Ginting, M. H. S. (2018). Production of bioplastic from avocado seed starch reinforced with microcrystalline cellulose from sugar palm fibers. *February 2020*.

Harunsyah. (2018). The effect of clay nanoparticles as reinforcement on mechanical properties of bioplastic base on cassava starch. *0–7.*

Hell, J., Kneifel, W., Rosenau, T., & Boehmdorfer, S. (2014). Analytical techniques for the elucidation of wheat bran constituents and their structural features with emphasis on dietary fiber–a review. *Trends in food science & technology*, *35*(2), 102-113.

Imre, B., & Pukánszky, B. (2013). Compatibilization in bio-based and biodegradable polymer blends. *European Polymer Journal*, *49*(6), 1215-1233.

Ibrahim, M. I. J., Sapuan, S. M., Zainudin, E. S., Zuhri, M. Y. M., Sapuan, S. M., Zainudin, E. S., & Zuhri, M. Y. M. (2019). Physical, thermal, morphological, and tensile properties of cornstarch-based films as affected by different plasticizers. *International Journal of Food Properties*, *22*(1), 925–941.

Iriani, E. S. (2019). The Effect of Agricultural Waste Nanocellulose on The Properties of Bioplastic for Fresh Fruit Packaging.

Jain, R., & Tiwari, A. (2015). Biosynthesis of planet-friendly bioplastics using renewable carbon sources. *Journal of Environmental Health Science and Engineering*, *13*(1), 1-5.

Jianlei Yang 1, Yern Chee Ching 1, and C. H. C. 2 1. (2019). Applications of Lignocellulosic Fibers and Lignin in Bioplastics: *A Review*. 1–26.

Jouhara, H., Czajczynsa, D., Ghazal, H., Anguliano, L., Reynolds, A., & spencer, N. (2017, November 5). Municipal waste management systems for domestic use. *Journal of Energy, 139*(1), pp.485-506.

Kalia, S., Kaith, B. S., & Kaur, I. (2009). Pretreatments of natural fibers and their application as reinforcing material in polymer composites—a review. *Polymer Engineering & Science*, *49*(7), 1253-1272.

Kasmani, J. E., & Samariha, A. (2011). Some Chemical and Morphological Properties of Wheat Straw. *Middle-East Journal of Scientific Research*, *8*(4), 823–825.

Kaur M, and Singh S 2016 *International Journal of Food Properties*19 2432

Kaushik, A., & Singh, M. (2011). Isolation and characterization of cellulose nanofibrils from wheat straw using steam explosion coupled with high shear homogenization. *Carbohydrate Research, 346(1), 76-85.*

Kelly, Cristina Coelho, De Carvalho Benini, Jacobus Cornelis Voorwald, Maria Odila Hil, Mirabel Cerqueira Rezende, and Valdeir Arantes. 2018. ―Preparation of Nanocellulose from Imperata Brasiliensis Grass Using Taguchi Method.‖ *Carbohydrate Polymers*, 1–19.

Kershaw, P. J. (2016). Marine plastic debris and microplastics–Global lessons and research to inspire action and guide policy change.

Keziah, V. S., Gayathri, R., & Priya, V. V. (2018). Biodegradable plastic production from corn starch. Research articles, 10(7), 1315–1317.

Khan, T. S., & Mubeen, U. (2017). *Wheat Straw : A pragmatic overview*. *November 2012*.

Kuorwel, k., Cran, M., Sonneveld, k., Miltz, J., & Bigger, S. (2011, November). Essential oils and their principal constituents as antimicrobial agents for synthetic packaging films. *J Food Science, 76*(9), Pp 164-177.

Leta, S., & Mesele, F. (2014). Spatial analysis of cattle and shoat population in Ethiopia: growth trend, distribution, and market access. *SpringerPlus*, *3*(1), 1-10.

Li, Jinpeng, Bin Wang, Kefu Chen, Xiaojun Tian, Jinsong Zeng, Jun Xu, and Wenhua Gao. (2018). "Optimization of Pretreatment and Alkaline Cooking of Wheat Straw on Its Pulpability Using Response Surface Methodology." *BioResources* 13 (1): 27–42.

Liu, R., Yu, H., & Huang, Y. (2005). Structure and Morphology of Cellulose in Wheat Straw. *June 2014*.

Liu, W., Mohanty, A. K., Drzal, L. T., Askel, P., & Misra, M. (2004). Effects of alkali treatment on the structure, morphology, and thermal properties of native grass fibers as reinforcements for polymer matrix composites. Journal of Materials Science, 39(3), 1051-1054.

Lucas, Nathalie, Christophe Bienaime, Christian Belloy, Michèle Queneudec, Françoise Silvestre, and José-Edmundo Nava-Saucedo. "Polymer biodegradation: Mechanisms and estimation techniques–A review." Chemosphere 73, no. 4 (2008): 429-442.

Luchese, C. L., Garrido, T., Spada, J. C., Tessaro, I. C., & de la Caba, K. (2018). Development and characterization of cassava starch films incorporated with blueberry pomace. *International journal of biological macromolecules*, *106*, 834-839.

Ma, H., & Deng, M. (2017). An optimized procedure for determining the amylase/amylopectin ratio in common wheat grains based on the dual wavelength iodine binding method Journal of Polymer & Composites 1(1), 23–30.

Markus Klar, D. G. A P. C. H. U. D., (2014). Everything you don't want to know about plastics, *s.l.: Swedish society of nature conservation.*

Mashek, W. B., Krieger, P., & Martin, K. (2016). Watching: Bioplastics. Plastics Market Watch. Washington, DC.

Maulida. (2018). Utilization of mango seed starch in the manufacture of bioplastic reinforced with microparticle clay using glycerol as a plasticizer. 0–7.

Maulida, M. S., & Tarigan, P. (2016). Production of starch based bioplastic from cassava peel reinforced with microcrystalline celllulose avicel PH101 using sorbitol as plasticizer. In *J. Phys. Conf. Ser* (Vol. 710, p. 12012).

McCleary, B. V., & Monaghan, D. A. (2002). Measurement of resistant starch. *Journal of AOAC International, 85(3), 665-675.*

Mehta, V., Darshan, M., & Nishith, D. (2014). Can starch-based plastic be an option of environmentally friendly plastic? *Journal of global biosciences*, *3*(3), 681-685.

Mohanty, A. K., Wibowo, A., Misra, M., & Drzal, L. T. (2003). Development of renewable resource-based cellulose acetate bioplastic: Effect of process engineering on the performance of cellulosic plastics. *Polymer Engineering & Science*, *43*(5), 1151-1161.

Mohsen Esmaeili, Gholamreza Pircheraghi, R. B. (2017). Optimizing mechanical and physical properties of thermoplastic starch via tuning the molecular microstructurethrough co-plasticization by sorbitol and glycerol. *Polymer International*, 66/6, 809-819

Montero, G., Coronado, M. A., Torres, R., Jaramillo, B. E., García, C., Stoytcheva, M., Ana, M. V, Lambert, A. A., & Valenzuela, E. (2016). Higher heating value determination of wheat

Mosissa .G. (2018). Addis Ababa institute of technology school of chemical and bioengineering, Production and characterization of bioplastics from corn starch reinforced with sugar cane bagasse.

Muche, M. (2018) Production and Characterization of Starch-Based Antimicrobial Packaging Film thesis done from Addis Ababa University

Mukhopadhyay, R., Sree, K. D., Saneeha, R., Kale, P., & Iram, U. (2017). Preparation and characterization of biodegradable plast ics. International Journal for Research in Applied Science & Engineering Technology **(IJRASET)**, 5(8), 134–142.

Munoz, L.A.; pedreschi, F.; Lieva, A.; Aguilera, J. . (2015). *Loss of birefringence and swelling behavior in native starch granules: Microstructural and thermal properties. J. Food Eng. 152*, 65–71.

N. Johar, I. Ahmad, and A. D. (2012). "Extraction, preparation and characterization of cellulose fibers and nanocrystals from rice husk*," Industrial Crops and Products, vol. 37, no. 1, pp. 93–99*.

Naela Ulul Maslahah1, Darmawan Alisaputra1, and E. S. 1. (2021). Biodegradation Bioplastic Based on Arrowroot Starch with Glycerol Plasticizer and ZnO Fillers.

Nakason, C., Wohmang, T., Kaesaman, A., & Kiatkamjornwong, S. (2010). Preparation of cassava starch-graft-polyacrylamide superabsorbents and associated composites by reactive blending. *Carbohydrate Polymers, 81(2), 348-357*.

Nanang Eko Wahyuningtiyas 1,*, H. S. (2019). Analysis of Biodegradation of Bioplastics Made of Cassava Starch.

Naseri, A., Shekarchizadeh, H., & Kadivar, M. (2019). Octenylsuccination of sago starch and investigation of the effect of calcium chloride and ferulic acid on physicochemical and functional properties of the modified starch film. *Journal of Food Processing and Preservation*, *43*(3), e13898.

Nazir, M. S., Wahjoedi, B. A., Yussof, A. W., & Abdullah, M. A. (2013). Eco-friendly extraction and characterization of cellulose from oil palm empty fruit bunches. *BioResources*, *8*(2), 2161-2172.

Nigussie, A., Kedir, A., Adisu, A., Belay, G., Gebrie, D., & Desalegn, K. (2015). Bread wheat production in small-scale irrigation users agro-pastoral households in Ethiopia: Case of Afar and Oromia regional state. *Journal of Development and Agricultural Economics,* 7 (4), 123–130.

Njoku, C. E., Omotoyinbo, J. A., Alaneme, K. K., & Daramola, M. O. (2020). Characterization of Urena lobata fibers after alkaline treatment for use in polymer composites. *Journal of Natural Fibers,* 1–12.

Nuruddin, M., Tcherbi-Narteh, A., Hosur, M., Chowdhury, R. A., Jeelani, S., & Gichuhi, P. (2013). Cellulose microfibrils extracted from wheat straw: a novel approach. Proceedings of the 45th ISTC.

Obasi, H., Igwe, I., Ogbobe, O., Madufor, I., & Egeolu, F. (2012). Analysis of the mechanical and degradation performances of selected starch/polypropylene blends.

Offiong, E. U., & Ayodele, S. L. (2016). Preparation and characterization of thermoplastic starch from sweet potato. International Journal of Scientific & Engineering Research, 7(5), 438–443.

Oladayo, O. O., Umunna, Q. C. Joseph, O. S. and Oluwasegun, W. (2016). Physicochemical chemical properties of cassava starch and starch- keratin prepared biofilm. *Songklanakarin J. Sci. Technol.* 38 (4):349-355.

Orezzoli, A. V., Zavaleta, E., Pajares-Medina, N., Adolfo, S., Lescano, L., & Linares, G. (2018). Research Article Physicochemical and Mechanical Characteristics of Potato Starch-Based Biodegradable Films.

P, Jantrawut, T, Chaiwarit, and K, J. (2017). "Effect of Plasticizer Type on Tensile Property and In Vitro Indomethacin Release of Thin Films Based on Low-Methoxyl Pectin". *Molecular Diversity Preservation International and Multidisciplinary Digital Publishing Institute. pp 2*.

Pilla, S. ed. (2011). Handbook of Bioplastics and Biocomposites Engineering Applications, Scrivener Pub., Hoboken, NJ, Wiley; Salem, Mass.

Prachayawarakorn, J., Ruttanabus, P., & Boonsom, P. (2011). Effect of cotton fiber contents and lengths on properties of thermoplastic starch composites prepared from rice and waxy rice starches. *Journal of Polymers and the Environment*, *19*(1), 274-282.

Priedniece, V., Spalvins, K., Ivanovs, K., & Pubule, J. (2017). a review of bioproducts from potatoes. Environmental and Climate Technologies, 21, 18–27.

Prinsen, P., Gutiérrez, A., Faulds, C. B., & del Río, J. C. (2014). A comprehensive study of valuable lipophilic phytochemicals in wheat bran. *Journal of agricultural and food chemistry*, *62*(7), 1664-1673.

Rajam, R., & Parthasarathi, S. (2020). Bio-Based Biodegradable Plastics - *Boom In Food Industry*. *9*(03), 3018–3024.

Rajinipriya, M., Nagalakshmaiah, M., Robert, M., & Elkoun, S. (2018). Importance of agricultural and industrial waste in the field of nanocellulose and recent industrial developments of wood-based nanocellulose: a review. *ACS Sustainable Chemistry & Engineering*, *6*(3), 2807-2828.

Reddy, R. L., Reddy, V. S., & Gupta, G. A. (2013). Study of bio-plastics as a green and sustainable alternative to plastics. *International Journal of Emerging Technology and Advanced Engineering, 3(5), 76-81.*

Sain, M., & Panthapulakkal, S. (2006). Bioprocess preparation of wheat straw fibers and their characterization. *Industrial crops and products, 23(1), 1-8.*

Santana, Á. L., & Meireles, M. A. A. (2014). New starches are the trend for industry applications: a review. *Food and public health, 4(5), 229-241.*

Saridewi, N., & Malik, M. (2019). Food packaging development of bioplastic from basic waste of cassava peel (manihot uttilisima) and shrimp shell. In *IOP Conference Series: Materials Science and Engineering* (Vol. 602, No. 1, p. 012053). IOP Publishing.

Sariningsih, N., Putra, Y. P., Pamungkas, W. P., Agustin, Y. E., & Padmawijaya, K. S. (2018). Bioplastic from chitosan and yellow pumpkin starch with castor oil. IOP Conf. Series: Materials Science and Engineering, 333 (2018) 012087.

Shah, M., Rajhans, S., Pandya, H. A., & Mankad, A. U. (2021). Bioplastic for future: A review then and now. *World Journal of Advanced Research and Reviews*, *9*(2), 056-067.

Shamsuddin, I. M., Jafar, J. A., Shawai, A. S. A., Yusuf, S., Lateefah, M., & Aminu, I. (2017). Bioplastics as better alternative to petroplastics and their role in national sustainability: a review. *Advances in Bioscience and Bioengineering*, *5*(4), 63.
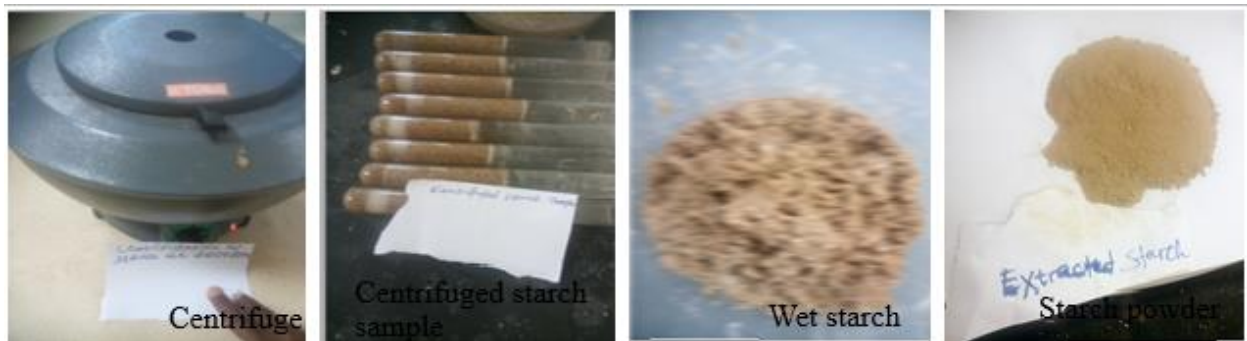
Shiferaw, E., Tadilo, W., Melkie, I., & Shiferaw, M. (2019). Sero-prevalence and trends of transfusion-transmissible infections among blood donors at Bahir Dar district blood bank, northwest Ethiopia: A four-year retrospective study. *PLoS One*, *14*(4), e0214755.

Slopiecka, K., Bartocci, P., & Fantozzi, F. (2012). Thermogravimetric analysis and kinetic study of poplar wood pyrolysis. *Applied Energy*, *97*, 491-497.

Suppakul, P., Chalernsook, B., Ratisuthawat, B., Prapasitthi, S., & Munchukangwan, N. (2013). Empirical modeling of moisture sorption characteristics and mechanical and barrier properties of cassava flour film and their relation to plasticizing–antiplasticizing effects. *LWT-Food Science and Technology*, *50*(1), 290-297.

Swamy, J. N., & Singh, B. (2010). Bioplastics and global sustainability. Plastics Research Online. *Society of Plastics Engineers*, *10*.

Talja, R. A., Helén, H., Roos, Y. H., & Jouppila, K. (2008). Effect of type and content of binary polyol mixtures on physical and mechanical properties of starch-based edible films. *Carbohydrate Polymers*, *71*(2), 269-276.

Tanetrungroj, T. and Prachayawarakorn, J. (2015). Effect of starch types on properties of biodegradable polymer based on the thermoplastic starch process by an injection molding technique. *Songklanakarin J. Sci. Technology.,* 37 (2): 193-199.

Tegangan, S., & Air, P. (2011). *Tensile and water absorption properties of biodegradable composites derived from cassava skin / polyvinyl alcohol with glycerol as a plasticizer, journal of biotechnology. 40(7), 713–718.*

Tang, X., Alavi, S., & Herald, T. J. (2008). Barrier and mechanical properties of starch-clay nanocomposite films. *Cereal Chemistry, 85(3), 433-439.*

Thielen, M. (2014). Sustainability Opportunities and Challenges of Bioplastics.

Tufail, T., Saeed, F., Imran, M., Arshad, M. U., Anjum, F. M., Afzaal, M., ... & Hussain, S. (2018). Biochemical characterization of the wheat straw cell wall with special reference to bioactive profile. *International journal of food properties*, *21*(1), 1303-1310.
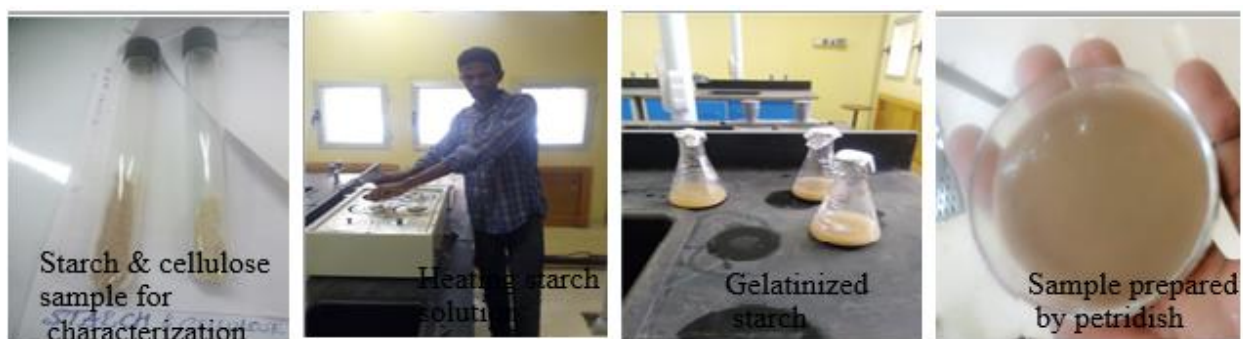
Uliana, A. (2019). Development of a Cassava Starch-Based Foam Incorporated grape stocks. *Journal of polymers and the environment, Journal home page*

Qasim, U., Ali, Z., Nazir, M. S., Ul Hassan, S., Rafiq, S., Jamil, F., ... & Saqib, S. (2020). Isolation of cellulose from wheat straw using alkaline hydrogen peroxide and acidified sodium chlorite treatments: Comparison of yield and properties. *Advances in Polymer Technology*, *2020*.

V, Koester, V. (2015). *"*Plasticizers – Benefits, Trends, Health, and Environmental Issues*".* *Chemistry Views.*

Van den Oever, M., Molenveld, K., van der Zee, M., & Bos, H. (Bio-based and biodegradable plastics: facts and figures: *focus on food packaging in the Netherlands* (No. 1722). Wageningen Food & Biobased Research.

Van der Harst, E., Potting, J., & Kroeze, C. (2014). Multiple data sets and modeling choices in a comparative LCA of disposable beverage cups. *Science of the Total Environment*, *494*, 129-143.

Wahyuningtiyas, N. E., & Suryanto, H. (2017). Analysis of biodegradation of bioplastics made of cassava starch. *Journal of Mechanical Engineering Science and Technology (JMEST)*, *1*(1), 24-31.

Wahyuningtiyas, N. E., & Suryanto, H. (2018). Properties of cassava starch-based bioplastics reinforced by nanoclay. Iranian Journal of Science and Technology, Vol. 1 No. 1, 2580-081.

Wakeyo, M., & Lanos, B. (2019). Analysis of price incentives for wheat in Ethiopia for the time period 2005-2012. *Gates Open Res*, *3(278)*, *27*.

Wang, Q.; Chen, Q.; Niida, H.; Mitsumura, N.; and Endo, T. (2014). Effect of water content on the crystalline structure of ionic liquids mixture pretreated microcrystalline cellulose (MCC). Materials Sciences and Applications. 5(4), 183–192.

Washam, C. (2010). *Plastics*. *April*, 10–12.

Wattanakornsiri, A., Pachana, K., Kaewpirom, S., Traina, M., & Migliaresi, C. (2012). Preparation and properties of green composites based on tapioca starch and differently recycled paper

cellulose fibers. *Journal of Polymers and the Environment*, *20*(3), 801-809.

Wittaya, T. (2012). Rice starch-based biodegradable films: properties enhancement. *Structure and function of food engineering*, *5*, 103-134.

Yue, H., Cui, Y., Yin, G., & Jia, Z. (2014). Preparation and environment-friendly cottonseed protein bioplastics. Porous Organic Polymers, 311-313.1851

Yehuala, G. A., & Emire, S. A. (2013). Antimicrobial activity, physicochemical and mechanical properties of aloe (Aloe debrana) based packaging films. *British Journal of Applied Science & Technology*, *3*(4), 1257.

Yussuf, A. A., Massoumi, I., & Hassan, A. (2010). Comparison of polylactic acid/kenaf and polylactic acid/rise husk composites: the influence of the natural fibers on the mechanical, thermal and biodegradability properties. *Journal of Polymers and the Environment*, *18*(3), 422-429.

Zaini, F., Kanani, A., Falahati, M., Fateh, R., Salimi-Asl, M., Saemi, N., ... & Nazeri, M. (2012). Identification of Prototheca zopfii from bovine mastitis. *Iranian journal of public health*, *41*(8), 84.

Zerihun, M., Worku, T., & Sakkalkar, S. R. (2016). Development and characterization of antimicrobial packaging films. Journal of ready to eat food, 03(02), 13–24.

Zhang, Y. R., Zhang, S. D., Wang, X. L., Chen, R. Y., & Wang, Y. Z. (2009). Effect of carbonyl content on the properties of thermoplastic oxidized starch. *Carbohydrate Polymers*, *78*(1), 157-161.

Zhou, H. (2016). Physicochemical Properties of Bioplastics and its Application for Fresh-cut Fruits Packaging. 1–117.

Appendixes

Appendix A: Supporting pictures during the study.

1. HCL 2. Ethanol
3. NaOH 4. H2O2
5. Glycerol

Centrifuge | Centrifuged starch sample | Wet starch | Extracted Starch Starch powder

size reduction of starch | Grounded powder | Furnace | Size reduction of straw by scissor

Ethanol dewaxing WS

Digested fiber

Stainless steel autoclave

Cellulose fiber

Starch & cellulose sample for characterization

Heating starch solution

Gelatinized starch

Sample prepared by petridish

Drying of film by oven

Controlled film

Figure A: laboratory works types of equipment, chemicals, and products.

Appendix B: Design expert 11 data

Table B₁: Fit summary for tensile strength

Source	Sequential p-value	Lack of Fit p-value	Adjusted R²	Predicted R²	
Linear	0.0238	< 0.0001	0.3316	0.2246	
2FI	0.7743	< 0.0001	0.2424	-0.3276	
Quadratic	**< 0.0001**	**0.9142**	**0.9953**	**0.9929**	**Suggested**
Cubic	0.8505	0.6780	0.9936	0.9806	Aliased

Table B₂: Fit summary for elongation at break

Source	Sequential p-value	Lack of Fit p-value	Adjusted R²	Predicted R²	
Linear	< 0.0001	0.0023	0.9244	0.9021	
2FI	0.2654	0.0024	0.9307	0.8944	
Quadratic	**0.0004**	**0.0595**	**0.9841**	**0.9433**	**Suggested**
Cubic	0.1623	0.0610	0.9898	0.6183	Aliased

Table B₃: Fit summary for water absorption

Source	Sequential p-value	Lack of Fit p-value	Adjusted R²	Predicted R²	
Linear	< 0.0001	< 0.0001	0.7487	0.6401	
2FI	0.2352	< 0.0001	0.7745	0.6726	
Quadratic	**< 0.0001**	**0.3666**	**0.9981**	**0.9949**	**Suggested**
Cubic	0.2221	0.6921	0.9987	0.9962	Aliased

Table B4: Model adequacy measures for tensile strength

Std. Dev.	0.2099	R²	0.9975
Mean	16.21	Adjusted R²	0.9953
C.V. %	1.30	Predicted R²	0.9929
		Adeq Precision	56.6572

Table B5: Model adequacy measures for elongation at break

Std. Dev.	0.3133	R²	0.9916
Mean	11.55	Adjusted R²	0.9841
C.V. %	2.71	Predicted R²	0.9433
		Adeq Precision	43.8324

Table B6: Model adequacy measures for water absorption

Std. Dev.	0.0821	R²	0.9990
Mean	21.99	Adjusted R²	0.9981
C.V. %	0.3733	Predicted R²	0.9949
		Adeq Precision	132.2709

Table B₇: Diagnostics Case Statistics for TS

Run Order	Actual Value	Predicted Value	Residual	Leverage	Internally Studentized Residuals	Externally Studentized Residuals	Cook's Distance	Influence on Fitted Value DFFITS	Standard Order
1	17.90	17.78	0.1173	0.613	0.899	0.890	0.128	1.121	10
2	12.00	12.10	-0.0961	0.669	-0.795	-0.779	0.128	-1.108	3
3	12.30	12.23	0.0667	0.669	0.552	0.532	0.062	0.757	7
4	19.80	19.49	0.3148	0.166	1.642	1.823	0.054	0.814	16
5	12.80	12.75	0.0522	0.606	0.396	0.379	0.024	0.469	13
6	19.60	19.49	0.1148	0.166	0.599	0.578	0.007	0.258	19
7	17.50	17.65	-0.1523	0.669	-1.261	-1.305	0.321	-1.854	8
8	20.00	19.96	0.0439	0.669	0.364	0.347	0.027	0.494	6
9	14.00	13.91	0.0920	0.606	0.698	0.679	0.075	0.842	12
10	16.50	16.52	-0.0182	0.606	-0.138	-0.131	0.003	-0.162	11
11	14.20	14.24	-0.0370	0.669	-0.306	-0.292	0.019	-0.415	5
12	13.70	13.72	-0.0152	0.669	-0.125	-0.119	0.003	-0.169	4
13	19.40	19.49	-0.0852	0.166	-0.445	-0.426	0.004	-0.190	18
14	17.20	17.18	0.0217	0.606	0.165	0.156	0.004	0.194	14
15	11.50	11.55	-0.0452	0.613	-0.346	-0.331	0.019	-0.416	9
16	19.30	19.49	-0.1852	0.166	-0.966	-0.963	0.019	-0.430	17
17	13.00	12.90	0.1002	0.669	0.830	0.816	0.139	1.159	1
18	14.70	14.82	-0.1189	0.669	-0.984	-0.982	0.196	-1.396	2
19	19.70	19.49	0.2148	0.166	1.120	1.137	0.025	0.508	20
20	19.10	19.49	-0.3852	0.166	-2.010	-2.470	0.081	-1.103	15

Table B₈: Diagnostics Case Statistics for EA

Run Order	Actual Value	Predicted Value	Residual	Leverage	Internally Studentized Residuals	Externally Studentized Residuals	Cook's Distance	Influence on Fitted Value DFFITS	Standard Order
1	8.80	8.88	-0.0779	0.613	-0.400	-0.383	0.025	-0.482	10
2	17.00	17.51	-0.5065	0.669	-2.809	-5.807	1.594	-8.253	3
3	14.00	14.06	-0.0627	0.669	-0.348	-0.332	0.024	-0.472	7
4	11.00	10.86	0.1426	0.166	0.499	0.479	0.005	0.214	16
5	14.50	14.19	0.3143	0.606	1.598	1.757	0.393	2.178	13
6	11.10	10.86	0.2426	0.166	0.848	0.835	0.014	0.373	19
7	9.70	9.88	-0.1777	0.669	-0.985	-0.984	0.196	-1.398	8
8	8.10	7.80	0.3046	0.669	1.689	1.896	0.576	2.694	6
9	14.70	14.34	0.3600	0.606	1.831	2.130	0.515	2.641	12
10	8.50	8.57	-0.0738	0.606	-0.375	-0.359	0.022	-0.445	11
11	10.40	10.58	-0.1805	0.669	-1.001	-1.001	0.202	-1.423	5
12	12.90	12.92	-0.0215	0.669	-0.119	-0.113	0.003	-0.161	4
13	10.80	10.86	-0.0574	0.166	-0.201	-0.191	0.001	-0.085	18
14	9.80	9.83	-0.0281	0.606	-0.143	-0.136	0.003	-0.168	14
15	15.50	15.14	0.3575	0.613	1.835	2.138	0.534	2.693	9
16	10.70	10.86	-0.1574	0.166	-0.550	-0.530	0.006	-0.237	17
17	12.70	12.72	-0.0243	0.669	-0.135	-0.128	0.004	-0.182	1
18	9.40	9.54	-0.1392	0.669	-0.772	-0.756	0.121	-1.074	2
19	10.90	10.86	0.0426	0.166	0.149	0.142	0.000	0.063	20
20	10.60	10.86	-0.2574	0.166	-0.900	-0.890	0.016	-0.398	15

Table B₉: Diagnostics Case Statistics for WA

Run Order	Actual Value	Predicted Value	Residual	Leverage	Internally Studentized Residuals	Externally Studentized Residuals	Cook's Distance	Influence on Fitted Value DFFITS	Standard Order
1	18.80	18.83	-0.0279	0.613	-0.548	-0.527	0.048	-0.664	10
2	26.50	26.51	-0.0061	0.669	-0.129	-0.123	0.003	-0.175	3
3	23.70	23.70	-0.0035	0.669	-0.074	-0.071	0.001	-0.100	7
4	21.30	21.32	-0.0162	0.166	-0.215	-0.205	0.001	-0.092	16
5	25.50	25.60	-0.0962	0.606	-1.867	-2.195	0.536	-2.721	13
6	21.30	21.32	-0.0162	0.166	-0.215	-0.205	0.001	-0.092	19
7	19.80	19.86	-0.0631	0.669	-1.336	-1.398	0.360	-1.987	8
8	19.70	19.68	0.0203	0.669	0.429	0.411	0.037	0.584	6
9	24.00	24.00	-0.0001	0.606	-0.001	-0.001	0.000	-0.002	12
10	20.90	20.92	-0.0200	0.606	-0.388	-0.371	0.023	-0.460	11
11	20.70	20.77	-0.0701	0.669	-1.485	-1.595	0.445	-2.268	5
12	22.90	22.82	0.0843	0.669	1.785	2.051	0.643	2.915	4
13	21.40	21.32	0.0838	0.166	1.119	1.135	0.025	0.507	18
14	21.30	21.22	0.0761	0.606	1.478	1.585	0.336	1.966	14
15	22.90	22.89	0.0083	0.613	0.163	0.155	0.004	0.195	9
16	21.40	21.32	0.0838	0.166	1.119	1.135	0.025	0.507	17
17	23.10	23.02	0.0773	0.669	1.635	1.813	0.540	2.577[1]	1
18	22.10	22.08	0.0177	0.669	0.374	0.358	0.028	0.508	2
19	21.20	21.32	-0.1162	0.166	-1.550	-1.687	0.048	-0.754	20
20	21.30	21.32	-0.0162	0.166	-0.215	-0.205	0.001	-0.092	15

Table C₁: Sample Sequential Model Sum of Squares for TS

Source	Sum of Squares	df	Mean Square	F-value	p-value	
Mean vs Total	5255.28	1	5255.28			
Linear vs Mean	78.34	3	26.11	4.14	0.0238	
2FI vs Linear	7.99	3	2.66	0.3725	0.7743	
Quadratic vs 2FI	**92.46**	**3**	**30.82**	**699.22**	**< 0.0001**	**Suggested**
Cubic vs Quadratic	0.0789	4	0.0197	0.3271	0.8505	Aliased
Residual	0.3618	6	0.0603			
Total	5434.50	2	271.73			

Table C₂: Sample Sequential Model Sum of Squares for EA

Source	Sum of Squares	df	Mean Square	F-value	p-value	
Mean vs Total	2670.36	1	2670.36			
Linear vs Mean	109.92	3	36.64	78.44	< 0.0001	
2FI vs Linear	1.91	3	0.6350	1.48	0.2654	
Quadratic vs 2FI	**4.59**	**3**	**1.53**	**15.57**	**0.0004**	**Suggested**
Cubic vs Quadratic	0.6038	4	0.1509	2.40	0.1623	Aliased
Residual	0.3779	6	0.0630			
Total	2787.75	2	139.39			

Table C₃: Sample Sequential Model Sum of Squares for WA

Source	Sum of Squares	df	Mean Square	F-value	p-value	
Mean vs Total	9671.20	1	9671.20			
Linear vs Mean	54.26	3	18.09	19.87	< 0.0001	
2FI vs Linear	3.94	3	1.31	1.61	0.2352	
Quadratic vs 2FI	**10.55**	**3**	**3.52**	**521.81**	**< 0.0001**	**Suggested**
Cubic vs Quadratic	0.0381	4	0.0095	1.95	0.2221	Aliased
Residual	0.0293	6	0.0049			
Total	9740.02	20	487.00			

Appendix D: 2D interaction graphs of each factor on the three responses
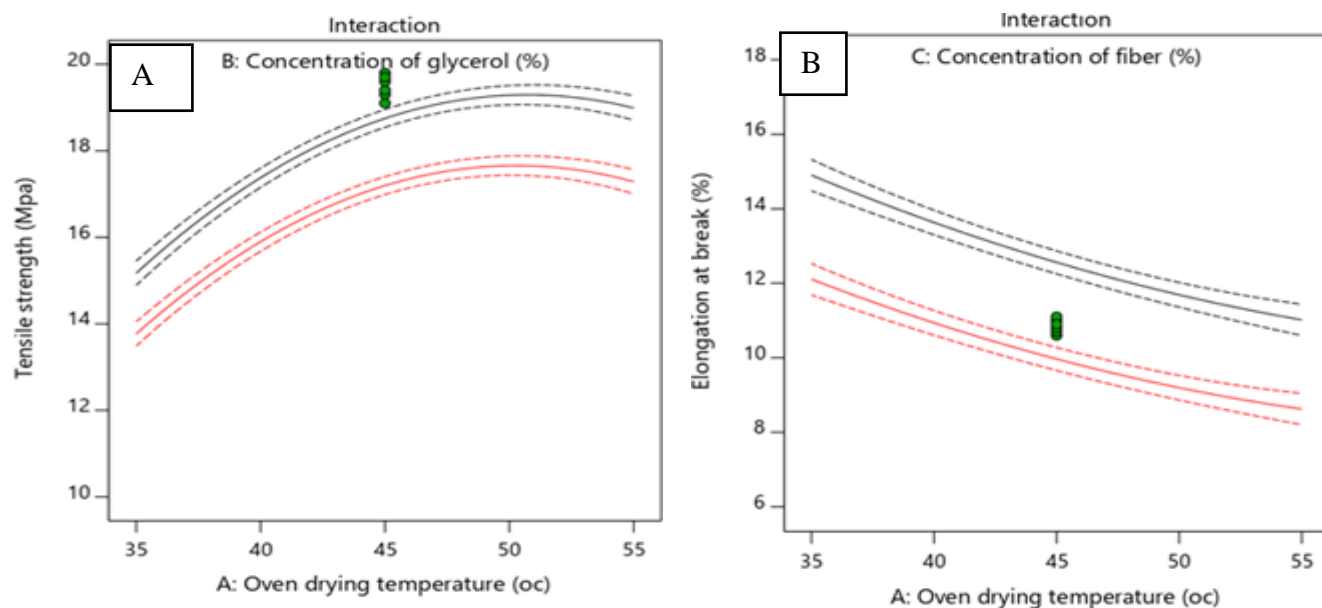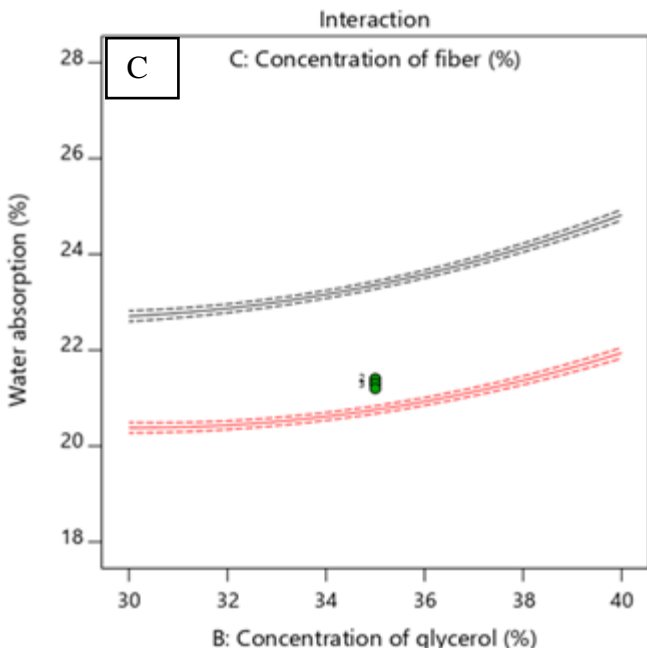
Figure D: A indicates the interaction effect of (AB) on the TS of the film, B indicates the interaction effect of (AC) on EA, and C indicates the interaction effect of (BC) on WA.

Appendix E₁: contour plots for significant factors for desirabilities, TS, EA and WA.
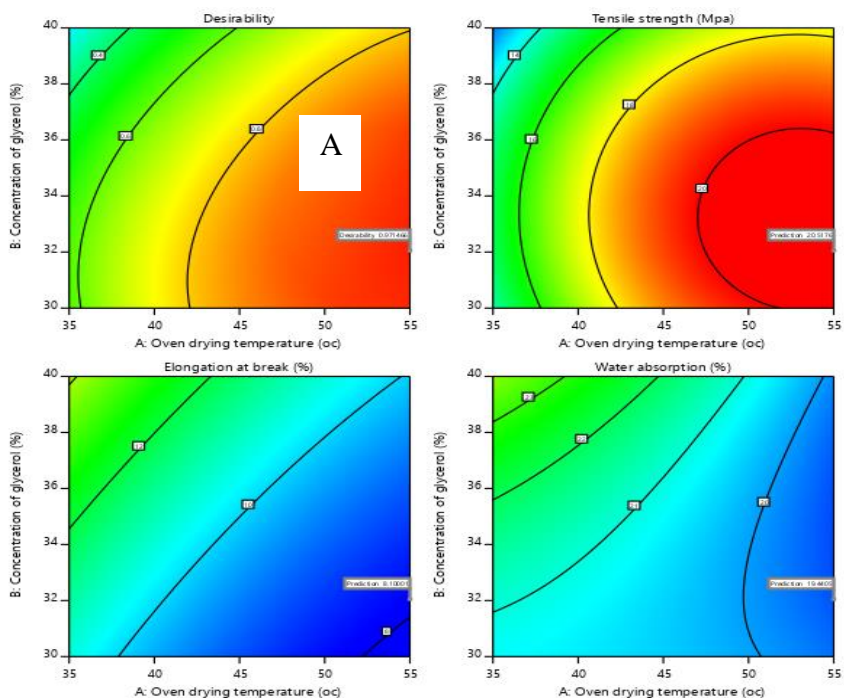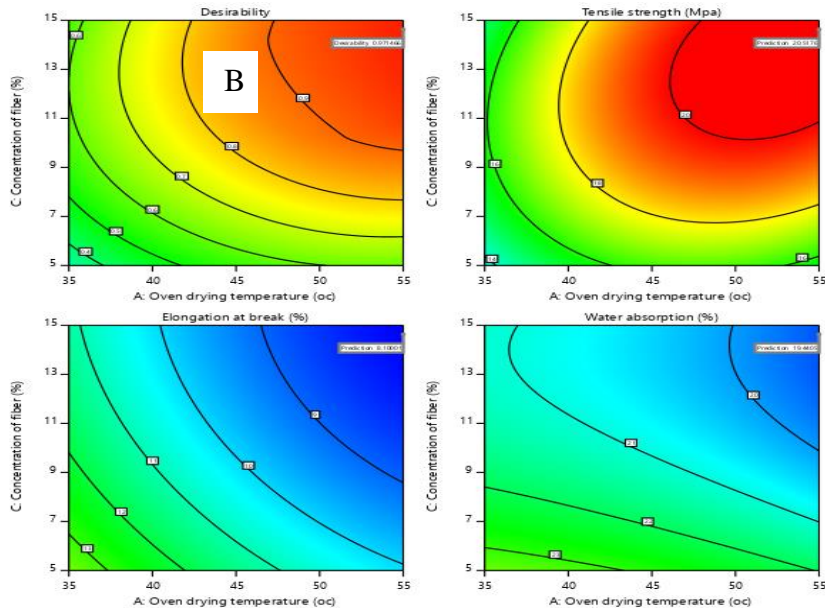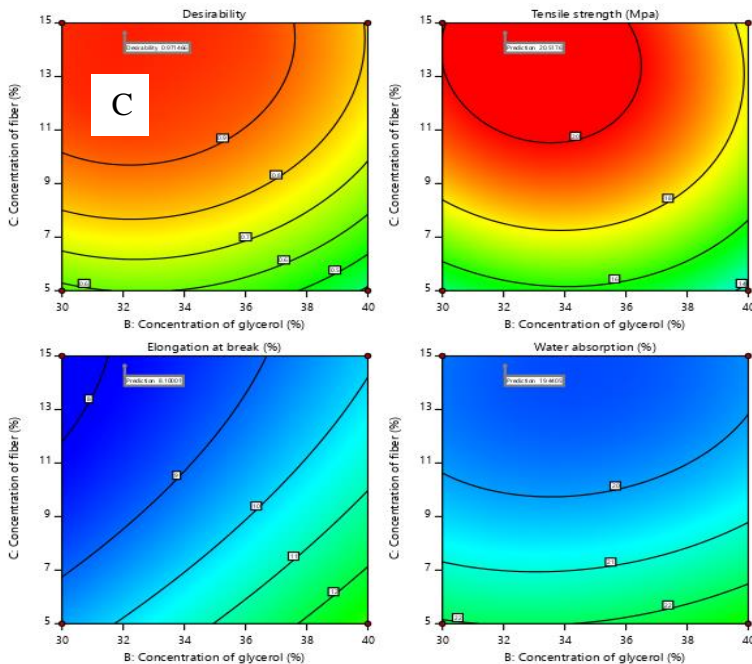
Figure E₁: A, B, and C indicate the oven drying temperature versus concentration of glycerol, oven drying temperature versus concentration of fiber, and concentration of glycerol versus concentration of fiber for desirability, tensile strength, elongation at break, and water absorption respectively of counterplot.
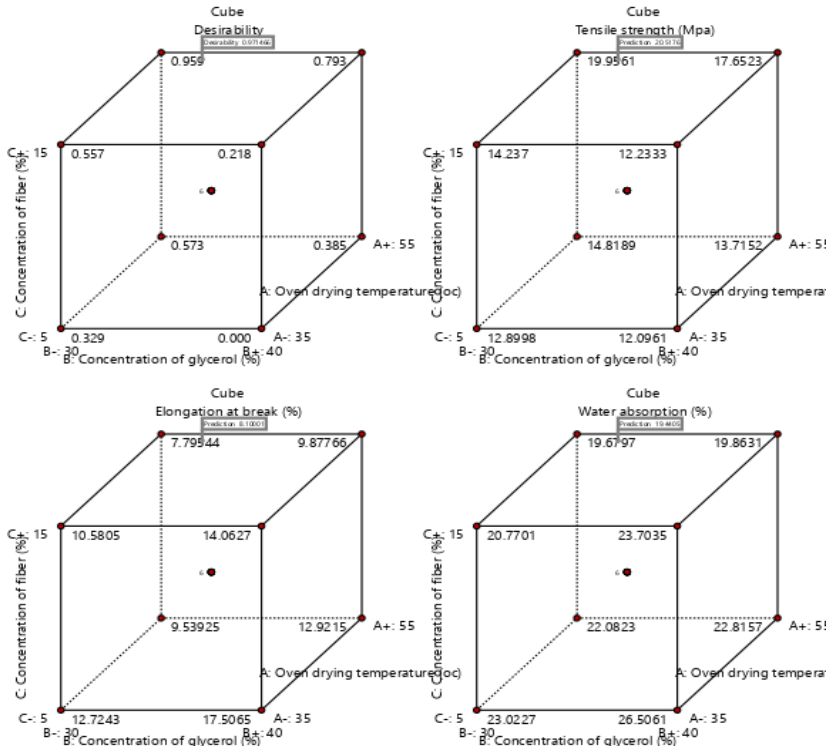
Appendix E₂: Perturbation graphs
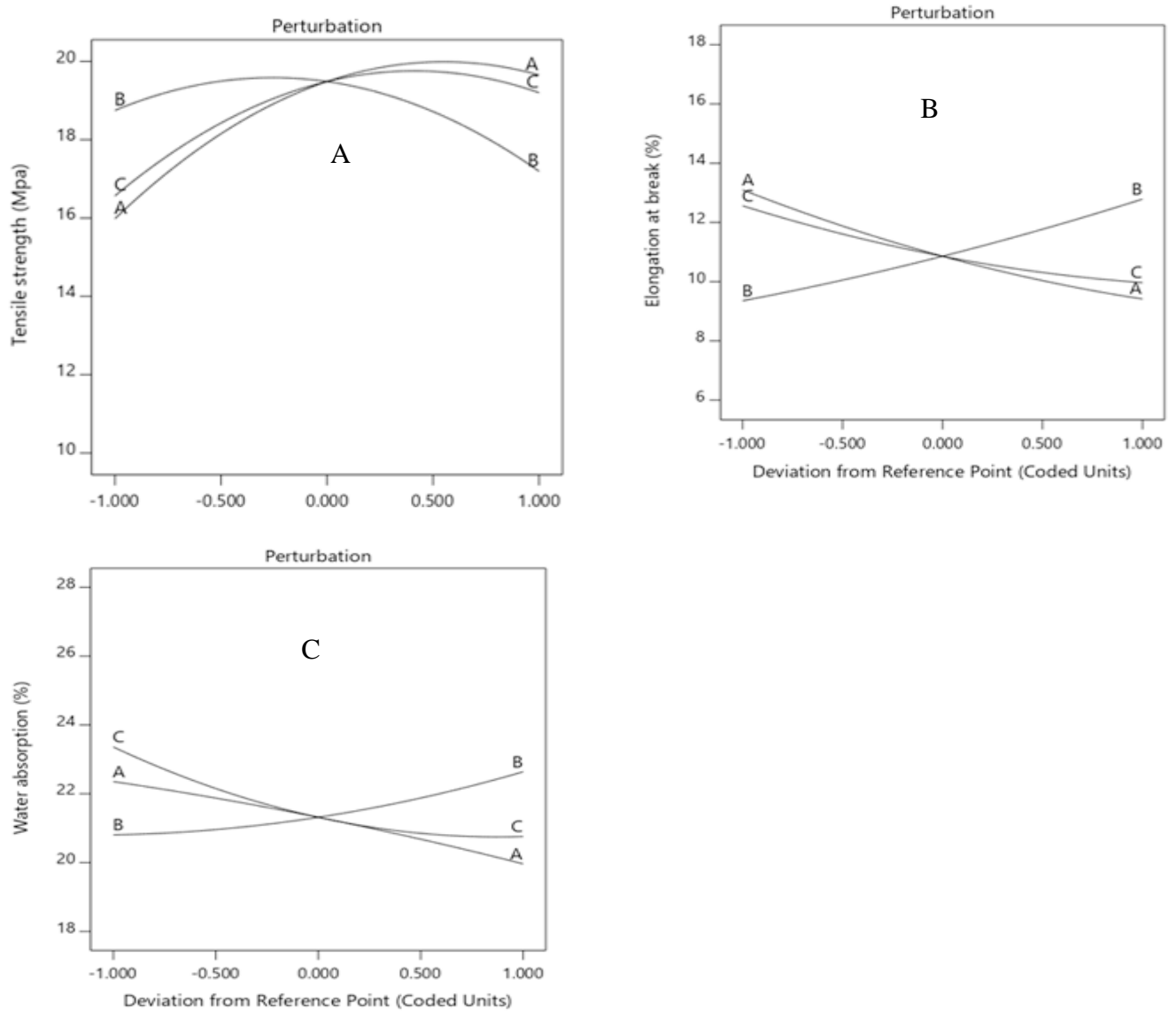
Figure E₂: Perturbation graphs of A (TS), B (EA), and C (WA).

Appendix E₃: cubic diagram

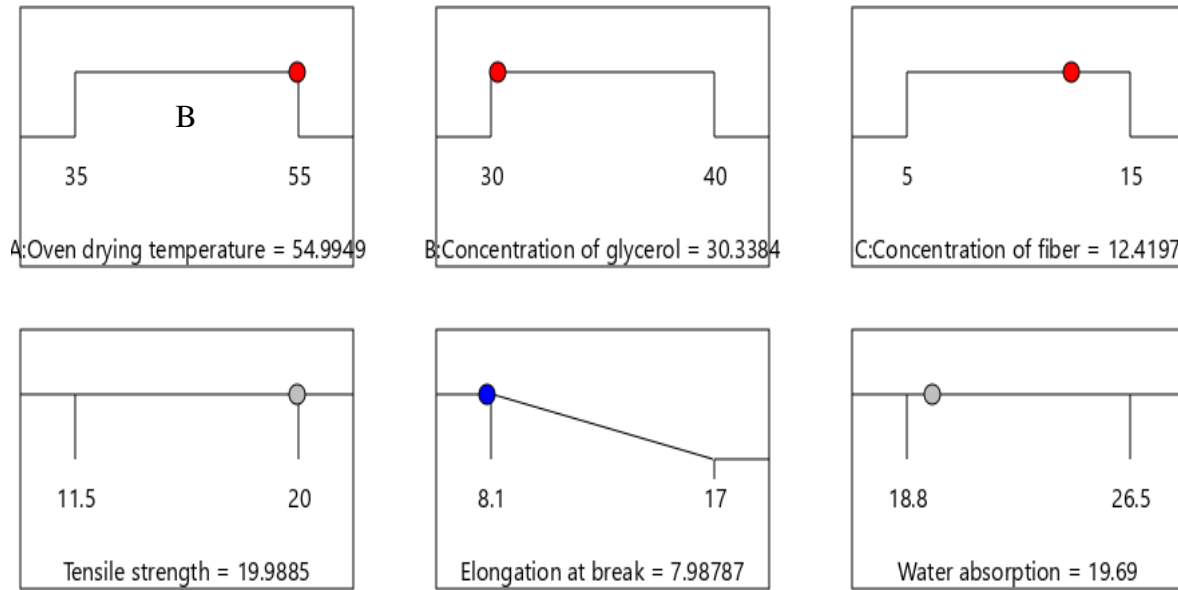**Figure E₃:** This is the cubic model for desirability, tensile strength, elongation at break, and water absorption concerning three independent factors.
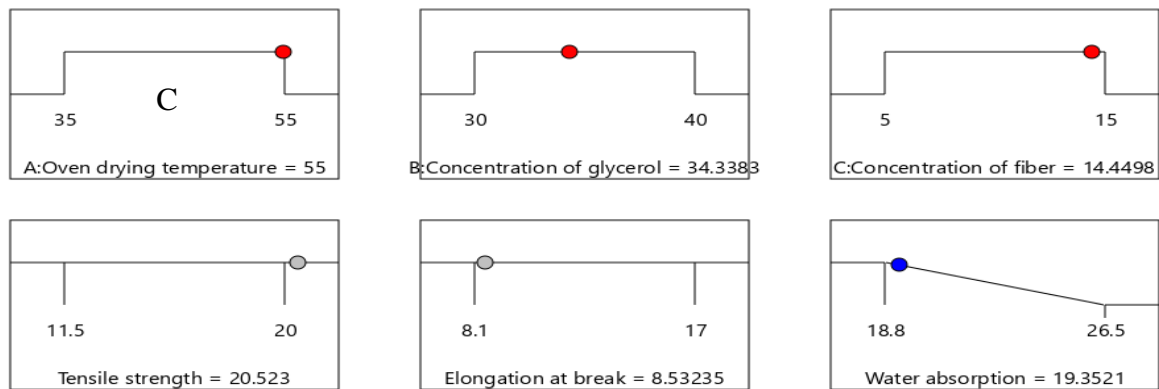
Appendix E₄: Desirability ramps for each response.
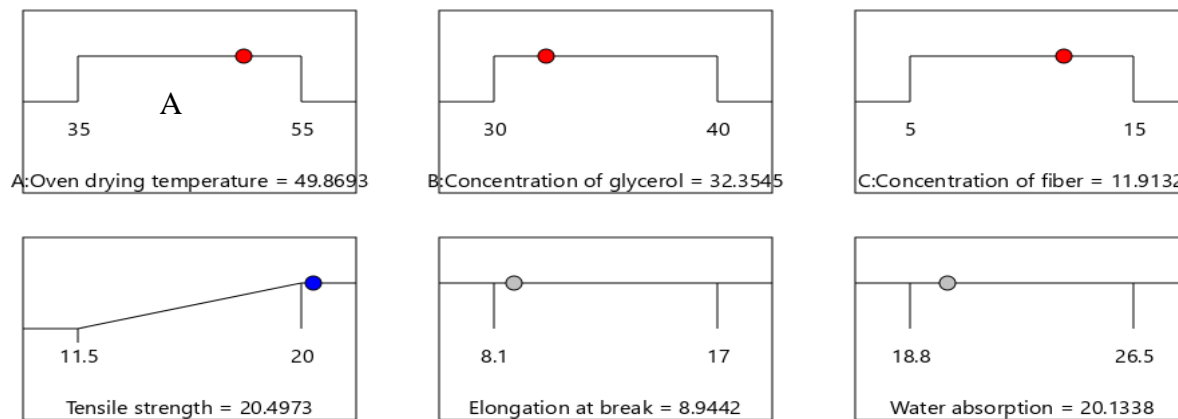
Desirability = 1.000
Solution 1 out of 10

35	55	
A:Oven drying temperature = 54.9949		

30	40
B:Concentration of glycerol = 30.3384	

5	15
C:Concentration of fiber = 12.4197	

11.5	20
Tensile strength = 19.9885	

8.1	17
Elongation at break = 7.98787	

18.8	26.5
Water absorption = 19.69	

Desirability = 1.000
Solution 1 out of 10

35	55
A:Oven drying temperature = 55	

30	40
B:Concentration of glycerol = 34.3383	

5	15
C:Concentration of fiber = 14.4498	

11.5	20
Tensile strength = 20.523	

8.1	17
Elongation at break = 8.53235	

|	
18.8	26.5
Water absorption = 19.3521	

Desirability = 0.928
Solution 1 out of 10

Figure E₄: Desirability ramp for the optimization of the response and the parameters A (TS), B (EA), and C (WA).

Appendix F: Absorbance of standard amylose solution

Table F₁: Amylose concentration and absorbance

Amylose concentration (mg/l)	Absorbance at 620 (nm)
5	0.048
10	0.097
15	0.145
20	0.192
25	0.238

Table F₂: Absorbance of sample solution

Sample	Absorbance at 620 nm
Wheat bran starch	0.235

Appendix G: A standard amylose calibration curve
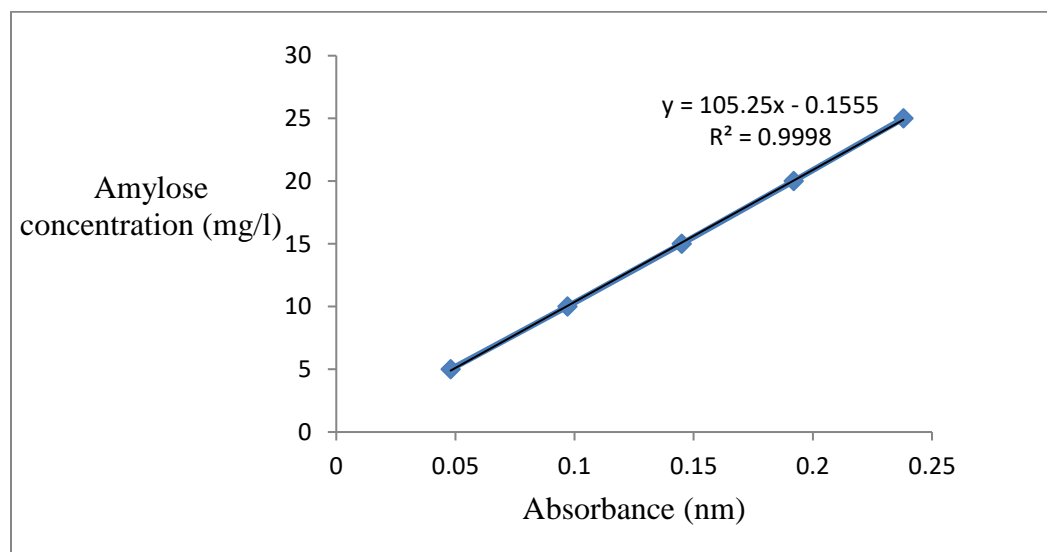
Figure G: standard amylose calibration curve

Table H: FTIR characteristics for wheat bran starch, wheat straw cellulose, and bioplastic film

Wavenumber (cm^{-1})	FTIR spectra of the samples			Functional group
	Wheat bran starch	Wheat straw cellulose	Bioplastic film	
3700 - 3200	3670	3657.6	3754 - 3542	O-H stretch for alcohol
3100 - 2850	2934	2934.8	3050 - 2839	C-H stretch for alkane
2140	-	-	2140	C≡C stretch for alkyne
1810 - 1680	1726	1702.1	1750	C = O stretch for alkene
1680 - 1620	-	-	1610	C = C stretch for alkene
1436 -1313	1436 -1313	1492-1315	1430	C-H bend of alkane
1313 - 500	1313 - 681	1315 - 662	951	C-O and C-C stretch in a D glucose ring